AUTOMATIC CALIBRATION OF THE PITMAN MODEL USING THE SHUFFLED COMPLEX EVOLUTION METHOD

Report to the

Water Research Commission

by

J G Ndiritu

School of Civil and Environmental Engineering

University of the Witwatersrand

WRC Report Number: KV 229/09

November 2009

Obtainable from

Water Research Commission
Private Bag X03
Gezina 0031
South Africa

orders@wrc.org.za

The publication of this report emanates from a project entitled *Automatic Calibration of the Pitman Model using the Shuffled Complex Evolution Method* (WRC Project No. K8/566/1)

ISBN 978-1-77005-897-2
Printed in the Republic of South Africa

EXECUTIVE SUMMARY

Motivation

This project was motivated by the need to evaluate automatic calibration for hydrological modelling in southern Africa – a region where manual calibration is predominant. The Pitman model was selected for the task because it is widely applied in Southern Africa for water resources assessment. With few exceptions, the Pitman model has been calibrated manually mostly as the rainfall-runoff module in Water Resources Simulation Model (WRSM 2000) (Bailey, 2008) and in earlier versions of the system (WRSM 2000 (Pitman et al., 2000); WRSM 90 (Midgley et al., 1994)). The Pitman model is also one of the models included in the SPATSIM modelling framework (Hughes, 2002). Hughes (in Knight Piesold et al. (2003)) mentions that the SADC team working on extending the WR90 study to SADC region identified the need for standardisation in the approach to model calibration to ensure that parameter regionalizations are based on a consistent modelling approach. Such standardization is likely to be difficult to implement with manual calibration and much easier with a guided automatic calibration approach. Considerable research on automatic model calibration has been undertaken elsewhere and the shuffled complex evolution (SCE-UA), an effective and efficient automatic calibration technique, has been developed (Duan et al., 1992) and widely applied globally (Tables 2.4 and 2.5). Discussions with many hydrological modellers in Southern Africa pointed to a perception that automatic calibration is dangerous because the calibrated parameters may not be hydrologically meaningful. While there may be merit in this, there does not seem to be any published research in southern Africa to support or disapprove it. Research in other parts of the world does not highlight this perceived danger and automatic calibration has been incorporated in some catchment modelling systems (e.g. catchment modelling toolkit (www.toolkit.net.au/rrl), Soil Water Assessment Tool (www.brc.tamus.edu/swat/)). Manual calibration on the other hand is often viewed as subjective, tedious and time consuming. This project set out to make an assessment of the dangers of automatic model calibration and also to compare its performance with manual calibration. The SCE-UA method was selected as the most suitable optimizer for the task.

Project aims

The aims of the project were to:

- Develop a user-friendly software for the shuffled complex evolution (SCE-UA) method of automatic model calibration that can be easily linked and applied to any catchment model.
- Use the Pitman model to demonstrate the application of the software.
- Compare automatic and manual calibration of the Pitman model and identify any dangers of automatic calibration and offer solutions for them.

Development of the automatic calibration software

The shuffled complex evolution (SCE-UA) algorithm was coded in Microsoft PowerStation Fortran, debugged and tested extensively using several optimization problems. After the code was considered to be free from bugs, it was then modified to allow for its application for the automatic calibration of any catchment model without the need for re-coding. A graphical user interface was then developed in Delphi for the calibrator to enable user-friendly calibration in a Windows environment. The main features of the software are presented in Chapter 3 and the software in the accompanying CD ROM includes an

example application. In order to use the calibrator, minimal coding of the catchment simulation model to be calibrated is required to allow the exchange of information between the model and the calibrator. Details of how this coding needs to done are also given in Chapter 3 and in the example application provided in the software.

Automatic calibration of the Pitman model and comparison with manual calibration

Three basins that had previously been calibrated manually by the Pitman model were selected for automatic calibration. These are:

- The Buffelspruit River catchment in Mpumalanga province in South Africa that had been calibrated by Hughes (2004).
- The Kafue basin in Zambia that had been calibrated by Mwelwa (2004).
- The Amatole basin in the Eastern Cape province of South Africa that had been calibrated by Kleynhans (2007).

The Pitman model that was used for automatic calibration had been obtained in 1999 from Dr V W Pitman, the developer of the Pitman model. This version of the Pitman model was not identical to those applied in manual calibration (SPATSIM version (Hughes, 2004) for Buffelspruit and Kafue and the WRSM2000 version (Pitman et al., 2000) for Amatole) but the differences were considered not significant enough to invalidate comparison of manual and automatic calibration. In addition, the calibration of Kafue basin (Mwelwa, 2004) initially involved automatic parameter search using a genetic algorithm before resorting to manual calibration. This calibration (Mwelwa, 2004) was therefore effectively a combination of automatic and manual calibration. In the current study, Buffelspruit was calibrated as a single catchment while 7 subcatchments located on the north east of Kafue basin were calibrated simultaneously. Three subcatchments of Amatole located in separate areas within the basin were each modelled as a single catchment. Sections 4.2, 4.3 and 4.4 present the analysis for Buffelspruit, Kafue and Amatole basin respectively. For all basins, 10 randomly initialised calibration-validation runs were carried out. The manual calibrations did not include any validation runs which limited the scope of comparison.

It was found that:

- None of the parameters obtained by automatic calibration for any catchment were considered hydrologically unrealistic. Uncharacteristically high PI values were obtained for Kafue basin and this was attributed to the hydrological functioning of dambos in the basin.
- Automatic calibration was able to help identify which parameters were well identified and which were poorly identified with reasonable objectivity as illustrated graphically in Figures 4.1, 4.2, 4.11 and 4.12.
- Automatic calibration helped infer the probable impacts of dambos in Kafue basin on parameters PI and ST. Previous manual calibration (Mwelwa, 2004) was not able to provide any inference although that study had indicated that dambos are expected to have significant impacts on several parameters of the Pitman model. Unlike the Buffelspruit and the Amatole, validation performance of Kafue basin was notably poorer than calibration and this was seen as evidence of the inadequacy of the Pitman model structure in incorporating the hydrological functioning of dambos.

- Automatic calibration performed better than manual calibration for the Buffelspruit and one of the three Amatole catchments while the manual and automatic performance for Kafue basin was practically identical.
- It was easy to objectively find out if the provided parameter search range for automatic calibration was adequate or whether it needed to be adjusted to allow for improved model performance and better parameter values.
- Reasonable time series of soil moisture storage and separation of slow and quick flow were obtained by automatic calibration. These time series were not available from manual calibration for a comparison to be made.

It took about 5 minutes to complete 10 calibration runs of a single catchment (Buffelspruit and the Amatole catchments) while 10 calibration runs of the Kafue basin (involving 77 parameters) took about 1 hour 40 minutes. Additional time was needed to assess the performance and how realistic the results were. If automatic calibration takes considerable time, (like for Kafue basin in this study) the modeller has time available for other activities while the calibrator is running.

Potential dangers and challenges of automatic calibration

The analysis did not reveal any glaring danger of automatic calibration. The main danger that could arise would be the fitting of model parameters that do not make hydrological sense. This can be avoided by setting the parameter search range limits realistically – a task which is not difficult and that manual calibration implicitly requires. This was easily accomplished in the calibrations here by setting an initial search range and search range limits for every parameter. By carrying out multiple randomly initialized calibration runs, the parameters consistently locating at the search range limit were identified and the search range adjusted if hydrologically and conceptually realistic. Using this approach lead to unexpectedly high values of precipitation index (PI) parameter for Kafue basin – thereby revealing the hydrological significance of dambos in the basin.

Although manual calibration induces the modeller to learn more about the catchment and the model structure than automatic calibration, Section 4.5.1 reveals that both manual and automatic calibration could obtain conceptually inconsistent parameter sets. Realistic calibration whether manual or automatic requires i) the understanding of the model structure and the catchment processes including any unique features ii) an idea of the expected parameter search ranges, iii) careful analysis and interpretation of the calibration results and the simulated time series and iv) verification of calibrated parameters using an independent data set.

Automatic model calibration requires the specification of an objective function whose selection needs to be guided by the aim/s of the modelling and its ability to maximise the utilization of available information and data. Different objective functions give different parameter sets (see for example Table 4.11 and 4.12) but this need not be viewed as a disadvantage of automatic calibration. It is a reminder that i) the model is an idealization of the reality, ii) the data applied are also mostly approximated and the precise values are hardly ever known and, iii) the modelling needs to be linked to the specific needs that may indicate how the objective function needs to be formulated. Manual calibration also works on the basis of the objective of matching the simulated and the observed data. Consequently, the considerations applicable in objective function selection of automatic calibration also apply in manual calibration.

Conclusions and Recommendations

This project was motivated by the need to evaluate automatic calibration for hydrological modelling in southern Africa – a region where manual calibration is predominant. The project aimed to develop an easy-to-use automatic calibrator based on the Shuffled Complex Evolution (SCE-UA) method and to demonstrate automatic calibration using the widely used Pitman model. The SCE-UA was coded and a graphical user interface was developed to enable user friendly calibration in a windows environment.
Automatic calibration using the calibrator was demonstrated by calibrating the Pitman model on 3 basins in southern Africa; the Buffelspruit, the Kafue and the Amatole. The three basins had been calibrated manually thereby allowing a comparison of manual and automatic calibration. For each catchment, 10 randomly initialised calibration runs were made and served to i) ensure that the applied parameter search ranges were adequate ii) assess the adequacy of optimization iii) assess the level of parameter identification and, iv) identify parameter inter-dependences within and across catchments. Sections 4.2, 4.3 and 4.4 provide the details of automatic calibration for the Buffelspruit, the Kafue and the Amatole catchments. Although automatic calibration is often faulted on the basis of its inability to relate parameter values to the physical features of the catchment, the calibration of Kafue basin revealed that automatic calibration can actually help infer relationships between parameter values and physical catchment features – an accomplishment that manual calibration of the basin was not able to achieve. Automatic calibration also performed considerably better than manual calibration for the Buffelspruit and one of the three Amatole basin catchments thereby revealing the value of the more exhaustive parameter search that automatic calibration can achieve in comparison to manual calibration.

No specific danger of automatic calibration was identified and the only caution is considered the careful identification of parameter search ranges and the use of all available information to try and obtain the best possible understanding of the hydrological processes and features in the catchment. In addition, thoughtful checking and interpretation of the calibration results is necessary.

The developed calibration software is available on the accompanying CD ROM and has been designed to enable easy implementation and simplicity in use. An example on how to link a catchment model to the calibrator is included in the software.

ACKNOWLEDGEMENTS

The author gratefully acknowledges the contributions of the following people:

- Ms Riana Steyn of Alborak Systems Engineering for creating the GUI for the calibration software.
- Prof Denis Hughes of the Institute for Water Research, Rhodes University for providing data and calibration results for Kafue basin.
- Mr Allan Bailey of Stewart Scott International for providing data and calibration results for Amatole basin.
- Dr Renias Dube formerly of the Water Research Commission (WRC) for his guidance at various phases of the project.

Funding for this project was provided by the WRC and the WRC is gratefully acknowledged for providing this support.

TABLE OF CONTENTS

LIST OF FIGURES

LIST OF TABLES

1 INTRODUCTION

This proposal is motivated by the need to evaluate and apply the global advances in model calibration for hydrological modelling in southern Africa – a region where manual calibration is predominant and where there is a perception that automatic model calibration is dangerous. Many hydrological models are in use in Southern Africa and the Pitman model has been selected for this project because it is widely used in southern Africa for practical water resources assessment. The Pitman model is calibrated manually in the Water resources Simulation Model 2000 (WRSM 2000) modelling system and no formal evaluation of: i) the uncertainty of parameters or the level of confidence one should have on them and ii) the prediction confidence limits of the model simulations is done. Considerable research on: i) automatic model calibration, ii) evaluation of model parameter uncertainty and ii) the consequent uncertainty in the predictive ability (confidence limits) of models has been undertaken globally. Hughes mentions (Page 130, Appendices, Knight Piesold et al. (2003)) that the SADC team working on extending the WR90 study to SADC identified the need for standardisation in the approach to model calibration to ensure that parameter regionalizations are based on a consistent modelling approach. Such standardization is likely to be difficult to implement with manual calibration and much easier with a guided automatic calibration approach. The evaluation of parameter and model predictive uncertainty would provide the modellers and water managers with additional information regarding the confidence with which to view modelling results. With the increasing climate variability/change, this information could have significant value in decision making. Although there is merit in considering in acknowledging the danger of automatic calibration, its widespread application (e.g. the HBV model (Yu and Yag (2000),), the NAM model (Madsen et al. (2002)), the Xinanjiang model (Cheng et al. (2002)), the SFB model (Thyer et al. (1999)), the MOD-HYDROLOG model (Chiew et al. (1994)), the HSPF model (Doherty and Johnston, (2003), Al-Abed and Whitely (2002)), the SMA-SAC (Gupta et al. (1999)), the PRMS model (Dagnachew et al. (2003)) is ample evidence that these perceived dangers may not difficult to prevent. Many of these and other publications mention the main disadvantages of manual calibration: it is subjective and could be very time consuming. Comprehensive evaluation of parameter uncertainty and model predictive uncertainty is also very difficult to undertake with the manual approach. This study aimed to i) assess the dangers associated with automatic calibration using the Pitman model and propose methods of dealing with them and ii) compare automatic and manual calibration. Although the analysis of parameter uncertainty is important, it is not within the scope of this project.

The specific aims of the project were:

- Develop a user-friendly software for the shuffled complex evolution (SCE-UA) method of automatic model calibration that can be easily linked and applied to any catchment model.
- Use the Pitman model to demonstrate the application of the software.
- Compare automatic and manual calibration of the Pitman model and identify any dangers of automatic calibration and offer solutions for them.
-

Chapter 2 reviews the literature on the Pitman model and automatic model calibration and Chapter 3 informs how the calibration software was developed. The automatic calibration of the three southern African basins presented in Chapter 4. This Chapter concludes with a discussion of the potential

dangers and advantages of automatic model calibration based on the calibration results. Conclusions and recommendations then follow in Chapter 5.

2 LITERATURE REVIEW

2.1 The Pitman Model

The Pitman model was developed by Pitman (1973) with the purpose of simulating runoff from both gauged and ungauged catchments in South Africa. The Pitman model is extensively used in South Africa and is the catchment process module within the Water Resources Simulation Model 2000 (WRSM 2000) (Pitman et al. (2000)) and the earlier version (WRSM 90) (Midgley et al. (1994)). The WRSM model is used extensively for water resources assessment in South Africa and has been recently upgraded to better model highly developed South African catchments (Bailey, 2008).

Figure 2.1 shows the main components of the original version of the Pitman model (Pitman, 1973). Each month is split into four iteration steps and rainfall is apportioned to each using a non-linear distribution. The rainfall first needs to satisfy interception storage. Surface runoff from the impervious part of the catchment is computed in proportion to the total catchment area. The proportion of the remaining rainfall that is absorbed by the catchment surface is determined using a function that assumes a triangular distribution of catchment absorption rates. This portion goes into the moisture store and the rest contributes to runoff. A non-linear power function determines the runoff amount that the soil store produces. One portion is considered to come from the upper zone (soil moisture runoff) and the other from the lower zone (baseflow runoff). Surface runoff occurs when the moisture storage capacity is exceeded. Evapotranspiration from the main moisture store depends on a model parameter, the potential evapotranspiration and the moisture state of the soil store. Pitman (1973) provides a more detailed description of the model. Modified versions of the original model have been used (e.g. Hughes, 1997; Gan et al., 1997; Hughes and Metzler, 1998) to cater for specific conditions. The WRSM 2000 model has recently been upgraded to improve the modelling of highly developed South African catchments (Bailey, 2008).

The Pitman model formulation has been modified in order to adequately model the hydrology of: i) surface water-ground water interactions, ii) afforestation, iii) alien vegetation, iv) dryland crops, v) off channel wetlands and vi) mine and irrigation water including quality aspects. According to Bailey (2005), these changes will increase the difficulty of calibration. Table 2.1 presents a brief description of the 12 parameters of the original model.

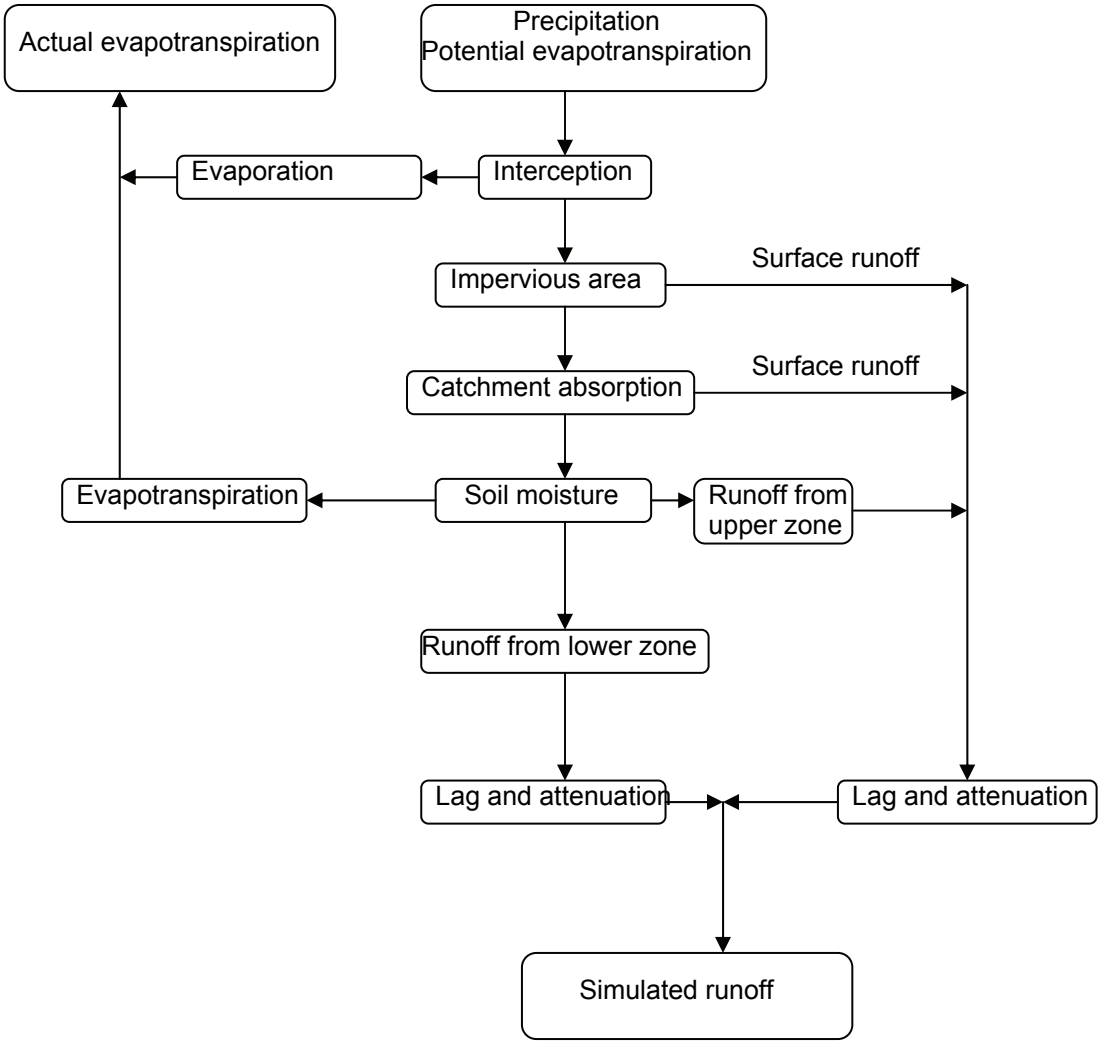

Figure 2.1 A flow chart of the Pitman model

2.2 Calibration of the Pitman model.

The Pitman model is typically calibrated manually with some of the 12 parameters often set to constant values. Pitman (1973) recommended initial parameter values for starting calibration and Midgley et al., 1994 provide preliminary parameter values for the Pitman model for the whole of South Africa.

In addition to the use of graphs (flow time series, duration curves etc.), the calibration performance is usually quantified using three measures: the mean annual flow (MAR), the standard deviation of the mean annual runoff (SD) and the seasonal distribution of flows quantified by the seasonal index (SI). Pitman (1973) proposed the parameter adjustment procedure presented in Table 2.2 to improve the matching of the three measures. These are used in addition to using the modeller's understanding of the catchment's hydrological processes to calibrate the model.

Table 2.1 Parameters of the original Pitman Model

Parameter	Units	Description
PI	mm	Interception storage
AI	none	Ratio of impervious to total area
ZMIN	mm/month	Minimum catchment absorption rate
ZMAX	mm/month	Maximum catchment absorption rate
ST	mm	Maximum moisture storage capacity
SL	mm	Moisture storage capacity below which no runoff occurs
FT	mm/month	Runoff from moisture storage at full capacity
GW	mm/month	Maximum groundwater runoff
R	none	Evaporation-moisture storage relationship parameter
POW	none	Power of the moisture storage-runoff equation
TL	months	Lag for surface and soil moisture
GL	months	Lag for groundwater runoff

Although the Pitman model has mostly been calibrated manually, automatic calibration has also been reported. Gan et al. (1997) carried out a comparative study of 5 models including the Pitman model using 4 catchments. The SCE-UA method was applied for all the calibrations but the focus was not evaluation of the adequacy of calibration. Ndiritu (2001) calibrated the Pitman model for 2 South African catchments applying a genetic algorithm (GA). Multiple randomly initialised calibrations obtained very close values of the objective function and the important parameters (which also gave very close values in the multiple runs) were clearly identified. Practically, the parameter sets obtained were considered as global optima.

Pitman model calibration is a multiobjective problem as three performance measures; the mean annual runoff, the standard deviation and the seasonal index need to be matched between the historic and the simulated flows. The use of several objectives recognizes that a single objective function is often an inadequate measure of the important characteristics of the observed data as Vrugt et al. (2003b) state. With the recent additions to the Pitman model in the upgrade of WRSM 2000, it is possible that water quality data will be involved in calibration in addition to streamflow thereby adding to the number of objectives involved. A review of model calibration with multiobjective functions is considered appropriate and is presented in the next Section.

Table 2.2 Effects of increasing Pitman model parameters on the characteristics of simulated runoff series

Parameter	Characteristic of simulated runoff		
	Mean annual flow	Standard deviation	Seasonal flow distribution
PI	decreased	increased	More peaked
AI	increased	decreased	Early wet season runoff increased
ZMIN	Decreased	increased	More peaked
ZMAX	Decreased	No effect	No effect
ST	decreased	Little effect	More uniform
SL	decreased	increased	More peaked
FT	increased	decreased	More uniform
GW	No effect	No effect	Dry season flows increased
R	Increased	decreased	More uniform
POW	decreased	increased	More peaked
TL	No effect	No effect	More uniform and lagged
GL	No effect	No effect	Dry season runoff increased

2.3 Multiobjective hydrologic model calibration

Hydrological modelling using multiobjectives can be grouped into two approaches; those that aggregate the objectives into a single objective and those that enable calibration whilst evaluating each objective independently using the concept of Pareto dominance.

2.3.1 Objective function aggregation method

Suppose we have a calibration problem that uses two objectives F_1 and F_2.
Weights can be used to combine F_1 and F_2 giving a single objective function F_w as

$$F_w(\theta) = wF_1(\theta) + (1-w)F_2(\theta) \tag{2.1}$$

where θ is the parameter set and w is a weight valued between 0 and 1 ($0 \le w \le 1$).
Depending on the objectives of the modelling exercise, it may be possible to choose w appropriately.
Euclidean distances can also used (Madsen, 2000) to obtain a single objective function F_e of the form

$$F_e(\theta) = \left[(F_1(\theta) + A_1)^2 + (F_2(\theta) + A_2)^2\right] \tag{2.2}$$

where A_1 and A_2 are transformation constants for the different objectives. The higher their value, the greater the importance given to the corresponding objective. Madsen (2000) explains how the values of A can be set obtain a balanced single objective F_e.

2.3.2 Pareto dominance approach

If the aggregated single objective is applied, the calibration will give a single solution just like in the case of single objective calibrations. The reality is that there are usually many other solutions that may obtain the same objective function but give simulated series of substantially different characteristics. This implies that a single 'best' parameter set does not exist and methods capable of obtaining a group of non dominated solutions are a better reflection of reality. The concept of Pareto dominance that was introduced by Goldberg (1989) can be applied to obtain these sets.

For the same problem of two objective functions F_1 and F_2, a parameter set θ_j dominates another parameter set θ_k if $F_1(\theta_j)$ is better than $F_1(\theta_k)$ and $F_2(\theta_j)$ is better than $F_2(\theta_k)$. Using this rule, it is possible to perform a search that identifies the curve that consists of parameter sets that are not dominated by any other as illustrated in Figure 2.2. If all non dominated points are ranked 1 while the dominated ones are ranked as 1 plus the number of other points dominating them, using the ranks as fitness values leads the search towards Pareto front (dotted line). All points (parameter sets) on the Pareto front can be considered as alternative optimal solutions to the problem.

The use of the Pareto front in practical hydrological modelling may pose some challenges not dealt with when using a single 'best' set but it reflects the reality of the uncertainties better. Analysis of the Pareto front parameter correlations can add insight into the way the model works and possible approaches to improvements. It could also form a much better basis of regionalization than the use of single parameter sets.

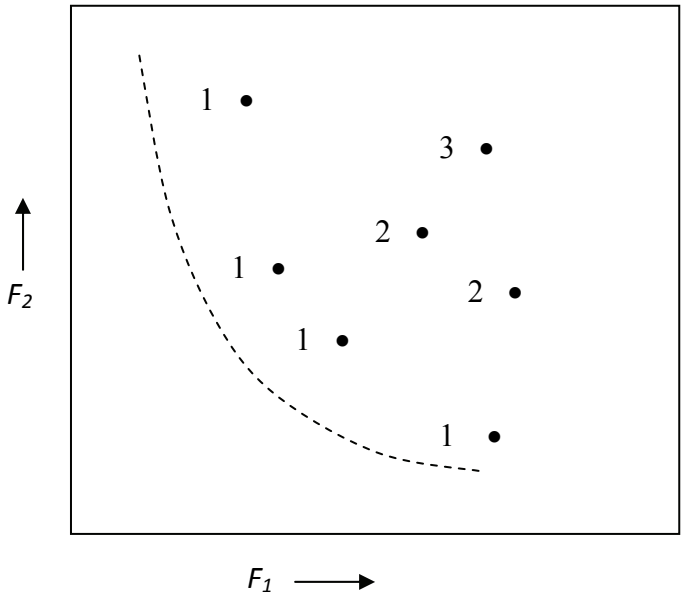

Figure 2.2 An illustration of Pareto dominance

The Pareto dominance approach has been used in several multiobjective model calibrations (Yapo et al., 1998; Boyle et al., 2000; Madsen, 2003). While this approached has generally worked, Vrugt et al. (2003b) report that it has the tendency to obtain a cluster of solutions around the region that agrees with the several objectives and miss out regions close to the edges of the Pareto front. Vrugt et al. (2003b) adopted an approach designed to deal with the clustering problem called the Strength Pareto approach which is described next.

2.3.3 Strength Pareto dominance approach

This method was developed by Zitler and Thiele (1999) and Vrugt et al. (2003b) also provide a clear description of the method. A brief description of the approach using Figure 2.3 as provided by Vrugt et al. (2003b) is described. Suppose we need to obtain the fitness of a problem of two functions F_1 and F_2 that need to be minimized. Figure 2.3a shows the fitness of 8 members using the traditional Pareto dominance approach described in Section 2.3.2. While this method leads the search towards the Pareto front, it does not provide a means of maintaining diversity of search because all non dominated solutions have the same fitness irrespective of their position. This results in clustering of solutions along a small portion of the Pareto front as shown in Figure 2.3b. The strength Pareto approach deals with this problem by encouraging growth of non dominated members that are on sparsely populated regions of the search space. To do this, the fitness of a member is based on both non dominance and the number of members it is dominating and dominating more members leads to a lower fitness. In Figure 2.3c, the fitness of the non dominated solutions is obtained as the ratio of the number of members it dominates to the total population. The fitness of the dominated solutions is obtained as the sum of the fitness of all dominating solutions that cover (dominate) the member plus unity (1). Adding one ensures that no non dominating member obtains a higher fitness than any dominating member. Vrugt et al. (2003b) found this method to have the weakness of many non dominating solutions having the same fitness (e.g. 3 members in the shaded region of Figure 2c have the same fitness of 12/8) and thereby making it difficult to improve search. They dealt with this by adding the Pareto rank obtained by the conventional approach (as in Figure 2a) to the fitness obtained by the Strength Pareto approach

and thereby obtained an effective method. Figure 2.3d shows a better distribution of Pareto front members that the improved approach obtained.

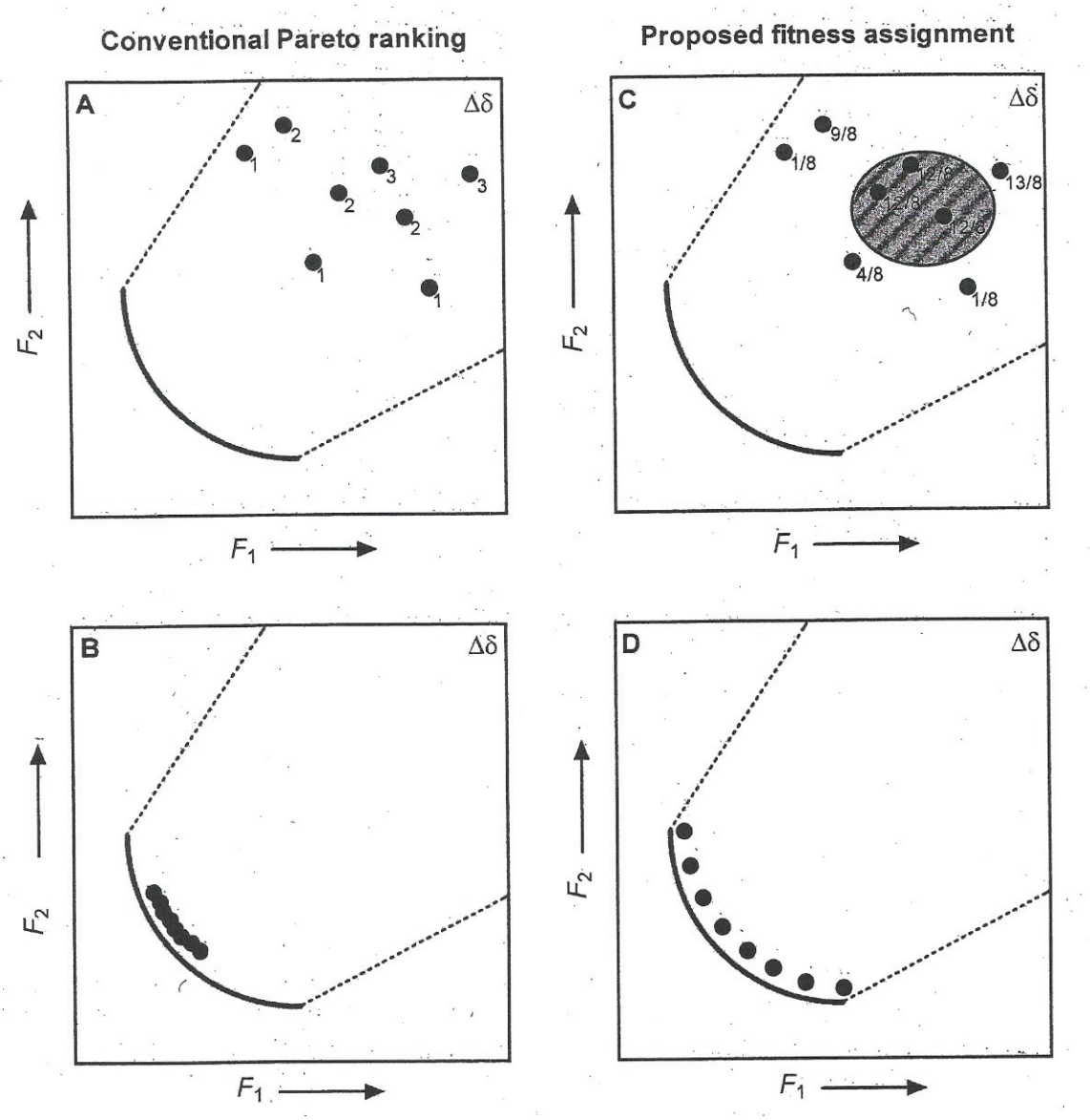

Figure 2.3 Illustration of the Strength Pareto ranking approach

2.4 The Shuffled Complex Evolution (SCE-UA) method

In a detailed study of the hydrological model calibration problem, Duan et al. (1992) identified five major characteristics that complicate model calibration as presented in Table 2.3. They then developed the Shuffled Complex Evolution (SCE-UA) method that is capable of dealing with these main characteristics of the model calibration problem. The SCE-UA is based on four concepts;

- Combination of deterministic and probabilistic approaches
- Systematic evolution of a complex of points spanning the parameter space in the direction of global improvement
- Competitive evolution
- Complex shuffling

A population of solutions is generated and divided into a number of complexes. Each complex evolves independently using the downhill simplex method for a set number of evolutions. The complexes are then shuffled thereby enabling exchange of information among them. If convergence is not reached, a new set of evolutions for each complex is carried out. A more detailed explanation of the method as provided by Duan et al. (1992, 1993) now follows. These two references can be consulted for more details on the derivation and numerical tests of the effectiveness and efficiency of the method.

Table 2.3 Characteristics complicating the optimization problem in hydrological model calibration

1. Regions of attraction	More than one main convergence region
2. Minor local optima	Many small 'pits' in each region
3. Roughness	Rough discontinuous surface with discontinuous derivatives
4. Sensitivity	Poor and varying sensitivity of response surface in region of optimum and non-linear parameter interaction
5. Shape	Non-convex response surface with long curved ridges

2.4.1 Steps of the Shuffled Complex Evolution Algorithm

1. To initialise the process, select $p \geq 1$ and $m \geq n+1$ where p is the number of complexes, m the number of points in each complex, an n is the dimension of the problem (the number of parameters to be optimized). Compute the sample size $s=pm$.
2. Generate the samples as follows. Sample s points $x_1, x_2, \ldots, x_i, \ldots, x_s$ in the feasible space $\Omega \subset R^n$. Compute the function value f_i at each point x_i. In the absence of prior information, use a uniform sampling distribution.
3. Rank the points as follows. Sort the s points in order of increasing function value. Store them in an array $D=\{x_i, f_i, i = 1, \ldots, s\}$, so that $i=1$ represents the point with the smallest function value.
4. Partition D into P complexes $A^1, \ldots, A^p$, each containing m points, such that
$$A^k = \left\{ x_j^{\,k}, f_j^{\,k} \,\middle|\, x_j^{\,k} = x_{k+p(j-1)}, f_j^{\,k} = f_{k+p(j-1)}, \qquad j = 1,\ldots,m \right\}$$
5. Evolve each complex $A^k, k=1,\ldots, p$, according to the competitive complex evolution (CCE) algorithm outlined below.
6. Shuffle the complexes as follows. Replace $A^1, \ldots, A^p$ into D, such that $D=\{A^k, k=1, \ldots, p\}$. Sort D in order of increasing function value.
7. Steps 1 to 6 consist of an epoch of the optimization. At this stage a convergence check is made. If the convergence criteria are satisfied, stop; otherwise return to step 4.

Following is the competitive complex evolution (CCE) algorithm required to evolve each complex in step 5 of the SCE algorithm.

1. To initialize the process, select q, α, and β, where $2 \leq q \leq m$, $\alpha \geq 1$ and $\beta \geq 1$.
2. Assign weights as follows. Assign a trapezoidal probability distribution to A^k, i.e.,
$$\rho_i = \frac{2(m+1-i)}{m(m+1)}, \qquad i = 1,\ldots,m$$
The point $x_1^{\,k}$ has the highest probability $\rho_1=2/(m+1)$ and the point $x_m^{\,k}$ has the lowest probability $\rho_m=2/m(m+1)$.
3. Select parents by randomly choosing q distinct points $u_1, \ldots, u_q$ from A^k according to the probability distribution specified above. The q points define a 'subcomplex'. Store the points in

array $B=\{u_i,v_i,\ i=1,\ldots q\}$ where v_j is the function value associated with point u_j. Store in L the locations of A^k which are used to construct B.

4. Generate offspring according to the following procedure:
    a. Sort B and L so that the q points are arranged in order of increasing function value and compute the centroid g using the expression $g = \frac{1}{q-1}\sum_{j=1}^{q-1} u_j$
    b. Compute the new point $r=2g-u_q$ (reflection step).
    c. If r is within the feasible space Ω, compute the function value f_r and go to step d; otherwise compute the smallest hypercube $H \subset R^n$ that contains A^k, randomly generate a point z and set $f_r=f_z$ (mutation step).
    d. If $f_r < f_q$, replace u_q by r, go to step f; otherwise compute $c=(g+u_q)/2$ and f_c (contraction step).
    e. If $f_c < f_q$, replace u_q by c, go to step f; otherwise randomly generate a point z within H and compute f_z (mutation step). Replace u_q by z.
    f. Repeat steps a to e α times where $\alpha \geq 1$ is a user-specified parameter.
5. Replace parents by offspring as follows: Replace B into A^k using the original locations stored in L. Sort A^k in order of increasing function value.

Iterate by repeating steps 2 to 5 β times, where $\beta \geq 1$ is a user-specified parameter which determines how many offspring should be generated or how far the complex should evolve.

Suitable values for the user specified parameters as a function of the number of parameters to optimize as recommended by Duan et al., 1994 are; $m=(2n+1)$, $q=(n+1)$, $\alpha=1$ and $\beta=(2n+1)$. Using these values leaves the number of complexes p as the only variable that needs to be specified.
The flow charts for the SCE-UA and the CCE algorithm as given by Duan et al., 1992 are presented in Figure 2.4 and 2.5 respectively.

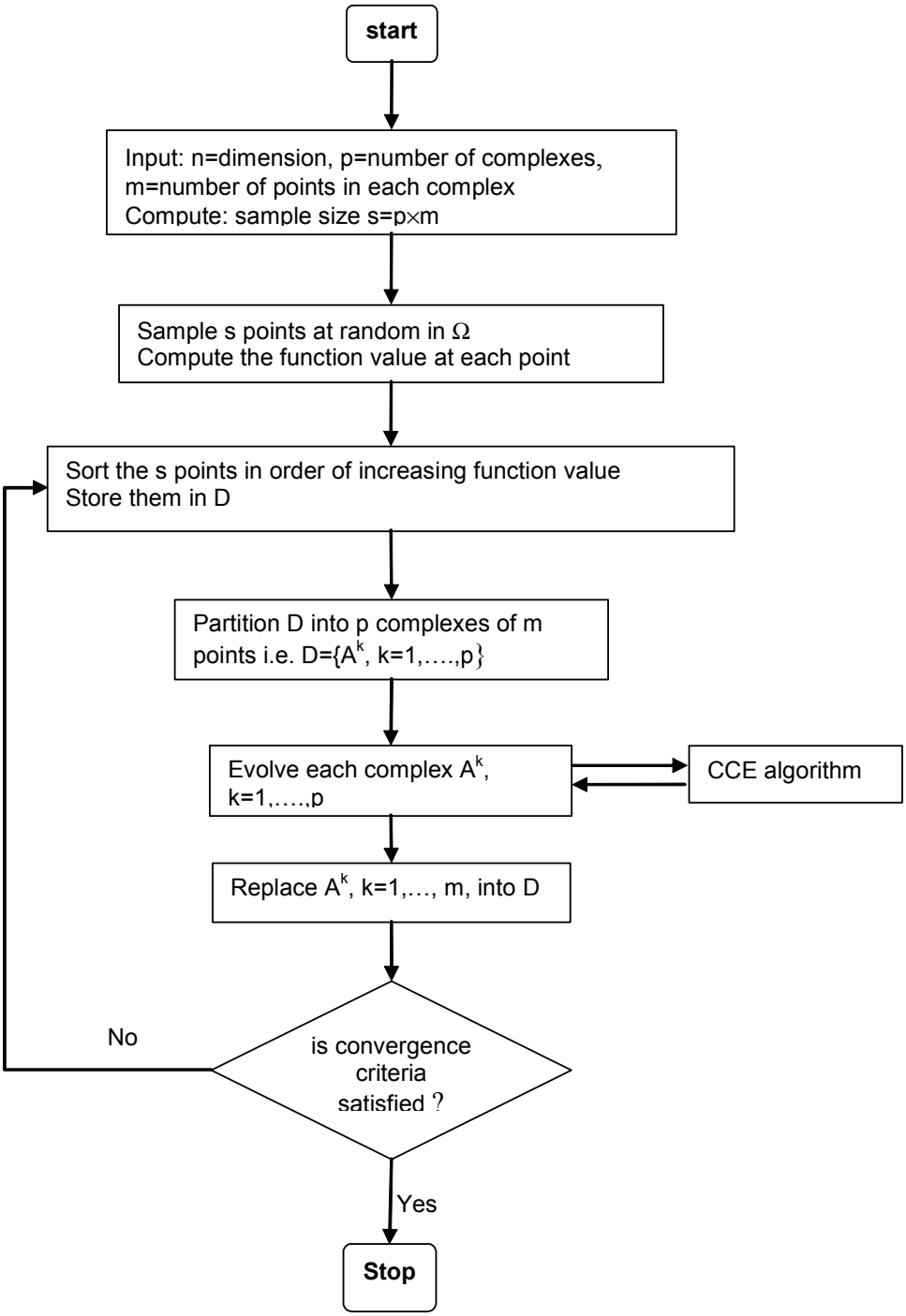

Figure 2.4 Flow chart of the shuffled complex evolution (SCE-UA) method

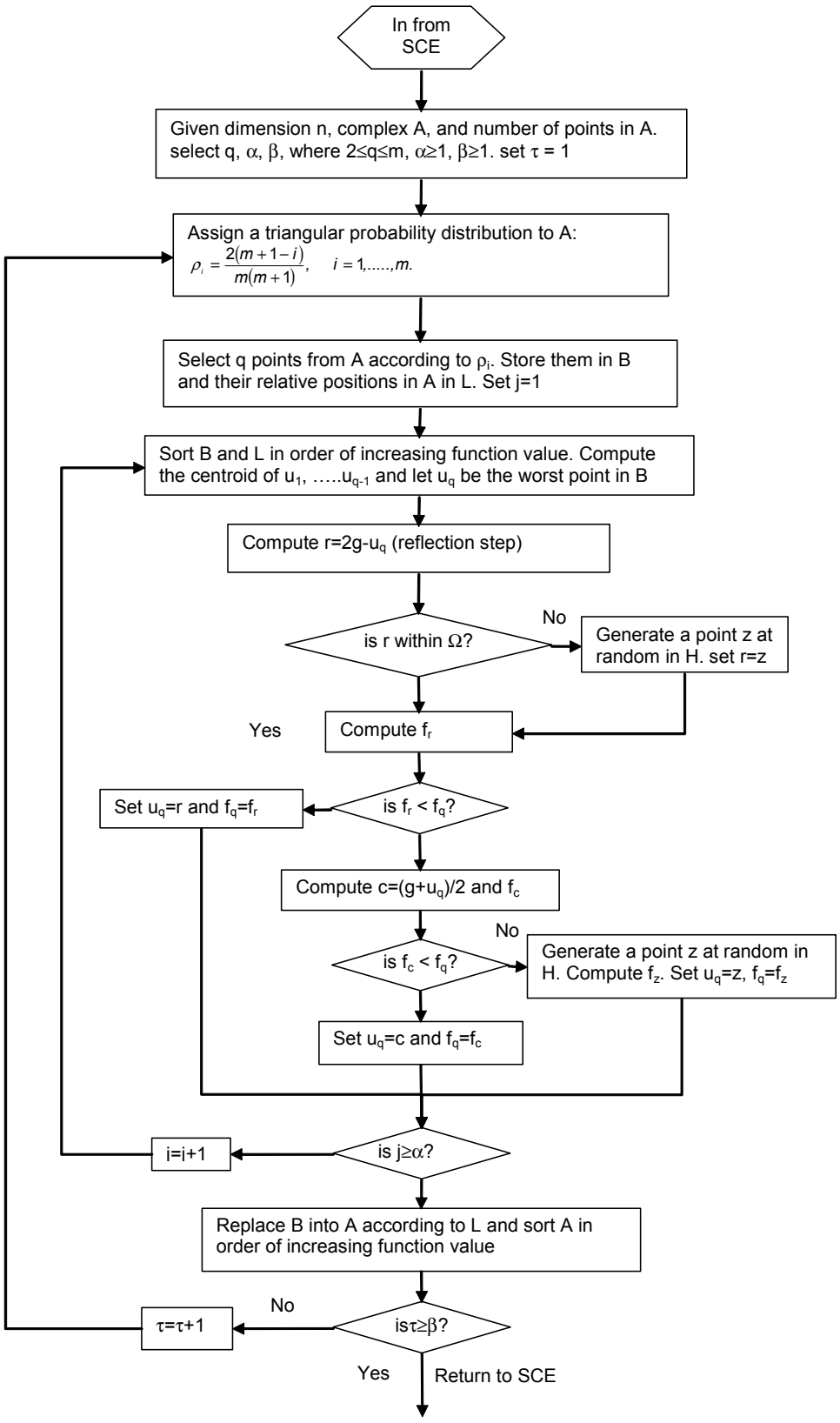

Figure 2.5 Flow Chart of the competitive complex evolution (CCE) algorithm

2.5 Comparative studies and applications of the SCE-UA method

The SCE-UA has arguably become the most popular method for the automatic calibration of hydrological models and has consistently proved to be more efficient and effective than many other

methods in numerous studies. Table 2.4 provides a summary of some of these studies. In Table 2.5, a sample of some of the recent applications of the SCE-UA method is provided.

The SCE-UA was developed for the optimization of a problem consisting of a single objective function and variants of the optimizer to handle multiple objectives and parameter uncertainty have also been developed. A brief discussion of these developments is presented in the next Section.

2.6 Further developments of the SCE-UA Method

Yapo et al. (1998) modified the SCE-UA to deal with multiobjective problems using the concept of Pareto dominance described in Section 2.3.2. The resulting method, called the Multiobjective Complex Evolution (MOCOM-UA) has been tested on several problems and been found to be an effective method of obtaining Pareto solution sets (Gupta et al., 1998; Boyle et al., 2000; Xia et al., 2002). These and other applications of MOCOM-UA however revealed some weaknesses pointed out by Vrugt et al. (2003b). MOCOM-UA had the tendency not to explore the search space adequately for the Pareto solutions and tended to obtain these in a cluster. The method also converged prematurely in some cases especially those involving large numbers of parameters and where the different objective functions were strongly correlated. Vrugt et al. (2003b)) incorporated the following two techniques into MOCOM-UA to deal with these problems.

- The modified Strength Pareto dominance approach (Zitler and Thiele, 1999) as described in Section 2.3.2
- The Metropolis algorithm (Metropolis et al., 1953)

The resulting method, entitled the Multiobjective Shuffled complex Evolution Metropolis (MOSCEM-UA) algorithm was found to improve the identification of the Pareto front significantly.

Vrugt et al. (2003a) developed the Shuffled Complex Evolution Metropolis (SCEM-UA) Algorithm, a method closely related to MOSCEM-UA for identifying the posterior distribution of calibrated parameters and Vrugt et al. (2004) used the SCEM-UA to calibrate a physically based hydrological model of the vadose zone.

Nittin and Liong (2004) modified the SCE-UA method by specifying initial starting points instead of using a randomly generated initial population. This method was found to improve performance for theoretical functions of few decision variables but no improvement was obtained for the two 10 decision variable functions.

2.7 Choice of calibration method

Pitman model calibration is a multiobjective function problem, and looking into the future, it is possible that additional objectives will be required if water quality modelling gets incorporated into the WRSM 2000 system. Out of the 4 possible calibration methods; the original SCE-UA, the MOCOM-UA, the SCEM-UA and the MOSCEM-UA, MOSCEM-UA is the one best suited for the situation. However, it is possible to use SCE-UA if the objective function aggregation method (Section 2.3.1) is adopted. The use of the original SCE-UA with the possibility of incorporating the objective function aggregation method to handle multiple objectives was considered the best balance of complexity and applicability

that would best meet the objectives of this project. This also allows for updated to the other more complex approaches when the demand for this arises.

Table 2.4 Comparative hydrological model calibration studies involving the SCE-UA method

Reference	Brief description	Calibration methods compared	Results
Abdulla et al. (1999)	Estimation of 4 baseflow parameters of the ARNO model to historical data	SCE-UA, simplex (SX), simulated annealing (SA)	SCE-UA was found to be less sensitive to the changes in seed random generator and the specified bounds of the parameters.
Cooper et al. (1997)	Calibration of the TANK model	SCE-UA, Genetic algorithm (GA), Simulated annealing (SA)	SCE-UA provided better estimates of the global optimum than GA and SA, SCE-UA used fewer function evaluations than GA and SA
Duan et al. (1992)	Calibration of the 6 parameter SIXPAR model for a theoretical case with known global optimum	SCE-UA, Multistart simplex (MSX), Simplex method (SX), Adaptive random search (ARS)	Both SCE-UA and MSX located global optimum consistently, SCE-UA 3 times more efficient than MSX, SX obtained a 65% success rate, ARS consistently failed to locate optimum.
Franchini et al. (1998)	Calibration of the ADM model for a simple and a complex catchment. For both a theoretical case with known global optima and a real world case with historical data case were applied	SCE-UA, Genetic algorithm coupled with sequential quadratic programming (GA-SQP), Pattern search coupled with sequential quadratic programming (PS-SQP)	SCE-UA most reliable in locating global optimum of single basin and also more consistent for the real-world case. For the complex basin, none of the methods located the global optimum but the SCE-UA was closest. SCE-UA obtained more stable parameters than the other methods.
Gupta et al. (1999)	Calibration of the Sacramento soil moisture accounting model, 13 parameters calibrated	SCE-UA, Multilevel expert calibration	SCE-UA obtained calibrations comparable to that of a well-trained hydrologist using multilevel expert calibration.
Kuczera (1997)	Calibration of the 6-parameter MSFB model using historical data	SCE-UA, Genetic algorithm (GA)	SCE-UA obtained better objective functions and more consistent parameter sets
Sorooshian et al. (1993)	Calibration of SAC-SMA model,13 parameters, one case theoretical with known global optimum, other case with historical data	SCE-UA, Multistart simplex (MSX)	SCE-UA located the global optimum for all 10 runs of the theoretical case, the MSX failed in all. SCE-UA obtained better and more consistent parameters for historical data case with a third fewer function evaluations.
Thiemann et al. (1998)	Calibration of the GR3 model, 7 parameters were to be obtained	SCE-UA, global gradient search method (Globex)	SCE-UA was significantly superior to Globex in effectiveness and efficiency
Thyer et al. (1999)	Calibration of the 6 parameter SFB model using historical data.	SCE-UA, simulated annealing (SA-SX)	For low-yielding catchments, SCE-UA was twice as robust. For high yielding catchments, the SCE-UA was 6 times more efficient than SA-SX

Table 2.5 Some applications of the SCE-UA method

Reference	Description
Ajami et al. (2004)	Calibration of a semi-distributed version of the SAC-SMA model to investigate the level of detail required for optimal streamflow estimation along a river system.
Bandaragoda et al. (2004)	Calibration of parameter multipliers of TOPNET, a networked version of the TOPMODEL.
Bell et al. (2002)	Optimization of the parameters of a contaminant transport model applied for assessing landfill liner design.
Brath et al. (2004)	An investigation of the effect of data length and raingauge network density on calibration performance using a distributed catchment model.
Cheng and Wang (2002)	Calibration of a linear reservoir flood model to evaluate the hydrological effects of urbanization
Contractor and Jenson (2000)	The calibration of a finite element groundwater flow model to minimize the difference between simulated and observed water levels.
Di Luzio and Arnold (2004)	Calibration of a physically based distributed model Soil and Water Assessment Tool (SWAT) to investigate improvements through the use of high precision gridded precipitation data.
Duan et al. (1994)	An investigation of how the algorithmic parameters of the SCE-UA affect its performance and development of guidelines for the selection of suitable values of these.
Eckhardt and Arnold (2001)	Calibration of the SWAT (Soil and Water Assessment Tool) for a mesoscale catchment
Eusuff and Lansey (2004)	Calibration of groundwater flow modelling tools MODFLOW, MTD3 and MODPATH in the development of a soil-aquifer treatment (SAT) management model that may be applicable where recharged wastewater effluent may be used for potable consumption in water stressed conditions.
Hsieh and Wang (1999)	Calibration of a semi-distributed parallel-type linear rainfall-runoff flood model
Lee and Wang (1998)	Calibration of a 'coloured noise' model.
Liong et al. (2001)	Calibration of the Storm Water Management Model (SWMM) for a 6 km^2 catchment.
Madsen (2000)	Multiobjective calibration of the MIKE11/NAM catchment model
Mertens et al. ,(2004)	Calibration of the MIKE SHE model for a 80 m $\times$20 m hillslope
Scott et al. (2000)	Calibration of the physically based, variable saturated flow model HYDRUS to model multiyear observations of soil moisture recharge.
Senarath et al. (2000)	Calibration of the physically based two-dimensional distributed Hortornian model CASC2D to investigate the benefits of continuous rather than event-based calibration.
Van Griensven and Bauwens (2003)	Multiobjective calibration of the ESWAT catchment model of river quantity and quality.
Yapo et al. (1996)	An investigation of length of data on parameter identification.

3 DEVELOPMENT OF THE SCE-UA CALIBRATION SOFTWARE

3.1 Linking the SCE-UA optimizer and the catchment simulation model

The SCE-UA algorithm as described in Section 2.4 was coded using Microsoft PowerStation Fortran, debugged and tested extensively using several optimization problems including the 10 parameter griewank function that Duan et al. (1993) had applied and the daily IHACRES rainfall runoff model (Jakeman and Hornberger, 1993). After the code was considered to be free from bugs, it was then modified to allow for its application for the automatic calibration of any catchment model without the need to re-code the optimizer. Minimal coding of the catchment model to be calibrated would typically be required to allow the exchange of information between the model and the optimizer using text files. The method to do this is described here and also in the example on the software (in the accompanying CD-ROM). The optimizer generates parameter sets for the model that the model needs to use while the model simulates the catchment and computes an objective function that the optimizer needs. For the purpose of recording the final parameter sets and model simulation using the final parameter set in calibration and validation, the model needs to know when the optimizer has completed calibration. This is accomplished by including the **mode** that indicates whether;

the optimizer is still in the process of calibrating (mode=Calibrating),

calibration is complete and the final parameters values can be used for a final simulation using the calibration data set (mode=CalibrationResult)

calibration is complete and the final parameter set is to be used for simulation using a validation data set (mode=ValidationResult).

A text file named '**sceout.txt**' is generated by the optimizer and contains the following information placed in the order indicated.

Mode (Calibrating or CalibrationResult or ValidationResult)

Number of optimization parameters per subcatchment (nps)

Number of subcatchments (ncas)

Parameter values for all subcatcments (PV(i,j)) for i=1to ncas and j=1 to nps

As an example, suppose a 3 parameter model with 2 sub catchments is being calibrated and the optimizer has obtained the following values for the first and second sub catchment respectively: PV(1,1)=0.5, PV(1,2)=0.6,PV(1,3)=200, PV(2,1)=0.8,PV(2,2)=0.9, PV(2,3)=600. In the calibrating mode, file '**sceout.txt'** will contain the following information/data with each data placed in each column.

Calibrating

3

2

0.5

0.6

200

0.8

0.9

600

This information is then obtained by the catchment simulation model for a single run. This run generates a single objective function value that is dropped to a file called '**objective.txt'**. This file contains only this single objective function value. This objective function value is then picked up by the optimizer as the value corresponding to the parameter data set that the optimizer had dropped in file '**sceout.txt'**. The files '**sceout.txt'** and **'objective.txt'** need to be closed at every step (in every simulation).

As the modeller may be calibrating several catchments with the same model, the selection of calibration and validation data is done using the calibrator. Once this selection is done, the calibrator creates a text file named **'DataFiles.txt'** containing the full name (including the extension) of the calibration data file on the first row and the validation data file on the second row. The catchment simulation model needs to open this file and read the names of the calibration data and validation data file. Figure 3.1 illustrates how the link is established.

The linkage requires the catchment simulation model to be placed in a subdirectory named '***Model***' located in the '*sce*' directory where the GUI application '**SCE.exe'** is placed. The optimizer allows up to 20 randomly initialised calibrations of the same catchment.

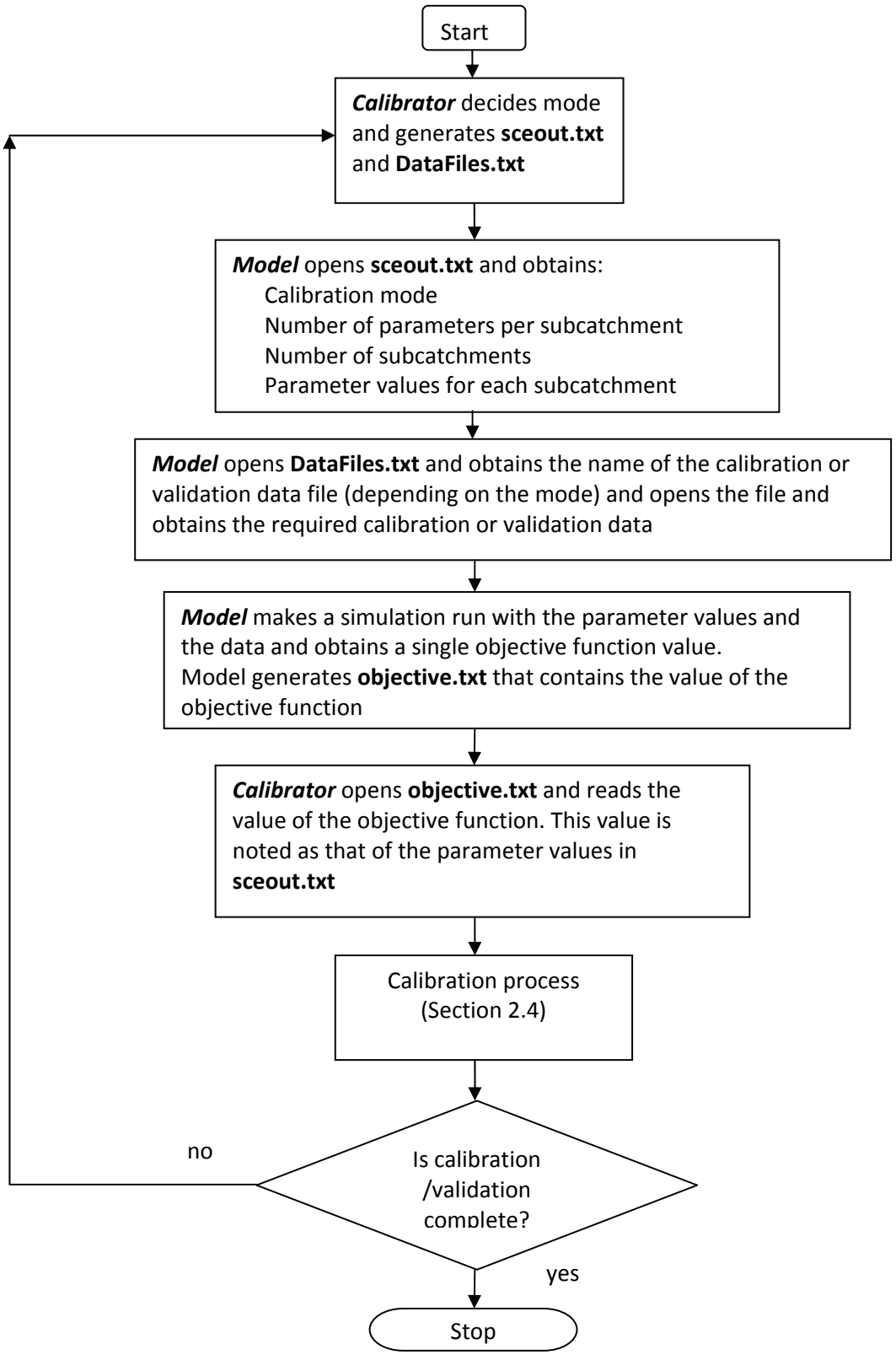

Figure 3.1 Linking the calibrator and the catchment model

3.2 The graphical user interface of the SCE-UA optimizer

The SCE-UA optimizer was coded in Fortran while the GUI was coded in Delphi. There are many features included in the GUI to ease the calibration process and these would be best understood by actually running the calibrator. An example showing the main steps in installing and applying the

calibrator in detail is provided on the 'help' menu of the software and the main features are also described here. The initial window shown as Figure 3.2 allows the modeller to;

- Create or edit optimization data of an existing catchment (a catchment that has already been calibrated and is on the database)
- Create or edit parameter ranges for an existing catchment (Figure 3.3)
- Run the calibrator
- View the calibration results (Figure 3.4)
- View the objective function values from the multiple calibrations (Figure 3.5).
- Export the optimization data, the parameter ranges, the calibrated parameters and the objective function values to a comma separated variables (*.csv) file.
- Create a new catchment
- Delete a catchment
- Copy a catchment
- Rename a catchment

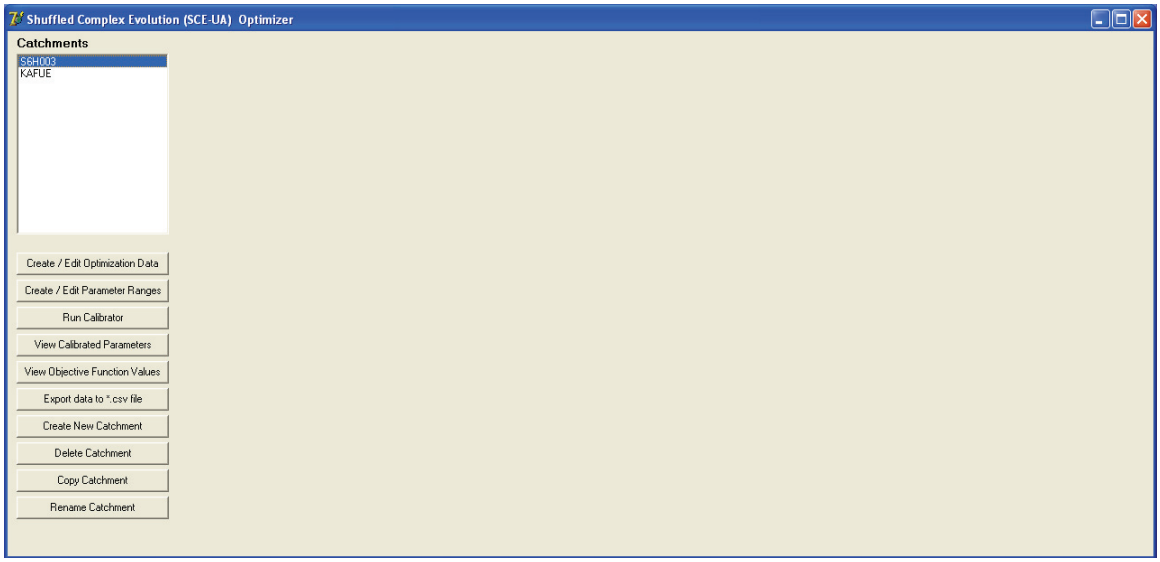

Figure 3.2 The main GUI of the SCE-UA optimizer

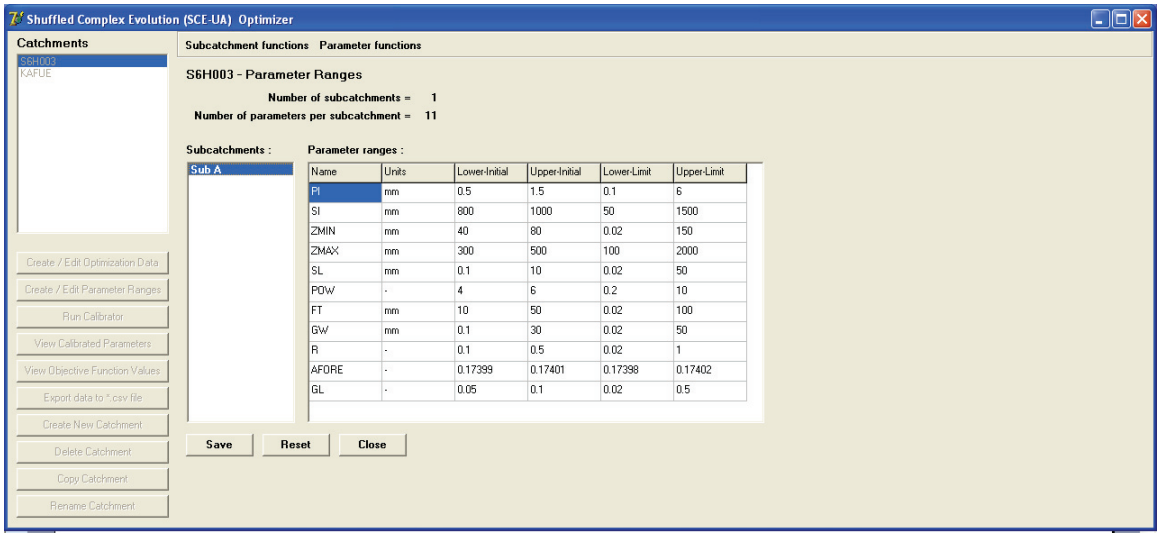

Figure 3.3 Entry of parameter ranges

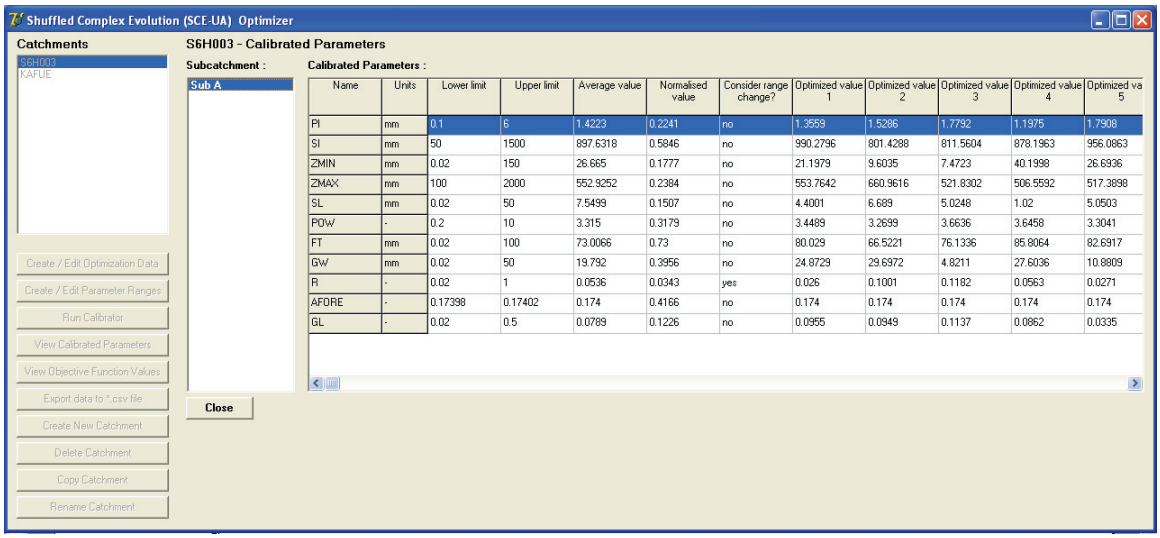

Figure 3.4 Viewing of calibrated parameter values

The calibrator requires the entry of two parameter search ranges as seen on Figure 3.3. The initial search ranges allow the modeller to select suitable starting parameters depending on available experience and judgement while the search range limits provide the limits beyond which search is not allowed for the particular set of runs. If the calibrated parameters from multiple runs are consistently close to one of the parameter range limits, this may indicate that the range needs to be extended if this makes physical/hydrological sense. If the average parameter value is located within 5% of the lower or the upper boundary, the 'Consider range change' column (see Figure 3.4) records 'yes'. The ratio of the lowest to the highest objective function value obtained from multiple runs gives an idea of how sufficient the optimization and is given as an additional output as seen on Figure 3.5. If this ratio is close to unity, then it is likely that the optimization was adequate and no rerun needs to be done with other SCE-UA optimization parameters. If not, then a rerun with new optimization parameters that are likely to optimize more thoroughly may help improve the calibration.

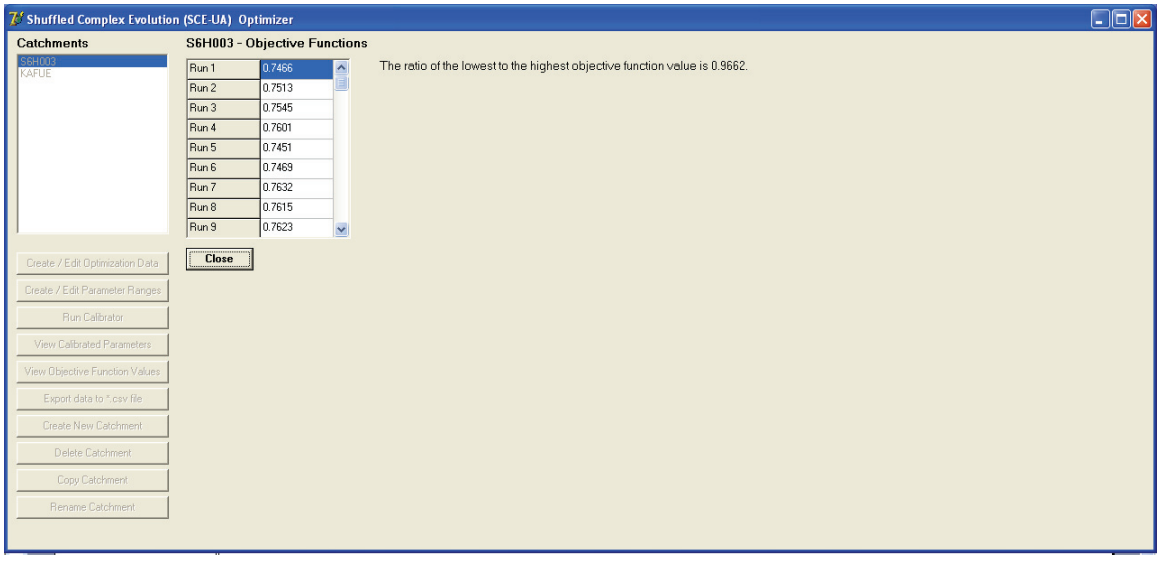

Figure 3.5 Objective function values from multiple calibration runs

4 AUTOMATIC CALIBRATION OF THE PITMAN MODEL AND COMPARISON WITH MANUAL CALIBRATION

4.1 Introduction

This Chapter reports on the automatic calibration of the Pitman model and comparison of automatic and manual calibration. The potential dangers of automatic calibration are investigated by finding whether unrealistic parameter values are obtained and by visual assessments of the simulated time series'. In addition, a study of the simulate soil moisture time series for one of the three test basins is carried out. Although the initial thought was to actually model the catchments manually (by modellers having varying levels of experience) as part of this research, it was found more practical to use catchments that had been previously calibrated manually using the Pitman model. The following three catchments that had been calibrated (or whose calibration had been guided) by highly experienced modellers were selected for the comparison.

- The Buffelspruit River catchment in Mpumalanga province in South Africa that had been calibrated by Hughes (2004).
- The Kafue basin in Zambia that had been calibrated by Mwelwa (2004).
- The Amatole basin in the Eastern Cape province of South Africa that had been calibrated by Kleynhans (2007)
-

The SPATSIM version of the Pitman model (Hughes, 2004) had been applied for Buffelspruit River and Kafue Basin while the WRSM2000 version of the Pitman model had been used for the Amatole basin. The Pitman model that was used for automatic calibration had been obtained in 1999 from Dr V W Pitman, the developer of the Pitman model. The SPATSIM version of the Pitman model includes modifications to the rainfall variability and canopy interception and modifications to improve groundwater modelling have lately been included (Hughes, 2004). Although the WRSM 2000 version of the model was expected to be identical to the version applied in automatic model calibration, some unexplained differences in the flows generated by identical parameter sets were observed. It was therefore not possible to use completely identical models as neither the STATSIM nor the WRSM 2000 versions were available for automatic calibration. The differences among the three versions of the Pitman model imply that the comparison was not perfect but these differences were not considered significant enough to invalidate the comparisons. The calibration of Kafue basin (Mwelwa, 2004) initially searched for parameter values using a genetic algorithm and then searched for them manually. This calibration can therefore be considered a combination of automatic and manual calibration.

Buffelspruit catchment was calibrated as a single catchment while 7 subcatchments located on the north east of Kafue basin were calibrated simultaneously. Three subcatchments of Amatole located in separate areas within the basin were each modelled as a single catchment. Sections 4.2, 4.3 and 4.4 present the analysis for Buffelspruit, Kafue and Amatole basin respectively while Section 4.5 summarises the Chapter by discussing the potential dangers, challenges and advantages of automatic calibration.

4.2 Calibration of the Buffelspruit Basin

According to Hughes (2004), the 581 km^2 Buffelspruit catchment has an undulating terrain with moderate to deep sandy loams developed on quartizites and shales in the upper parts and on metamorphosed migmatite and gneiss in the lower areas. There also exists a narrow band of dolomites of high storativity and transmissivity in the middle of the basin. The remaining area is however underlain by a fractured rock aquifer of low storativity and transmissivity. The mean annual rainfall is 870 mm and the annual potential evaporation is about 1400 mm. The basin is relatively still natural with low irrigation levels and a few farm dams that were ignored in the analysis. Twenty nine years of streamflow data from 1971 to 1999 was applied in the current analysis. This data was obtained from the Department of Water Affairs and Forestry (DWAF). DWAF also provided the potential evaporation data while the rainfall data was obtained from Lynch (2004).

All 11 parameters of the Pitman model presented in Table 2.1 were calibrated and the 29 years (348 months) of data was divided into two parts; one 180 months (1971 to 1985) and the other 168 months (1986 to 1999) long. Each of these in turn acted as the calibration and validation data. The initial and final search ranges for the parameters were subjectively selected using the available knowledge on the expected ranges in the literature. The SCE-UA parameter selection presented on Table 4.1 was based on the guidelines by Duan et al. (1994) while the search termination parameters were selected based on the experience gained with the SCE-UA and other evolutionary optimization methods. Ten randomly initialised calibration runs were then made and the optimized parameter values analysed to find if some of the parameters were consistently at the boundary of the search range limits. If this happened, the search range for the specific parameters was increased and the 10 calibration runs repeated. The objective of the calibration was to minimize the coefficient of mean absolute deviation of monthly (CMAD) defined as

$$CMAD = \frac{\sum_{i=1}^{n} \left| q_i^{sim} - q_i^{o} \right|}{\sum_{i=1}^{n} q_i^{o}} \qquad 4.1$$

where q_i^{sim} and q_i^{o} is the simulated and the observed monthly flow respectively and *n* is the number of months of analysis.

Table 4.1 SCE-UA optimization and search termination parameters for Buffelspruit Catchment

Description of parameter and [recommended value]	Notation	value
number of decision variables	n	11
number of complexes	p	10
number of points in each complex [m>=n+1, m=2n+1]	m	23
sample size = pm	s	230
number of points to select in complex [2<=q<=m] use q=n+1	q	12
optimization parameter [α>=1] use α=1	alp	1
optimization parameter (β>=1) [β=2n+1] - use β=n	bet	11
maxepoch = maximum number of epochs for termination	maxepoch	100
change in epoch objective function prompting termination	conv	0.02
spacing of epochs in checking for convergence	iconv	10

Tables 4.2 and 4.3 present the optimised parameter values and parameter search range limits for each of the 10 calibration runs. All the parameter values were considered realistic. The objective function values for the 10 runs (see Tables 4.2 and 4.3) were almost identical suggesting very effective optimization. It was also observed that the simulated time series for both calibration and validation were practically identical for the multiple runs providing additional evidence that the global optimum was practically obtained for all the runs. Figures 4.1 and 4.2 show the variation of the optimized parameter values for the two calibrations scaled to take values in the range 0 to 1 within the respective search range limits while Figures 4.3 and 4.4 scale the individual parameter values by the respective averages from the 10 runs. Figures 4.3 and 4.4 are considered to provide a less subjective assessment of parameter identification as the computation involved does not include the subjectively selected parameter range limits. It is observed from Figures 4.3 and 4.4 that parameters ST, ZMAX, POW and FT are identified much more closely than the other parameters. This result can be used to reduce the number of parameters to calibrate in catchments that are hydrologically similar to Buffelspruit. Figure 4.5 illustrates the correlation between SL and FT for the first period (1971 to 1985).

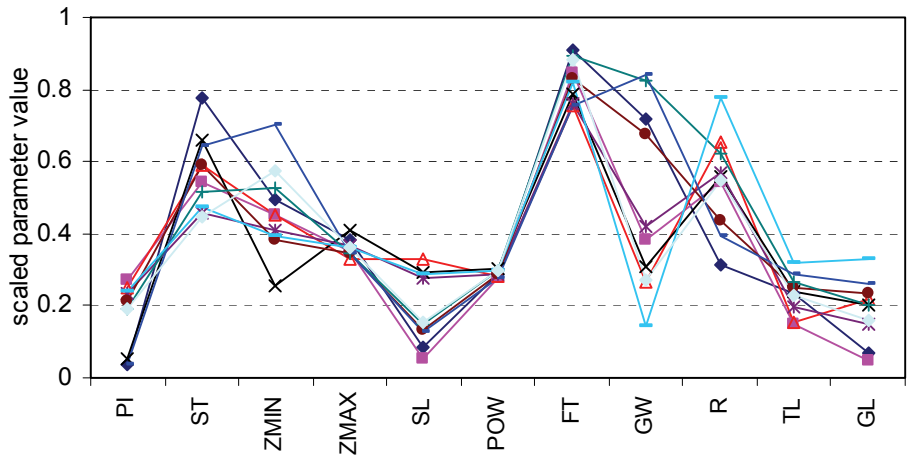

Figure 4.1 Scaled parameter values for Buffelspruit catchment (1971 to 1985).

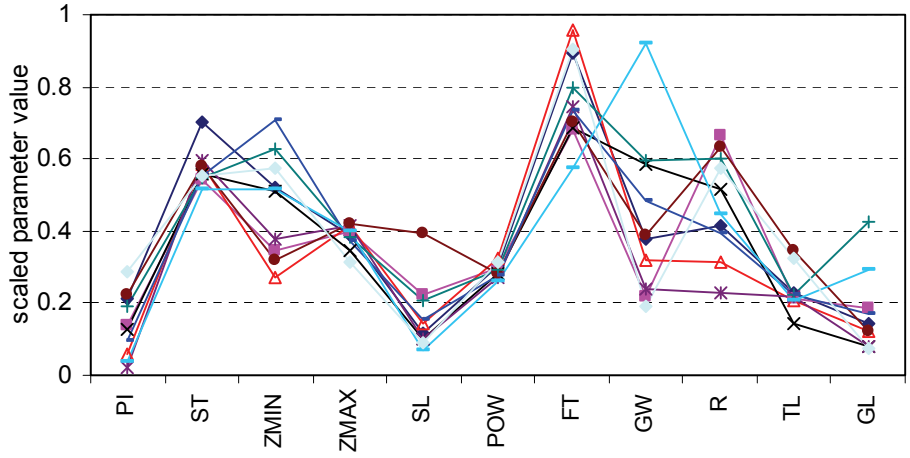

Figure 4.2 Scaled parameter values for Buffelspruit catchment (1986 to 1999).

Table 4.2 Parameter values for 10 randomly initialized calibrations for Buffelspruit catchment – 1971 to 1985

Run	n-epoch[1]	n-sim[2]	Objective function	PI (mm)	ST (mm)	ZMIN (mm)	ZMAX (mm)	SL (mm)	POW	FT (mm)	GW (mm)	R	TL (months)	GL (months)
1	3	1725	0.4182	0.33	1174	74.3	826	4.4	2.99	91	35.9	0.33	0.47	0.35
2	3	1720	0.4118	1.69	833	67.8	766	2.5	2.91	84	19.2	0.55	0.30	0.25
3	3	1699	0.4265	1.56	905	67.7	723	16.5	2.95	76	13.3	0.66	0.31	1.10
4	3	1703	0.4046	0.41	1007	38.1	875	14.7	3.18	79	15.6	0.57	0.48	1.03
5	3	1704	0.4112	1.49	716	61.5	793	13.7	3.03	76	20.9	0.58	0.39	0.77
6	3	1720	0.4079	1.37	906	57.5	752	6.6	3	83	33.8	0.45	0.50	1.18
7	3	1713	0.4106	1.22	795	78.7	759	7.6	3.12	89	41.2	0.63	0.53	1.04
8	3	1703	0.4186	0.31	984	105.5	756	6.3	2.93	75	42	0.40	0.58	1.33
9	3	1709	0.4148	1.51	738	59.0	792	14.4	3.14	82	7.1	0.78	0.64	1.67
10	3	1729	0.4033	1.23	694	86.0	783	7.7	3.13	88	13.6	0.56	0.46	0.81
Parameter search range limits		lower limit		0.1	50	0.0002	100	0.0002	0.2	0.02	0.02	0.02	1E-07	0.02
		upper limit		6	1500	150	2000	50	10	100	50	1	2	5

[1] n-epoch: number of epochs [2] n-sim: number of simulations

Table 4.3 Parameter values for 10 randomly initialized calibrations for Buffelspruit catchment – 1986 to 1999

Run	n-epoch[1]	n-sim[2]	Objective function	PI (mm)	ST (mm)	ZMIN (mm)	ZMAX (mm)	SL (mm)	POW	FT (mm)	GW (mm)	R	TL (months)	GL (months)
1	3	1713	0.418	1.35	1072	78.4	838	6	3.18	90	19	0.43	0.45	0.74
2	3	1741	0.4008	0.93	837	52.1	857	11.2	3.11	68	11	0.67	0.42	0.94
3	3	1714	0.4104	0.44	897	40.9	890	7.2	3.36	96	15.9	0.33	0.41	0.62
4	3	1709	0.4143	0.85	857	76.5	761	4.9	2.96	69	29.2	0.53	0.29	0.41
5	3	1697	0.4043	0.22	910	56.3	887	5.1	2.86	75	11.9	0.24	0.44	0.42
6	3	1704	0.4023	1.42	890	47.6	894	19.7	2.99	70	19.4	0.64	0.69	0.62
7	4	2251	0.4079	1.25	843	93.8	827	10.4	3.08	80	29.9	0.61	0.45	2.13
8	3	1714	0.4083	0.67	852	106.0	805	7.6	2.92	74	24.1	0.40	0.45	0.88
9	3	1718	0.4052	0.32	799	77.3	854	3.4	2.76	57	46	0.46	0.42	1.49
10	3	1723	0.4151	1.80	851	86.5	700	4.5	3.28	91	9.6	0.59	0.65	0.39
Parameter search range limits		lower limit		0.1	50	0.0002	100	0.0002	0.2	0.02	0.02	0.02	1E-07	0.02
		upper limit		6	1500	150	2000	50	10	100	50	1	2	5

[1] n-epoch: number of epochs [2] n-sim: number of simulations

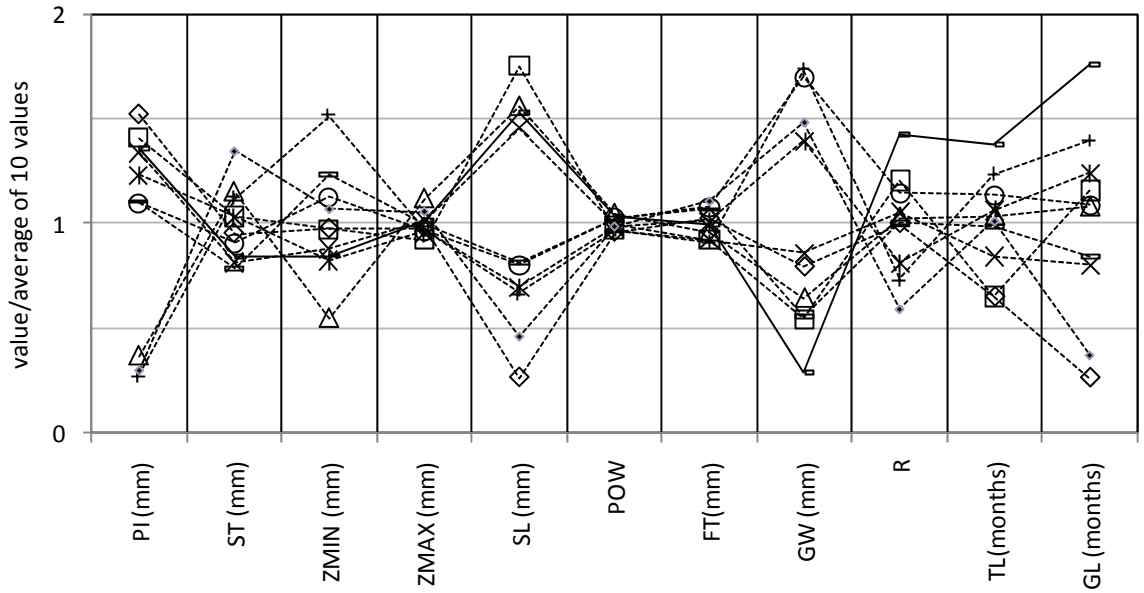

Figure 4.3 Parameter locations from 10 calibration runs of Buffelspruit catchment (1971-85)

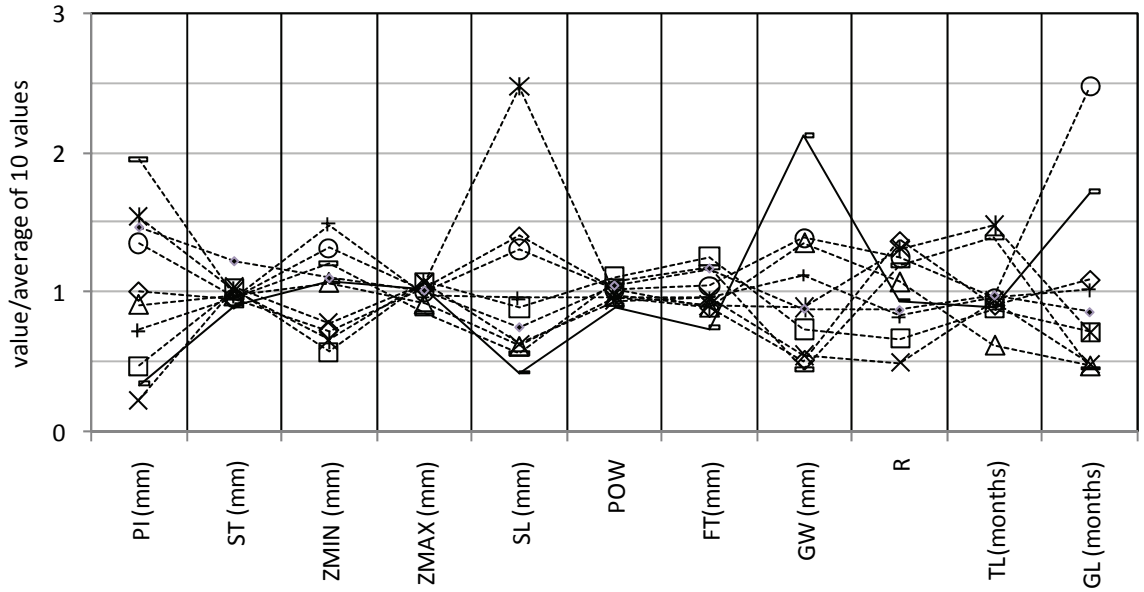

Figure 4.4 Parameter locations from 10 calibration runs of Buffelspruit catchment (1986-99)

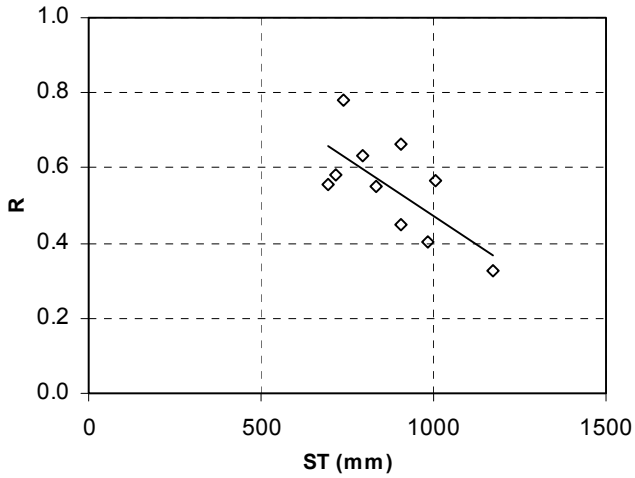

Figure 4.5 Correlation between parameters ST and R for Buffelspruit catchment (1971 to 1985).

To evaluate the quality of the modelling and the calibration, the Nash and Sutcliffe coefficient of efficiency (CE), the coefficient of determination (R^2), the bias (BIAS), the coefficient of mean absolute deviation (CMAD) and a residual mass curve coefficient (RMCC) were used. The first three are commonly used and need not be defined while CMAD is defined in equation 4.1. The RMCC is defined in equations 4.2 to 4.5.

$$RMCC = 1 - \frac{\sum_{j=1}^{n} \left| q_j^{o\,res} - q_j^{sim\,res} \right|}{\sum_{j=1}^{n} q_j^{o\,res}} \tag{4.2}$$

$$q_j^{o\,res} = \sum_{i=1}^{j} \left(q_i^{o} - \overline{q^{o}} \right) \qquad j = 1,2, \quad ,n \tag{4.3}$$

$$q_j^{sim\,res} = \sum_{i=1}^{j} \left(q_i^{sim} - \overline{q^{sim}} \right) \qquad j = 1,2, \quad ,n \tag{4.4}$$

$$\overline{q^{o}} = \frac{1}{n} \sum_{i=1}^{n} q_i^{o} \qquad and \qquad \overline{q^{sim}} = \frac{1}{n} \sum_{i=1}^{n} q_i^{sim} \tag{4.5}$$

where q_i^{sim} and q_i^{o} is the simulated and the observed flow respectively and *n* is the number of months of analysis. RMCC is designed to quantify the extent of systematic errors in the simulated time series and takes an ideal value of 1.0.

Tables 4.4 and 4.5 present the simulation performance values for both the calibration and validation runs. With the exclusion of the RMCC, the calibration and validation runs gave reasonably close results. The large difference in the RMCC was caused by the large underestimation of a few of the observed flows in the first time series (1971-1985). Therefore, RMCC may be too sensitive to the simulated values in a single or two points and thereby fail to fulfil its intended purpose of quantifying systematic errors. The close calibration and validation results are an indication of the effectiveness of calibration and also of the robustness of the Pitman model. The calibration of the same basin by Hughes (2004) using manual calibration of the SPATSIM version of the Pitman model obtained a CE of 0.200 and a CD of 0.434 with normal flows and 0.660 and 0.674 for log transformed flows. The results obtained here, with the overall average CE and CD of 0.559 and 0.755 f

Representative time series comparing the observed and the simulated flows and the separation of the simulated flows into surface runoff and slow flow (baseflow) are presented in Figures 4.6 and 4.7.

Table 4.4 Calibration and validation performance with the first period (1971-1985) used for calibration

Run	Calibration (1971-1985)					Validation (1986-1999)				
	CE	R^2	BIAS	CMAD	RMCC	CE	R^2	BIAS	CMAD	RMCC
1	0.554	0.75	-0.019	0.363	0.11	0.558	0.75	0.052	0.37	0.44
2	0.569	0.761	-0.031	0.354	0.089	0.577	0.761	0.034	0.364	0.467
3	0.536	0.738	-0.054	0.36	0.07	0.558	0.748	0.009	0.366	0.51
4	0.553	0.749	-0.058	0.352	0.073	0.567	0.755	0.004	0.354	0.518
5	0.559	0.764	-0.122	0.348	0.074	0.569	0.762	-0.078	0.351	0.504
6	0.548	0.746	-0.078	0.352	0.086	0.55	0.746	-0.025	0.36	0.459
7	0.578	0.762	-0.011	0.354	0.081	0.576	0.763	0.05	0.363	0.481
8	0.538	0.744	-0.079	0.355	0.087	0.559	0.748	-0.022	0.362	0.502
9	0.577	0.763	-0.019	0.356	0.066	0.586	0.768	0.045	0.362	0.515
10	0.587	0.773	-0.075	0.346	0.085	0.58	0.764	-0.029	0.353	0.475
Average	0.559	0.755	-0.057	0.354	0.082	0.568	0.757	0.004	0.361	0.487

Table 4.5 Calibration and validation performance with the second period (1986-1999) used for calibration

Run	Calibration (1986-1999)					Validation (1971-1985)				
	CE	R^2	BIAS	CMAD	RMCC	CE	R^2	BIAS	CMAD	RMCC
1	0.537	0.761	-0.131	0.361	0.497	0.489	0.759	-0.179	0.359	0.101
2	0.576	0.764	-0.061	0.347	0.545	0.542	0.757	-0.116	0.35	0.063
3	0.557	0.758	-0.075	0.352	0.461	0.568	0.766	-0.116	0.35	0.093
4	0.553	0.747	-0.047	0.358	0.514	0.536	0.743	-0.1	0.353	0.07
5	0.566	0.756	-0.026	0.355	0.47	0.566	0.761	-0.083	0.349	0.094
6	0.573	0.773	-0.086	0.35	0.542	0.521	0.764	-0.143	0.353	0.072
7	0.577	0.771	-0.07	0.354	0.53	0.535	0.767	-0.124	0.352	0.082
8	0.564	0.761	-0.088	0.357	0.513	0.535	0.762	-0.138	0.353	0.088
9	0.566	0.758	-0.07	0.351	0.534	0.538	0.757	-0.127	0.352	0.069
10	0.55	0.754	-0.103	0.357	0.498	0.526	0.75	-0.143	0.355	0.08
average	0.562	0.760	-0.076	0.354	0.510	0.536	0.759	-0.127	0.353	0.081

The model underestimated many of the high flows both in calibration and validation. The objective function (CMAD) favours the reproduction of high flows and this observation therefore points out to inaccuracies in the data and/or inadequacy of the model structure. The simple least squares objective function, which favours the reproduction of high flows even more, was also applied and gave similar results. The plots of flow separation reveal a very high base flow contribution that averages to 79% of the total flow. This is much higher than those reported by Hughes (2004) (28% by the GW Pitman model and 50% by a digital filter). Comprehensive field tests could reveal which of the three is most realistic but such data is often not available and not easy to obtain. Moreover, a distinct separation of quick and slow flow may not exist in reality.

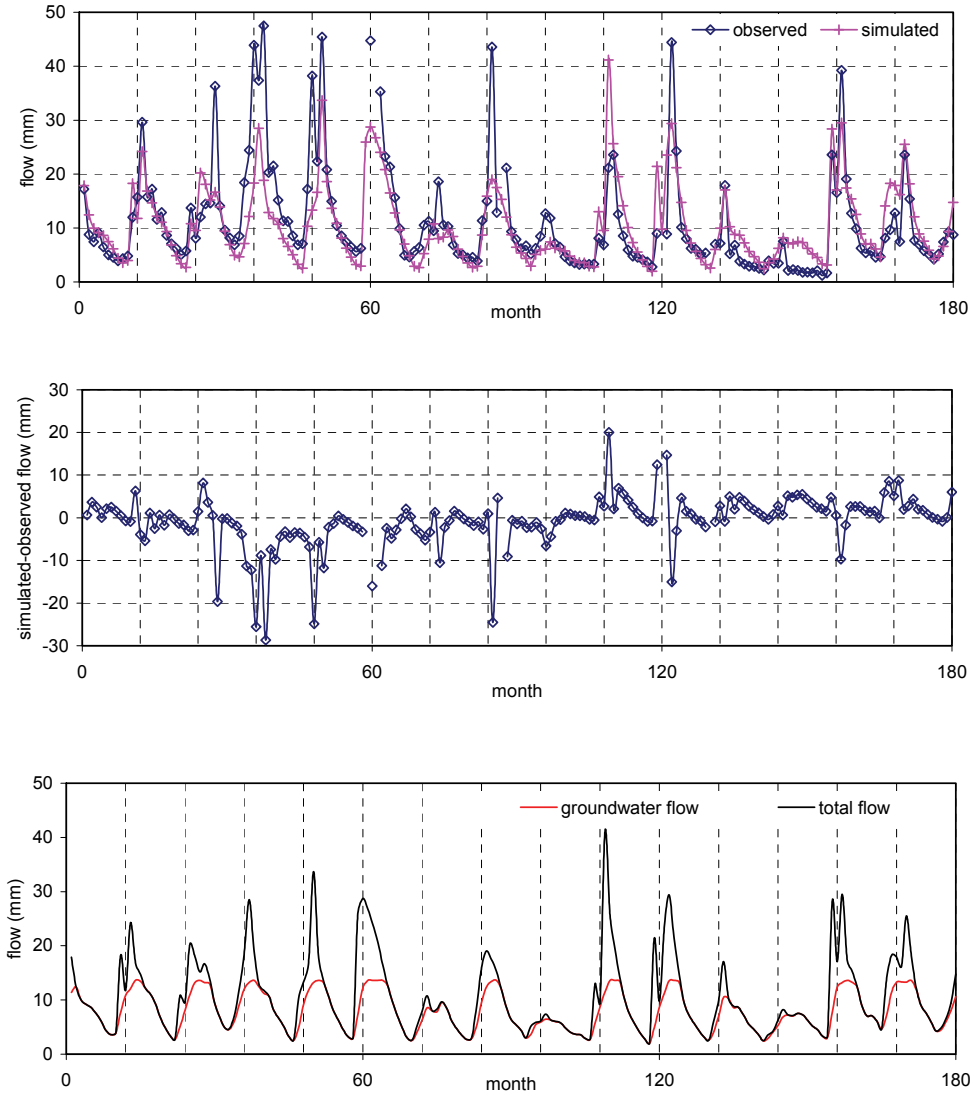

Figure 4.6 Streamflow time series and flow separation for Buffelspruit catchment (1971-1985 calibration)

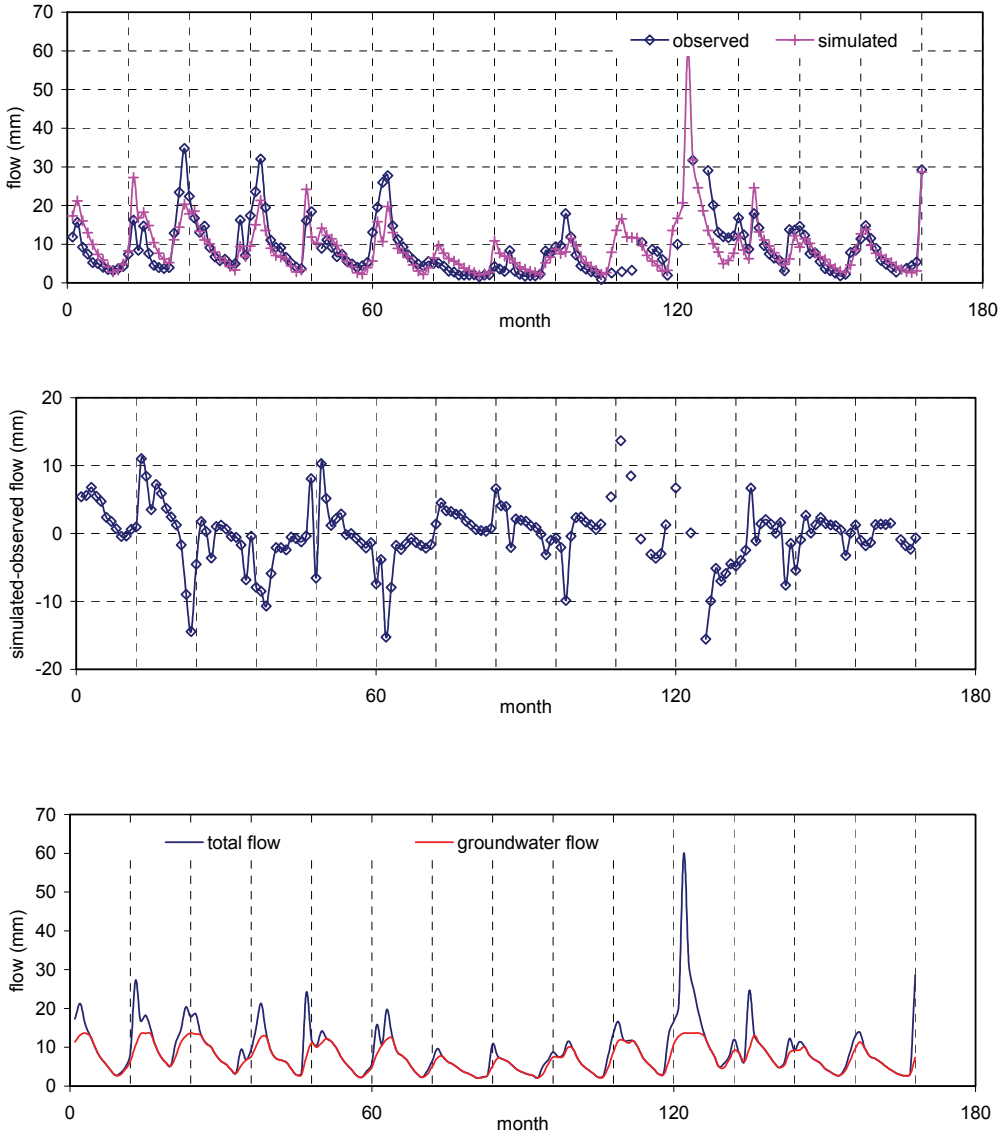

Figure 4.7 Streamflow time series and flow separation for Buffelspruit catchment (1986-1999 validation)

4.3 Calibration of the North Eastern Catchments of Kafue Basin

Kafue River is one of the major tributaries of the Zambezi River covering about 20% of Zambia's total land area. Mwelwa (2004) calibrated the whole basin but the analysis here was confined to seven subcatchments in the north eastern part of the basin covering an area of 18 726 km^2 as shown in Figure 4.8. The subcatchments included are A, C, D, E, F, G and H. The mean annual rainfall in this area is about 1300 mm while the average annual potential evaporation varies from about 1460 to 1640 mm. The weathering horizons in the basin range from 25 to 60 m and the upper soil horizons are very permeable and have high infiltration rates. Mwelwa (2004) provides more details on the climate, soils, the geology and the geomorphology of the basin. One unique feature of Kafue basin is the existence of dambos – pan-like features called that store water in subsurface zone and on which wetlands frequently form (Mwelwa, 2004).

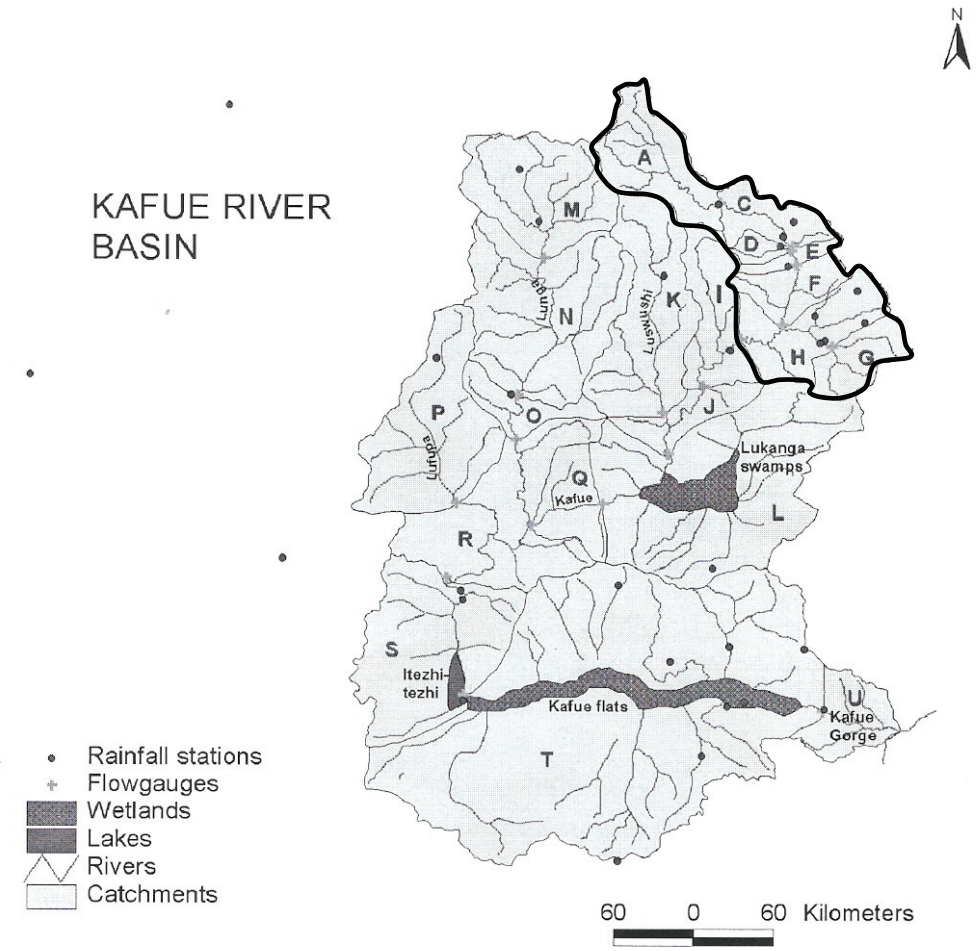

Figure 4.8 Kafue Basin highlighting the seven subcatchments modelled

The data set for Kafue Basin was provided by Prof Hughes of the Institute for Water Research (IWR), Rhodes University, South Africa and had been used in an MSc project (Mwelwa, 2004) as part of the Southern African FRIEND (Flow Regimes from International Experimental and Network Data) project. The period from 1959 to 1980 was selected for the current analysis after some preliminary calibrations and mass balance analysis indicated that the abstractions data for subcatchment G was unlikely to be reliable. The abstractions for this subcatchment increased with time and the impact of the perceived inaccuracy of the values up to 1980 was considered acceptable. The objective function for automatic calibration was based on the coefficient of efficiency (CE) computed using actual flows and logarithms of flows and was defined as 'minimize 1 – average CE' where the average CE is the average of the CE obtained from actual flows and from logarithms of flows. The objective function was computed ignoring months with missing data and calibration of all 11 Pitman model parameters for each subcatchment was done simultaneously resulting in an optimisation problem with 77 decision variables. Streamflow measurements at all the seven subcatchment outlets were used in calibration. Ten randomly initialised calibrations were carried out using the SCE-UA optimization parameters shown in Table 4.6 based on the recommendations of Duan et al. (1994). The last three rows of the Table show the search termination parameters adopted.

Table 4.6 SCE-UA optimization and search termination parameters for Kafue basin calibration

Description of parameter and [recommended value]	Notation	value
number of decision variables	n	77
number of complexes	p	10
number of points in each complex [m=2n+1]	m	155
sample size = pm	s	1550
number of points to select in complex [q=m]	q	155
optimization parameter [α>=1] use α=1	alp	1
optimization parameter (β>=1) [β=2n+1]	bet	155
maxepoch = maximum no. of epochs for termination	maxepoch	100
change in epoch objective function prompting termination	conv	0.02
spacing of epochs in checking for convergence	iconv	2

4.3.1 Kafue Basin calibration

The calibration of the basin required 2 adjustments of the search range limits as the some of the optimized parameter values consistently located close to the limits with the initial search ranges and after the first adjustment of the ranges. The second adjustment of the ranges however obtained parameter values that were well within all the set ranges. Figure 4.9 shows the objective function values obtained from the three sets of runs. The objective function values from multiple randomly initialized runs are very close revealing the effectiveness of the SCE-UA optimizer.

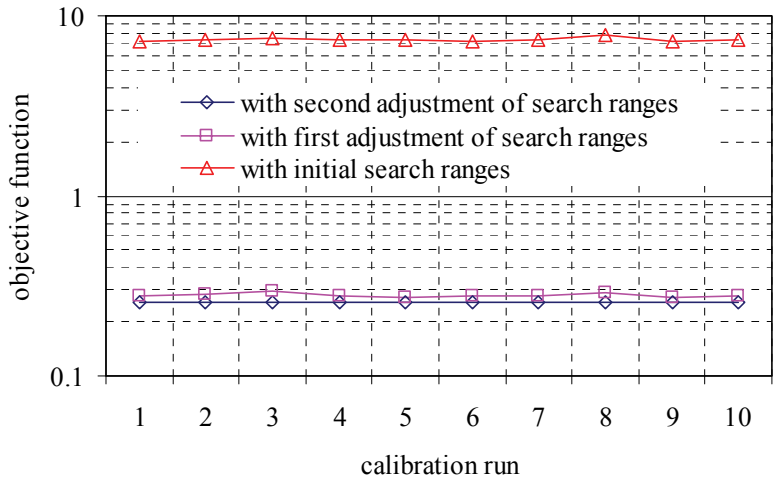

Figure 4.9 Objective function values for 10 calibration runs of Kafue basin.

Figure 4.10 shows the location of the parameter values scaled within the search range limits for selected subcatchments. The arrows on the Figure point to the cases where the optimized parameters converged on the search range limits from the multiple randomly initialised calibrations while the two numbers below each arrow are the average parameter values from the 10 runs and the set search range limit. The Figure indicates that upper limits of 1400 mm and 5 mm for ST and PI respectively were inadequate and R also took very low values for some subcatchments (Figure 4.10a and b). The upper search range limits of ST and PI could be increased while the lower search range limit for R had already been set to the lowest possible value of 0 and could not be reduced further. It is however noted that R tended to take higher values not located at the lower limit of 0 if both ST and PI did not locate close to the upper search range limits (Figure 4.10c). Tables 4.7a and 4.7b present the

parameter values obtained for the 10 calibration runs while Table 4.8 presents the performances from the 10 runs. All the parameter values were considered realistic but the unexpectedly high values of interception storage (PI) with average ranging from 9.0-13.4 mm for subcatchments E, F, G and H warranted further explanation. Additional calibrations that allowed ST to take high values but with PI limited to an upper limit of 8 mm were found to result in clearly suboptimal solutions in which the flow magnitudes were grossly overestimated. Further calibrations using the coefficient of mean absolute deviation (CMAD (equation 4.1)) as the objective function also revealed that PI still needed to take high values for satisfactory calibrations to be obtained.

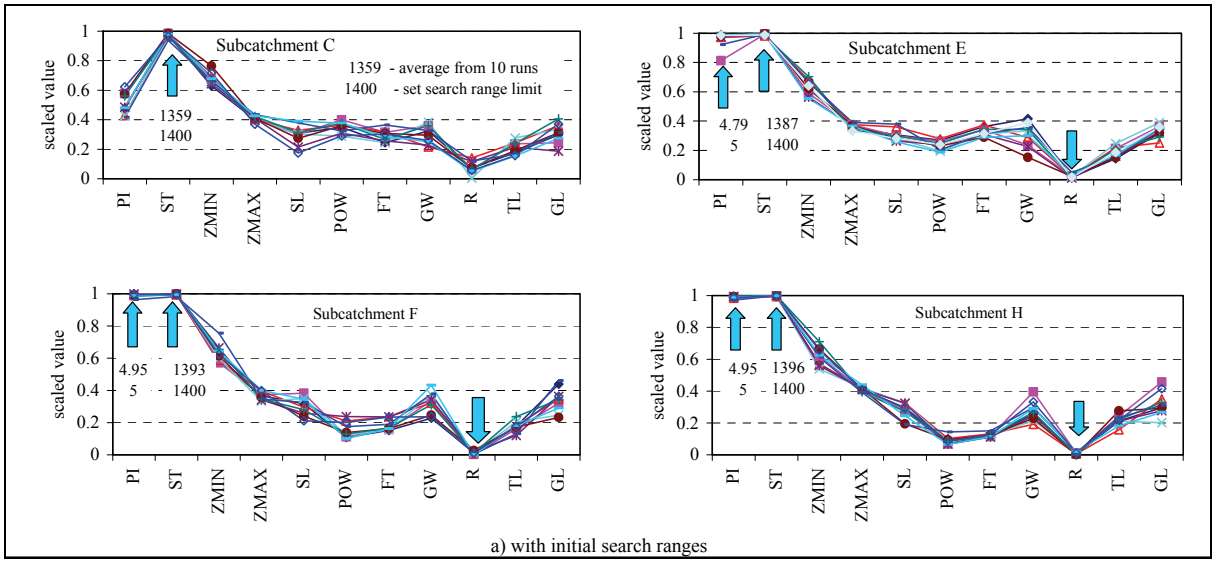

a) with initial search ranges

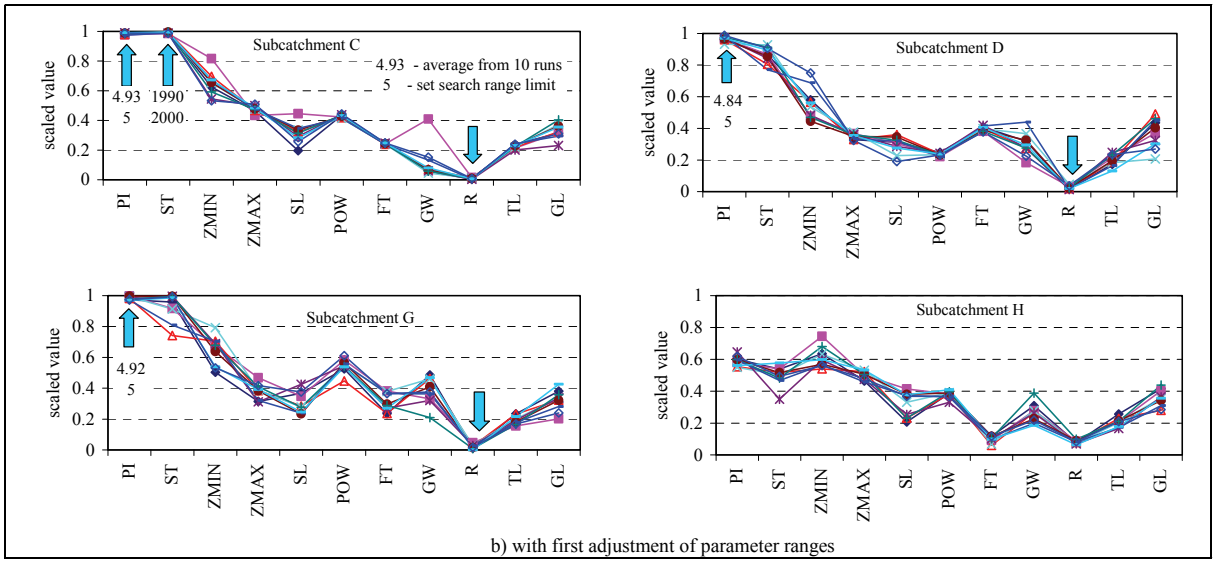

b) with first adjustment of parameter ranges

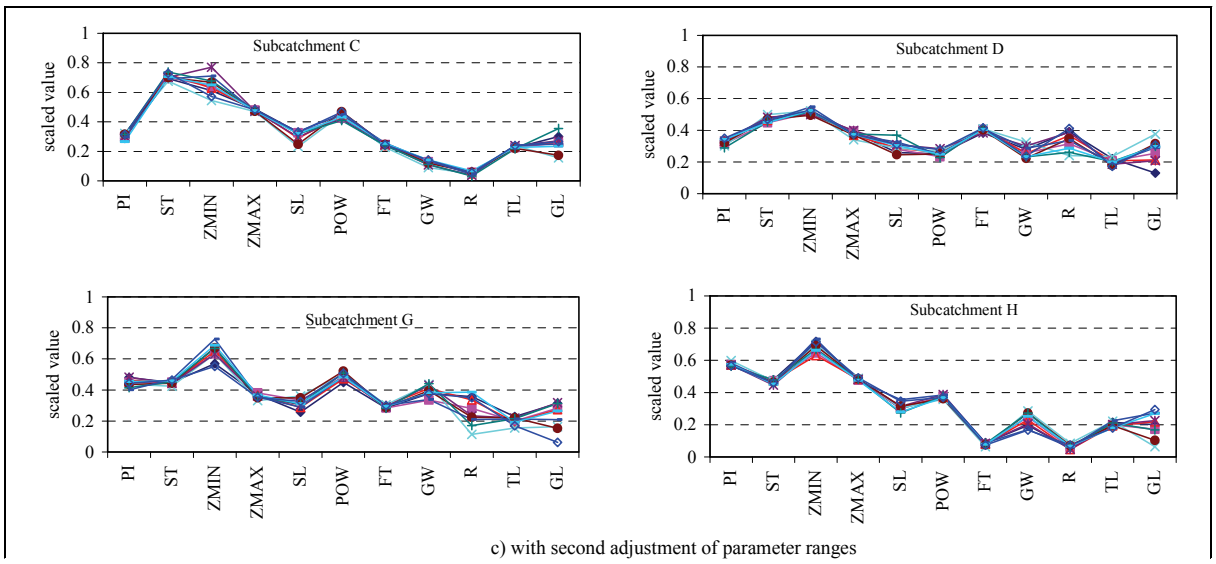

c) with second adjustment of parameter ranges

Figure 4.10 Scaled parameter values for 10 randomly initialised runs of five Kafue basin subcatchments

Table 4.7a Optimized parameter values for the first 5 runs of Kafue Basin

Sub-catchment	Run	parameter values										
		PI	ST	ZMIN	ZMAX	SL	POW	FT	GW	R	TL	GL
		mm	mm	mm	mm	mm	-	mm	mm	-	months	months
A	1	6.79	1166	108.2	1334	13.97	4.17	124.7	17.99	0.401	0.33	1.22
	2	5.76	1158	107.1	1339	14.91	4.33	121.6	17.94	0.348	0.36	1.40
	3	7.15	1147	107.9	1359	15.13	4.21	124.2	17.66	0.420	0.35	1.49
	4	6.75	1132	112.5	1340	12.37	4.20	116.4	17.31	0.187	0.41	1.48
	5	5.42	1155	104.3	1343	12.76	4.05	123.7	16.70	0.285	0.35	1.27
C	1	5.84	1980	91.7	1269	16.47	5.34	55.2	5.06	0.062	0.45	1.51
	2	6.05	1992	96.0	1252	16.27	5.41	56.5	5.16	0.057	0.45	1.30
	3	5.90	2029	94.3	1259	14.43	5.57	55.5	5.65	0.046	0.47	1.33
	4	6.50	1949	81.7	1228	11.61	5.60	53.3	3.63	0.047	0.48	0.79
	5	6.10	1992	115.5	1234	14.86	5.44	56.6	4.37	0.038	0.48	1.37
D	1	6.79	1370	78.5	1033	12.96	3.26	83.1	11.20	0.392	0.44	0.67
	2	6.33	1337	76.4	1048	14.07	3.10	87.0	10.29	0.315	0.41	1.29
	3	6.69	1356	78.7	986	14.40	3.32	88.0	10.12	0.367	0.42	1.08
	4	6.11	1399	78.4	918	14.41	3.40	87.7	13.04	0.240	0.47	1.89
	5	6.70	1379	74.8	1058	15.45	3.56	83.0	12.05	0.387	0.37	1.05
E	1	13.07	1470	91.5	862	13.59	4.26	60.8	14.09	0.098	0.38	0.98
	2	13.74	1441	90.5	850	14.73	4.02	59.9	14.25	0.074	0.38	1.19
	3	13.70	1474	92.5	862	16.59	4.13	56.6	14.30	0.061	0.41	1.06
	4	12.89	1409	80.5	855	11.44	4.56	62.0	17.86	0.092	0.33	0.44
	5	13.10	1448	85.1	853	14.80	4.34	57.6	14.42	0.041	0.40	1.02
F	1	11.30	1493	87.6	1346	16.36	4.19	32.2	10.03	0.053	0.41	1.91
	2	11.25	1452	85.0	1333	13.90	4.27	31.2	9.23	0.062	0.40	1.01
	3	11.08	1443	84.0	1343	14.62	4.45	31.3	11.02	0.059	0.39	1.19
	4	9.99	1452	84.3	1379	12.91	4.22	22.1	10.97	0.065	0.46	0.64
	5	10.59	1441	82.8	1373	14.72	4.54	29.9	8.52	0.063	0.39	0.95
G	1	9.66	1338	85.5	990	12.85	5.04	63.8	15.05	0.371	0.46	1.58
	2	9.05	1341	94.8	1012	16.68	5.36	63.9	13.40	0.296	0.40	1.43
	3	9.31	1334	97.6	979	14.37	5.25	67.0	16.39	0.349	0.39	1.38
	4	8.79	1308	94.9	893	18.08	5.51	67.8	17.44	0.131	0.31	0.83
	5	9.69	1329	94.7	968	15.19	5.32	65.4	17.20	0.248	0.44	1.60
H	1	11.39	1374	107.6	1258	15.05	4.35	26.8	7.86	0.055	0.43	1.02
	2	11.50	1368	97.0	1245	15.14	4.40	25.0	9.99	0.059	0.40	0.88
	3	11.45	1365	94.5	1259	15.48	4.30	25.2	9.21	0.046	0.39	1.11
	4	12.00	1364	104.6	1272	15.14	4.22	22.2	11.44	0.085	0.45	0.34
	5	11.44	1336	100.6	1257	15.71	4.49	26.2	8.26	0.047	0.40	1.14
Search range	lower lim.	0.1	800	0.02	100	0.02	2	10	0.02	0.0001	0.001	0.02
	upper lim.	20	2000*	150	2500	50	10	200	30	1	2	5

* 2500 for subcatchment C

Table 4.7b Optimized parameter values for the last 5 runs of Kafue Basin

Sub-catchment	Run	parameter values										
		PI	ST	ZMIN	ZMAX	SL	POW	FT	GW	R	TL	GL
		mm	mm	mm	mm	mm	-	mm	mm	-	months	months
A	6	6.49	1164	106.8	1328	13.66	4.35	125.7	17.77	0.288	0.34	1.65
	7	6.62	1125	110.4	1351	13.97	4.25	118.2	17.89	0.370	0.35	1.62
	8	6.06	1130	106.4	1364	16.49	4.44	122.9	16.34	0.329	0.35	1.73
	9	6.10	1154	108.5	1355	12.15	4.08	122.1	16.47	0.339	0.37	1.35
	10	6.46	1170	113.6	1365	15.10	4.04	124.4	17.38	0.291	0.36	1.50
C	6	6.39	1990	100.2	1232	12.37	5.75	56.9	4.81	0.058	0.44	0.88
	7	6.36	2054	101.6	1253	15.95	5.26	55.8	4.46	0.033	0.43	1.79
	8	6.00	1976	106.6	1226	16.70	5.58	58.9	5.45	0.045	0.48	1.26
	9	5.38	1998	97.4	1240	15.98	5.46	58.0	5.70	0.068	0.45	1.19
	10	6.33	2040	85.8	1258	16.46	5.72	56.6	5.61	0.055	0.48	1.34
D	6	6.48	1364	74.3	988	12.28	3.26	86.4	8.92	0.349	0.36	1.59
	7	5.86	1344	77.8	1004	18.47	3.05	88.9	9.29	0.260	0.41	1.51
	8	6.84	1349	82.1	994	16.27	3.25	87.5	11.48	0.335	0.39	1.47
	9	6.91	1339	78.8	998	15.17	3.25	86.7	9.34	0.287	0.40	1.50
	10	7.04	1363	79.0	1001	15.52	3.51	88.9	9.50	0.411	0.34	1.55
E	6	14.11	1422	86.7	875	17.60	4.13	59.5	14.00	0.073	0.44	0.98
	7	13.06	1470	92.6	854	13.46	4.53	63.2	17.64	0.069	0.34	0.87
	8	13.07	1431	86.9	859	15.56	4.19	57.5	14.59	0.075	0.43	1.46
	9	13.68	1441	89.4	845	13.65	4.40	61.0	14.38	0.053	0.41	1.06
	10	13.44	1469	90.9	861	16.37	4.29	63.4	11.96	0.068	0.39	1.21
F	6	11.27	1427	84.1	1370	15.11	4.33	32.4	6.99	0.054	0.39	1.13
	7	10.50	1427	84.2	1336	14.16	4.36	26.3	8.10	0.055	0.47	0.90
	8	10.57	1456	81.8	1355	16.23	4.48	27.2	10.62	0.061	0.39	1.44
	9	10.50	1436	83.4	1360	12.75	4.37	27.2	9.62	0.064	0.39	1.16
	10	11.32	1461	81.8	1323	15.21	4.35	32.0	10.60	0.075	0.41	1.04
G	6	8.75	1332	100.8	939	17.45	5.69	64.3	15.82	0.239	0.44	0.78
	7	8.35	1342	100.2	958	15.47	5.58	63.3	17.63	0.187	0.43	1.58
	8	8.08	1363	109.1	953	14.43	5.40	67.2	13.57	0.225	0.43	1.06
	9	9.15	1350	103.2	983	15.50	5.35	65.9	15.27	0.397	0.39	1.34
	10	8.92	1356	82.9	947	16.30	5.55	66.8	15.10	0.363	0.34	0.33
H	6	11.45	1355	103.5	1265	15.78	4.25	24.5	10.92	0.071	0.39	0.53
	7	11.32	1373	100.2	1259	13.67	4.40	25.5	10.89	0.065	0.42	0.86
	8	11.71	1349	109.8	1235	17.80	4.46	26.4	6.82	0.060	0.45	1.37
	9	11.53	1343	99.2	1241	13.97	4.31	24.8	10.09	0.067	0.36	1.36
	10	11.36	1351	107.0	1279	17.28	4.33	24.0	6.71	0.073	0.36	1.48
Search range	lower lim.	0.1	800	0.02	100	0.02	2	10	0.02	0.0001	0.001	0.02
	upper lim.	20	2000*	150	2500	50	10	200	30	1	2	5

* 2500 for subcatchment C

Table 4.8 Calibration performance for 10 randomly initialized runs of Kafue Basin

run	Sub catchment	Calibration (1959-1980)					run	Sub catchment	Calibration (1959-1980)				
		CE	R^2	BIAS	CMAD	RMCC			CE	R^2	BIAS	CMAD	RMCC
1	A	0.815	0.817	-0.03	0.304	0.339	6	A	0.812	0.814	-0.053	0.303	0.33
	C	0.724	0.734	0.062	0.338	0.36		C	0.73	0.733	-0.035	0.327	0.342
	D	0.697	0.702	-0.044	0.33	0.144		D	0.712	0.712	0	0.325	0.129
	E	0.684	0.711	0.049	0.397	0.223		E	0.702	0.707	-0.062	0.381	0.255
	F	0.592	0.594	-0.054	0.435	-0.038		F	0.592	0.598	-0.053	0.428	-0.055
	G	0.382	0.438	-0.278	0.619	0.279		G	0.421	0.446	-0.216	0.614	0.339
	H	0.67	0.682	0.083	0.411	0.376		H	0.674	0.677	0.049	0.406	0.359
2	A	0.812	0.814	0.018	0.309	0.374	7	A	0.808	0.808	-0.034	0.307	0.347
	C	0.729	0.736	0.042	0.338	0.331		C	0.721	0.721	-0.007	0.339	0.325
	D	0.709	0.711	0.036	0.331	0.111		D	0.708	0.717	0.081	0.333	0.089
	E	0.701	0.711	0.023	0.392	0.204		E	0.679	0.702	-0.027	0.389	0.262
	F	0.592	0.596	-0.061	0.43	-0.037		F	0.594	0.601	-0.016	0.428	0.033
	G	0.408	0.440	-0.23	0.617	0.317		G	0.441	0.453	-0.137	0.621	0.368
	H	0.674	0.674	-0.005	0.399	0.342		H	0.67	0.679	0.064	0.406	0.371
3	A	0.808	0.815	-0.071	0.304	0.342	8	A	0.809	0.812	-0.008	0.306	0.372
	C	0.731	0.733	0.017	0.334	0.353		C	0.718	0.733	0.048	0.338	0.328
	D	0.712	0.714	-0.021	0.323	0.135		D	0.709	0.714	-0.039	0.324	0.137
	E	0.697	0.702	-0.072	0.382	0.289		E	0.685	0.711	0.04	0.394	0.224
	F	0.588	0.596	-0.064	0.426	-0.032		F	0.591	0.598	-0.05	0.425	0.03
	G	0.407	0.438	-0.23	0.618	0.309		G	0.446	0.457	-0.022	0.652	0.4
	H	0.675	0.677	0.041	0.401	0.353		H	0.677	0.679	-0.043	0.397	0.339
4	A	0.794	0.806	-0.113	0.311	0.317	9	A	0.817	0.817	0.028	0.31	0.359
	C	0.723	0.728	-0.054	0.327	0.313		C	0.708	0.738	0.115	0.35	0.365
	D	0.715	0.716	-0.01	0.318	0.119		D	0.705	0.716	-0.06	0.322	0.132
	E	0.651	0.706	0.03	0.402	0.214		E	0.687	0.701	-0.095	0.379	0.289
	F	0.601	0.605	0.012	0.433	0.109		F	0.593	0.602	0.005	0.431	0.033
	G	0.434	0.454	-0.194	0.612	0.345		G	0.412	0.437	-0.211	0.62	0.318
	H	0.631	0.666	-0.145	0.408	0.286		H	0.676	0.677	0.027	0.4	0.352
5	A	0.814	0.817	0.062	0.314	0.37	10	A	0.815	0.815	-0.017	0.305	0.324
	C	0.729	0.734	0.021	0.335	0.328		C	0.719	0.721	-0.028	0.332	0.329
	D	0.679	0.687	-0.078	0.325	0.139		D	0.702	0.712	-0.074	0.321	0.155
	E	0.687	0.702	-0.036	0.383	0.275		E	0.697	0.709	-0.014	0.388	0.236
	F	0.585	0.601	0.003	0.431	0.01		F	0.587	0.594	-0.08	0.428	-0.039
	G	0.35	0.433	-0.347	0.622	0.273		G	0.433	0.452	-0.184	0.616	0.331
	H	0.68	0.684	0.017	0.396	0.367		H	0.681	0.682	0.021	0.4	0.357

A split sample calibration-validation analysis for the basin using 1959-72 for calibration and 1973-80 for validation obtained better calibration runs but notably poorer validations. Table 4.9 compares the overall automatic calibration and manual calibration performances and also includes the performances from the split sample calibration – validation tests.

Table 4.9 Comparison of automatic and manual calibration performance for Kafue basin

Calibration method and period of data		actual flows		logarithms of flows		average
		R^2	CE	R^2	CE	
Manual calibration 1960-1980 (Mwelwa, 2004)		0.705	0.638	0.761	0.668	0.693
automatic calibration1959-80	best run	0.669	0.657	0.761	0.750	0.709
	average of 10 runs	0.670	0.663	0.763	0.748	0.711
automatic calibration 1959-72 and validation1973-80	calibration best run	0.701	0.696	0.793	0.781	0.743
	calibration – av. of 10 runs	0.698	0.692	0.793	0.778	0.740
	validation best run	0.549	0.433	0.663	0.568	0.553
	validation – av. of 10 runs	0.545	0.423	0.66	0.561	0.547

A simple method to identify redundant parameters is to find whether the calibrated parameter values simply plot randomly and mostly within the initial search range. Figure 4.11, a plot of the scaled values of the calibrated values of SL for subcatchment E reveals that this parameter is most likely just taking on random values and has no impact on model performance. Using this method, parameters SL and ZMIN were found to be redundant for all the subcatchments.

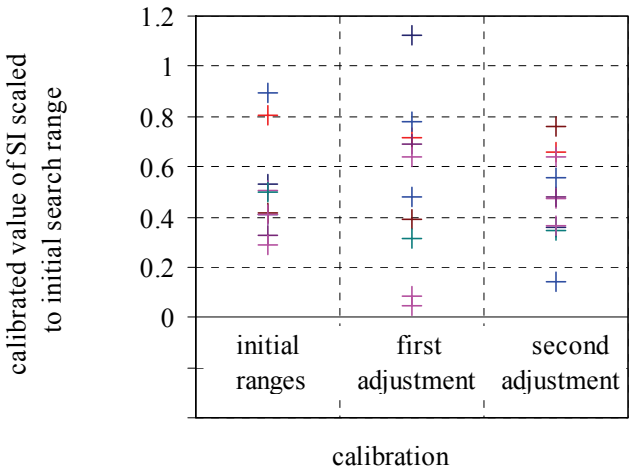

Figure 4.11 Scaled parameter values of parameter SL for subcatchment E.

Considering that the Pitman model works at a monthly time scale, the lag parameters, TL and GL were considered to be of low importance although they obtained a reasonable level of identification. Additional runs revealed that removing SL, ZMIN, TL and GL had negligible impact on model performance. Figure 4.12 plots the values of the remaining 7 parameters in a manner that illustrates i) the levels of identification of parameter values, ii) any interdependence of parameter values within individual subcatchments and iii) any correlation of parameter values across subcatchments.

From this Figure, it is observed that;

Parameter interdependence within subcatchments is either nonexistent or insignificant in the sense that it spans over a small range. For example, Figure 4.12(iv) suggests a high correlation between FT and PI for subcatchment A but the ranges of the 10 calibrated values are small (110-130 and 5-7.5 mm for FT and PI respectively).

Out of the 49 parameters plotted on Figure 4.12, 41 can be considered to be adequately identified. The 8 parameters not properly identified are parameter R for subcatchment A, D and G (Figure 4.12 (iii)) and parameter GW for subcatchment D, E, F, G and H (Figure 4.12 (viii)). Subcatchment C consistently obtained a significantly larger ST value compared with the other subcatchments. This observation and observation a) suggest insignificant levels of equifinality.

There is evidence of correlations of parameter values across subcatchments especially between PI and ST (excluding subcatchment C Figure 4.12 (i)).

Section 4.3.2 discusses the results and attempts to offer plausible explanations of the observations.

4.3.2 Discussion of Kafue basin calibration results

The uncharacteristic observations in the Kafue basin calibration were:

- the high values of interception index (PI) especially for subcatchments E, F, G and H,
- the notably poorer validation performance (for the Buffelspruit and Amatole, the validations were as good as the calibrations), and
- the high value of soil storage capacity ST for subcatchment C.

The interception storage (PI) in the Pitman model typically takes values lower than 5mm and is not expected to exceed 8 mm. The relationship that the Pitman model uses to obtain the monthly interception loss as a function of monthly rainfall was derived for interception storages in the range 0-8 mm. Since considerably larger PI values were obtained for subcatchments E, F, G and H, the relationship was applied beyond the range it was developed for.

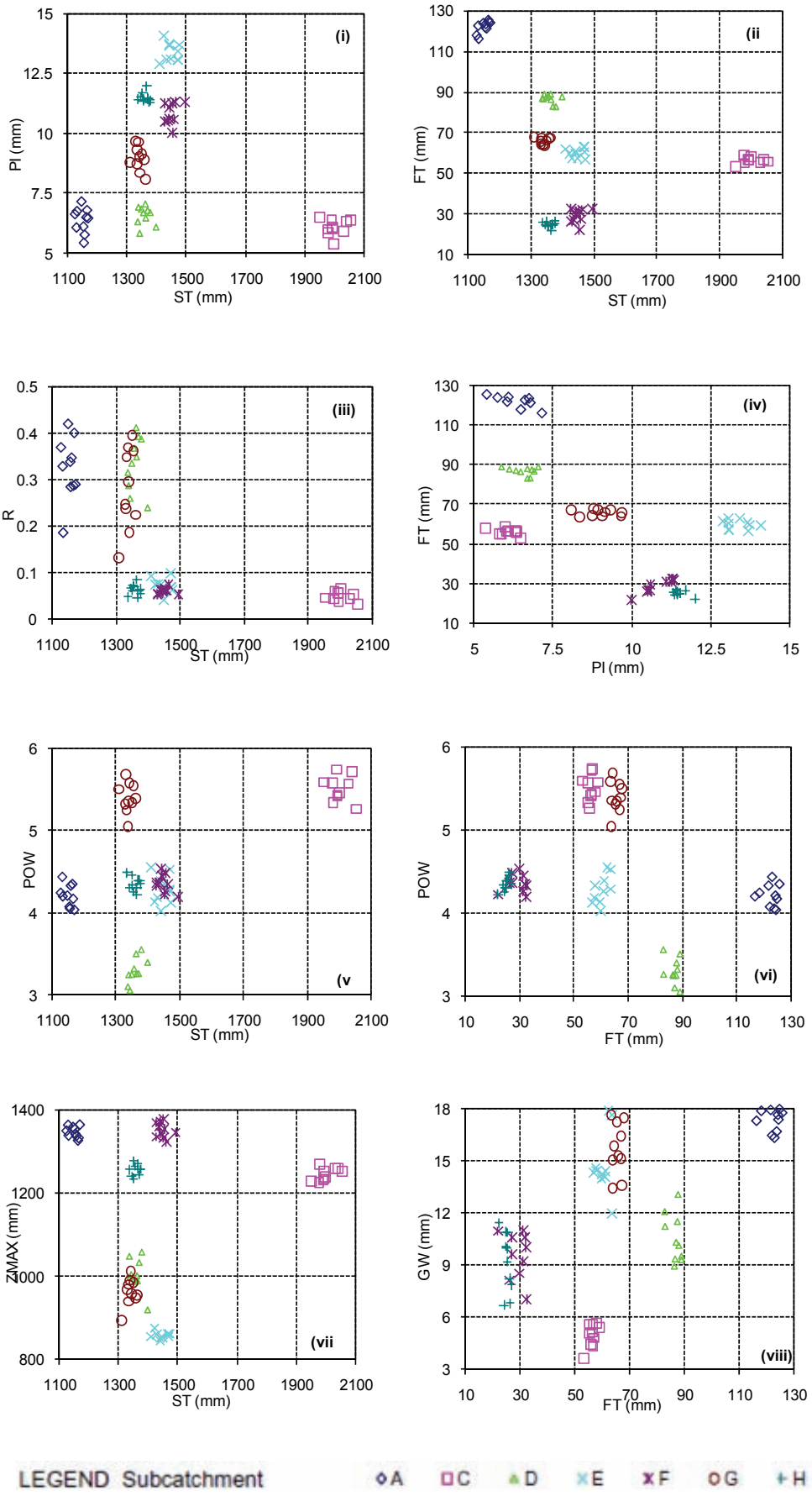

Figure 4.12 Plots of calibrated parameter values for Kafue basin subcatchments

The numerous dambos found in the Kafue basin were considered to be the reason for the large PI values and PI was considered to represent the interception storage in the dambos and not on vegetation as in normal Pitman model applications. Studies on dambos (Bullock (1992a,b); McCartney, 2000) suggest that their main hydrological impact is to reduce streamflow through evaporation loss. This offers a plausible explanation of the observed gross overestimation of simulated streamflow when PI was limited to an upper limit of 8 mm.

Since the Pitman model does not explicitly model dambos, the poorer validations for Kafue basin can be reasonably considered to be due to inability of the Pitman model structure to represent the processes occurring in the dambos adequately. The latest additions to the Pitman model (Bailey, 2008) include the modelling of wetlands directly connected to the stream but not over land where many dambos occur. Winsemius et al. (2006) have modelled dambos as processes over land and this may also be appropriate for the Pitman model.

Figure 4.13 shows a comparison of the simulated and observed flow for selected subcatchments. The simulation is generally considered satisfactory.

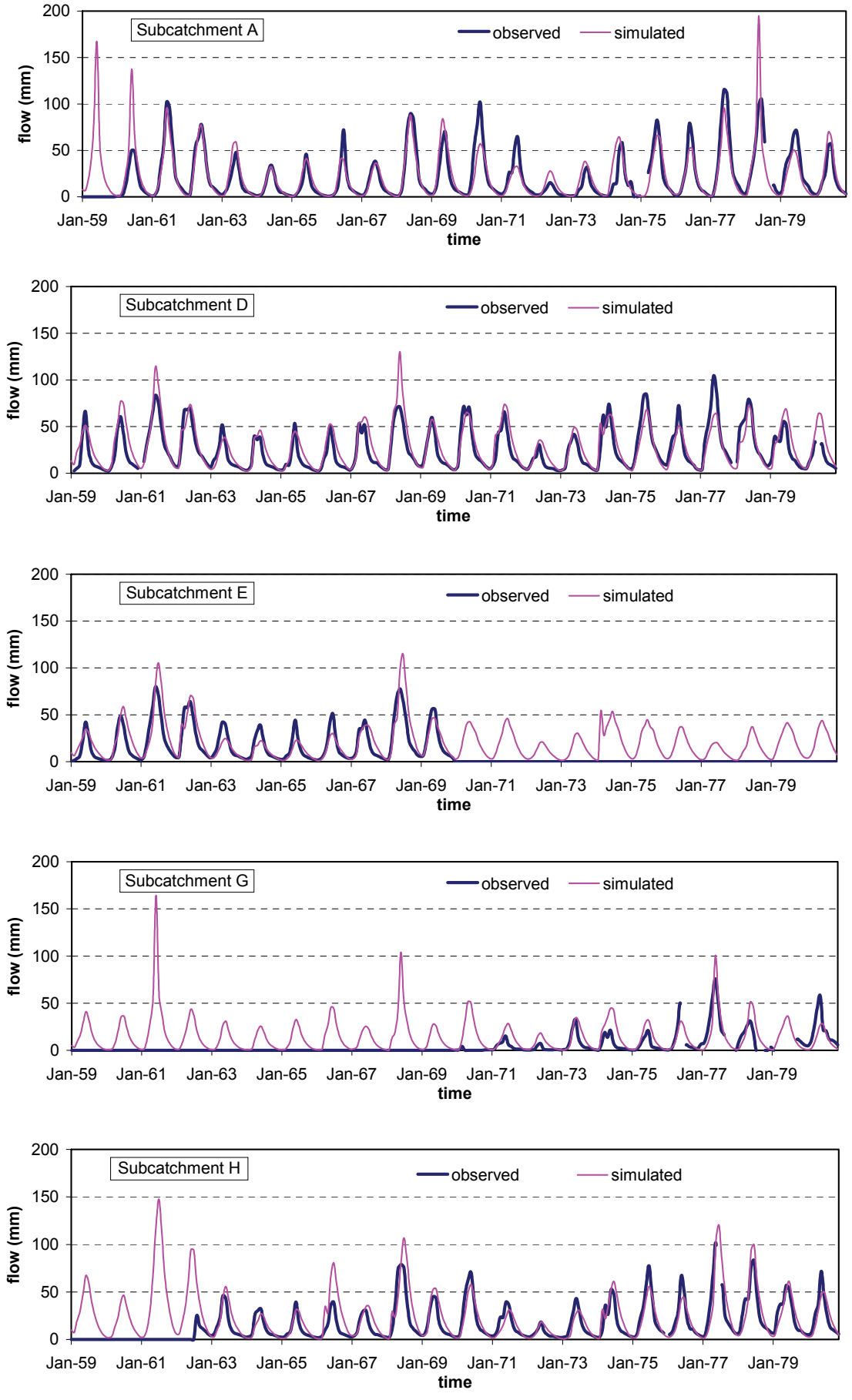

Figure 4.13 Comparison of simulated and observed streamflows for five Kafue basin subcatchments

4.4 Calibration of three Amatole Basin Catchments

4.4.1 Selection of subcatchments and objective function

The Amatole River Basin is located in the Eastern Cape province of South Africa had been manually calibrated (Kleynhans, 2007). The calibrated parameter values and simulated time series' were provided by Allan Bailey of Stewart Scott International. Three catchments in the basin whose flows were still mainly natural were selected for automatic calibration. Table 4.10 provides basic information on the three sites including the splitting of the data into calibration and validation sets. Manual calibration (Kleynhans, 2007) used all the available data and no validation runs were carried out.

Table 4.10 Basic information on three Amatole Basin catchments selected for analysis

Gauging Station	River	Catchment area (Km^2)	MAR (mm)	Available data	Percent of flows missing	Calibration data	Validation data
R2H009	Ngqokweni	258	574	1955-2003	21	1955-1979	1980-2003
R3R001	Nahoon	473	671	1966-2003	0	1966-1984	1985-2003
S6H003	Toise	215	668	1966-2003	14	1966-1984	1985-2003

As explained in Section 2.2 and described in Table 2.2, parameter adjustment in manual calibration of the original and the WRSM 2000 version of the Pitman model is mainly based on the matching of the mean annual runoff (MAR), the annual standard deviation (SD) and the seasonal index (SI) of the simulated and the observed flows in addition to graphical comparisons. For automatic calibration, a hybrid objective function that minimises the differences of the three measures between the simulated and the historic flows as described in equation 4.6 was applied.

$$minimize \quad \left(\frac{|MAR_{sim} - MAR_o|}{MAR_o} + \frac{|SD_{sim} - SD_o|}{SD_o} + \frac{|SI_{sim} - SI_o|}{SI_o} \right) \tag{4.6}$$

where MAR_{sim} and MAR_o is the simulated and observed mean annual runoff respectively, SD_{sim} and SD_o is the simulated and observed standard deviation of annual flows respectively and SI_{sim} and SI_o is the simulated and observed seasonal index respectively. The seasonal index is obtained as the range of the monthly cumulative net deviations of flows as described in equations 4.7 to 4.9 and illustrated on Figure 4.14.

$$SI = \text{maximum}\left(CumNetDev(j) j = 1,2,..12\right) \quad - \quad \text{minimum}\left(CumNetDev(j) j = 1,2,..12\right) \tag{4.7}$$

$$CumNetDev(j) = \sum_{k=1}^{J} NetDev(k) \qquad j = 1,2,....12 \tag{4.8}$$

$$NetDev(k) = 100\left[\frac{\sum_{i=1}^{n} q_{i,k}}{\sum_{k=1}^{12}\sum_{i=1}^{n} q_{i,k}} - \frac{1}{12} \right] \qquad k = 1,2,....12 \tag{4.9}$$

Where $q_{i,k}$ is the flow in month k of year i.

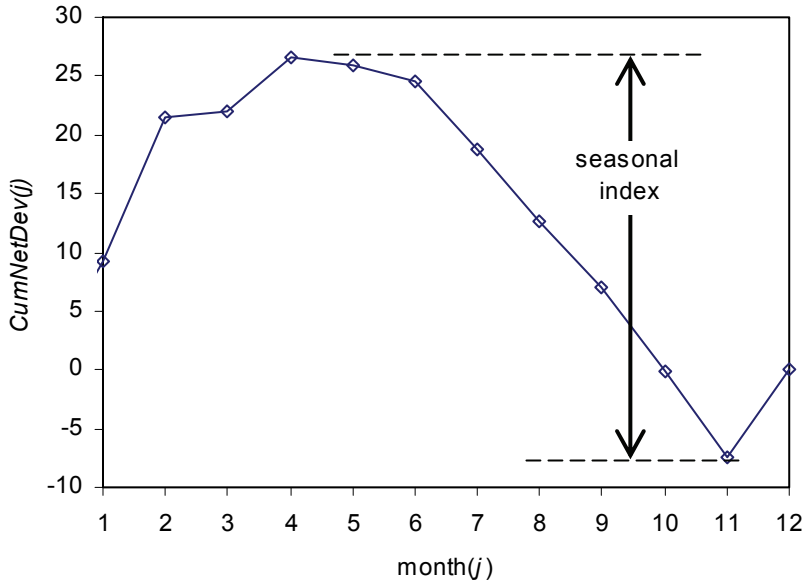

Figure 4.14 Determination of seasonal index

Another set of calibrations using the monthly coefficient of mean absolute deviation (CMAD) (equation 4.1) as the objective function was also carried out. The hybrid objective function was only applicable to the years without missing flows while the CMAD was applied for all months where observed flows were available. For this reason, the hybrid objective function is at times referred to as the annual objective function and the CMAD as the monthly objective function for the rest of this Section. Ten randomly initialised calibration runs were made for each catchment and each objective function. For the calibration of each catchment, the SCE-UA optimization parameters applied were the same as those used for Buffelspruit Basin (Table 4.1). For all the calibrations parameter TL was set to 0.5 months as in the manual calibrations (Kleynhans, 2007) and the rest of the parameters were calibrated.

4.4.2 Amatole Basin automatic calibration results and comparison with manual calibration

Tables 4.11 and 4.12 present the calibrated parameters obtained from all 10 runs using the hybrid and the coefficient of mean absolute deviation (CMAD) objective function. The parameters obtained from manual calibration (Kleynhans, 2007) are also presented in the Tables. Not unexpectedly, large differences are observed in the parameter values obtained manually and automatically and also with the two objective functions. Figure 4.15 compares the scaled parameter values for the 10 calibrations using the hybrid objective function and manual calibration for the three catchments. Table 4.11 and Figure 4.15 reveal the most prevalent differences as those in parameters SL, ST, POW, FT and GW. These parameters are mainly connected to the soil moisture-runoff relationship of the Pitman model and the modelling of this process is therefore analysed in more detail in Section 4.4.3. It is in particular noted that parameter POW takes on values much higher than the upper limit of 3.0 that is assumed in most manual calibrations and set in the WRSM 2000 model (Bailey, 2008).

Tables 4.13 to 4.16 present the calibration and validation performances for the three catchments using the 5 performance measures applied to Buffelspruit and Kafue basin and three additional measures

quantifying the closeness of the mean annual runoff (CMAR), the standard deviation of annual flows (CSD) and the seasonal index (CSI) of the simulated series to the that of the observed series. The three additional measures correspond to the three components of the hybrid objective function described in equation 4.6. A graphical comparison of the average performances obtained using the two objective functions in automatic calibration and the single value obtained from manual calibration are presented in Figure 4.16. Figure 4.16 plots the absolute deviation of each performance measure from the ideal value and not the actual performance measure as expressed in equation 4.10. Therefore, the closer a plotted value is to zero, the closer it is to the ideal and the better the performance.

$$average \quad absolute \quad deviation = \left| \frac{\sum_{i=1}^{n} \left| actual \quad value_i - ideal \quad value \right|}{n} \right| \tag{4.10}$$

Figure 4.16 reveals the following:

- Automatic calibration using the monthly (CMAD) objective function obtains better performance than using annual (hybrid) objective function. The main difference is in the validation of R2H009 where CMAD performance is notably superior for 5 of the 8 performance measures.
- Automatic calibration using the annual (hybrid) objective function performs slightly better than manual calibration. The notable differences are in the CE and RMCC values in the calibration of R2H009 and the RMCC value in the validation of S6H003.
- On the basis of the 8 performance measures, automatic calibration using the monthly objective function performs best while manual calibration performs the worst.
-

A closer look at the data set used for R2H009 revealed that only 3 years of annual data were complete for the calibration period (1955-1979) while 201 months of analysis were available for the same period. Calibrating with the monthly (CMAD) objective function therefore used 201 months while calibrating with the annual (hybrid) objective function used only 3 years (36 months). This difference probably explains the poorer performance of the annual objective function in the validation runs of R2H009. Manual calibration applied the complete period of analysis (1955-2003) which for R2H009 was 10 years of complete data suggesting that the poor manual calibration performance is more likely attributable to other factors.

Figure 4.17 shows plots of the historic and simulated flows from manual and automatic calibration using the hybrid (annual) objective function for selected periods. In Figure 4.18, a comparison of the validation time series for R2H009 for manual and automatic calibration using the CMAD function is shown. Automatic calibration using the monthly objective function provides an evidently superior fit in agreement with the observations on Figure 4.16 and Table 4.16.

Table 4.11 Parameter values for Amatole catchments using the hybrid objective function

Catchment R2H009													
run	n-epoch	n-sim	objf	PI (mm)	ST (mm)	ZMIN (mm)	ZMAX (mm)	SL (mm)	POW	FT (mm)	GW (mm)	R	GL (months)
1	11	12933	0.167	0.789	504	70.6	514	5.61	8.21	62.8	6.27	0.687	0.0996
2	11	13000	0.171	1.710	494	49.2	564	9.38	7.37	97.3	16.68	0.540	0.1039
3	11	12978	0.168	0.940	509	56.5	604	7.29	7.98	78.9	6.83	0.623	0.0974
4	11	12916	0.176	1.551	473	42.7	645	10.03	6.70	78.9	5.78	0.458	0.0465
5	11	12941	0.169	0.680	511	51.2	700	13.65	7.69	89.8	8.00	0.555	0.1189
6	11	13047	0.174	1.798	449	39.3	640	9.14	6.74	65.5	1.32	0.524	0.0342
7	11	13048	0.167	1.418	490	53.6	557	22.98	7.74	91.5	9.12	0.621	0.0879
8	11	12926	0.172	1.381	490	55.4	575	5.54	7.33	82.3	10.44	0.538	0.0605
9	11	12983	0.165	0.810	538	56.6	604	10.57	8.49	94.5	6.19	0.657	0.0996
10	11	12964	0.171	1.674	483	56.9	521	4.16	7.21	77.9	4.62	0.541	0.0731
average	11	12974	0.170	1.275	494	53.2	593	9.84	7.55	81.9	7.53	0.574	0.0822
Manual calibration				1.5	150	45	420	0	3	4	0	0.5	0

Catchment R3R001													
run	n-epoch	n-sim	objf	PI (mm)	ST (mm)	ZMIN (mm)	ZMAX (mm)	SL (mm)	POW	FT (mm)	GW (mm)	R	GL (months)
1	6	3551	0.0252	0.961	983	114	303	3.17	7.13	28.4	5.86	0.116	0.0703
2	6	3522	0.0236	1.401	905	127	263	7.59	7.59	41.1	6.92	0.166	0.0981
3	6	3560	0.0255	1.081	836	110	309	4.76	6.81	32.5	5.48	0.114	0.0739
4	6	3527	0.0258	1.155	906	103	307	4.43	5.71	8.2	7.26	0.220	0.0686
5	6	3547	0.0256	1.569	867	104	293	4.26	7.86	32.9	5.57	0.407	0.0736
6	7	4106	0.0246	1.466	1012	126	261	7.92	7.39	29.4	6.81	0.247	0.0326
7	6	3527	0.0248	0.517	910	126	303	7.34	6.53	13.6	12.35	0.164	0.1275
8	7	4118	0.0233	1.817	920	118	251	9.53	7.99	34.9	9.10	0.239	0.0649
9	6	3547	0.0254	1.157	862	112	295	10.02	6.26	13.5	8.19	0.218	0.0585
10	6	3592	0.0248	0.859	782	112	314	8.30	6.80	22.7	8.12	0.092	0.0925
average	6	3660	0.0249	1.198	898	115	290	6.73	7.01	25.7	7.57	0.198	0.0761
Manual calibration				1.5	120	90	400	0	3	3	0	0.5	0

Catchment S6H003													
run	n-epoch	n-sim	objf	PI (mm)	ST (mm)	ZMIN (mm)	ZMAX (mm)	SL (mm)	POW	FT (mm)	GW (mm)	R	GL (months)
1	9	5387	0.0010	0.889	963	43.4	426	3.55	4.44	42.1	16.1	0.340	0.0782
2	8	4841	0.0006	0.821	903	42.5	433	5.74	4.49	42.2	17.7	0.346	0.0868
3	8	4847	0.0008	0.934	895	36.3	442	4.07	4.47	43.4	12.4	0.315	0.0901
4	8	4866	0.0010	0.924	885	46.2	417	4.88	4.69	43.1	14.8	0.432	0.0750
5	9	5442	0.0004	1.138	920	47.2	402	4.31	4.34	38.4	17.8	0.387	0.0885
6	7	4232	0.0004	1.128	913	41.9	413	5.37	4.92	47.7	21.9	0.485	0.0772
7	8	4860	0.0009	0.842	909	48.8	414	4.67	4.57	40.8	13.7	0.414	0.0728
8	8	4831	0.0007	0.757	915	47.3	427	3.38	4.09	35.8	15.1	0.266	0.0909
9	8	4859	0.0008	0.739	908	43.9	433	5.67	4.61	43.3	15.9	0.376	0.0809
10	9	5420	0.0004	0.870	940	40.5	434	7.58	4.56	44.8	20.4	0.358	0.0756
average	8	4959	0.0007	0.904	915	43.8	424	4.92	4.52	42.2	16.6	0.372	0.0816
Manual calibration				1.5	60	75	500	0	3	20	2	0.5	2.5

Table 4.12 Parameter values for Amatole catchments using monthly coefficient of mean absolute deviation (CMAD) objective function

Catchment R2H009													
run	n-epoch	n-sim	objf	PI (mm)	ST (mm)	ZMIN (mm)	ZMAX (mm)	SL (mm)	POW	FT (mm)	GW (mm)	R	GL (months)
1	6	3448	0.7864	1.883	914	65.9	993	11.50	5.342	31.0	10.79	0.0272	0.0868
2	6	3407	0.7845	1.242	1047	54.4	1195	5.49	5.845	28.7	10.58	0.0836	0.0446
3	6	3423	0.7874	1.074	1067	94.2	866	9.87	5.992	34.3	12.30	0.065	0.0457
4	6	3427	0.7858	2.208	694	59.7	972	10.64	5.233	23.1	13.77	0.0433	0.1074
5	6	3454	0.7891	1.718	1073	85.3	792	15.73	5.964	46.8	2.07	0.0436	0.0911
6	6	3441	0.7861	1.092	945	71.8	1048	10.72	6.090	36.7	9.37	0.021	0.0694
7	6	3407	0.7843	1.798	831	52.7	1078	14.75	5.261	23.5	6.87	0.0463	0.1143
8	6	3435	0.7851	1.743	929	60.8	1072	11.39	5.514	28.5	17.21	0.0396	0.0503
9	6	3447	0.789	1.548	875	93.3	800	10.96	5.754	32.5	7.69	0.0535	0.0806
10	6	3416	0.7856	1.004	915	91.6	959	5.84	5.384	19.8	13.33	0.0458	0.1306
average	6	3431	0.786	1.531	929	73.0	978	10.69	5.64	30.5	10.40	0.047	0.0821
Manual calibration				1.5	150	45	420	0	3	4	0	0.5	0

Catchment R3R001													
run	n-epoch	n-sim	objf	PI (mm)	ST (mm)	ZMIN (mm)	ZMAX (mm)	SL (mm)	POW	FT (mm)	GW (mm)	R	GL (months)
1	6	3502	0.5737	0.483	661	87.6	449	5.51	8.40	15.3	3.08	0.197	0.1261
2	6	3486	0.5737	0.805	661	79.6	439	8.95	8.61	19.8	1.11	0.162	0.0768
3	6	3543	0.5744	0.591	738	83.3	449	6.17	7.87	15.7	7.44	0.155	0.0334
4	6	3492	0.5722	0.119	578	84.1	468	6.30	8.92	14.4	9.08	0.134	0.0924
5	6	3532	0.5737	1.106	593	66.6	435	3.11	8.83	16.9	5.46	0.210	0.0812
6	6	3504	0.5734	0.270	634	89.0	442	5.97	9.06	20.2	5.78	0.088	0.0449
7	6	3523	0.5747	0.772	744	80.1	442	6.08	8.71	18.4	4.72	0.189	0.0803
8	6	3528	0.5742	0.407	748	83.8	458	5.66	8.01	18.2	9.86	0.094	0.0688
9	6	3513	0.5732	0.694	625	71.4	462	3.34	8.24	15.0	6.81	0.148	0.0545
10	6	3530	0.5759	1.102	839	77.4	430	4.92	7.21	16.5	7.08	0.103	0.0662
average	6	3515	0.5739	0.635	682	80	447	5.60	8.39	17.0	6.04	0.148	0.0725
Manual calibration				1.5	120	90	400	0	3	3	0	0.5	0

Catchment S6H003													
run	n-epoch	n-sim	objf	PI (mm)	ST (mm)	ZMIN (mm)	ZMAX (mm)	SL (mm)	POW	FT (mm)	GW (mm)	R	GL (months)
1	6	3406	0.5390	0.376	690	2.91	706	3.51	5.32	78.1	34.6	0.226	0.0717
2	6	3448	0.5350	0.195	599	2.44	633	9.55	4.96	75.6	31.5	0.075	0.0943
3	6	3407	0.5318	0.445	552	0.30	640	14.11	4.93	61.4	24.1	0.189	0.0492
4	6	3433	0.5357	0.522	629	1.74	628	3.52	5.33	82.7	29.3	0.206	0.0661
5	6	3425	0.5338	0.465	608	0.24	671	3.75	5.48	69.1	25.3	0.305	0.0721
6	6	3424	0.5360	0.232	652	3.16	640	8.15	5.99	73.1	36.0	0.429	0.0476
7	6	3381	0.5357	0.436	643	3.25	655	11.45	4.99	73.5	48.1	0.196	0.0500
8	6	3438	0.5333	0.831	534	0.78	622	12.28	4.88	56.9	23.0	0.253	0.0563
9	6	3437	0.5329	0.609	586	1.69	648	10.14	4.91	58.1	12.7	0.255	0.0880
10	6	3408	0.5325	0.627	526	0.13	653	12.99	4.66	60.1	11.5	0.111	0.0477
average	6	3421	0.5346	0.474	602	1.7	649	8.94	5.15	68.9	27.6	0.225	0.0643
Manual calibration				1.5	60	75	500	0	3	20	2	0.5	2.5

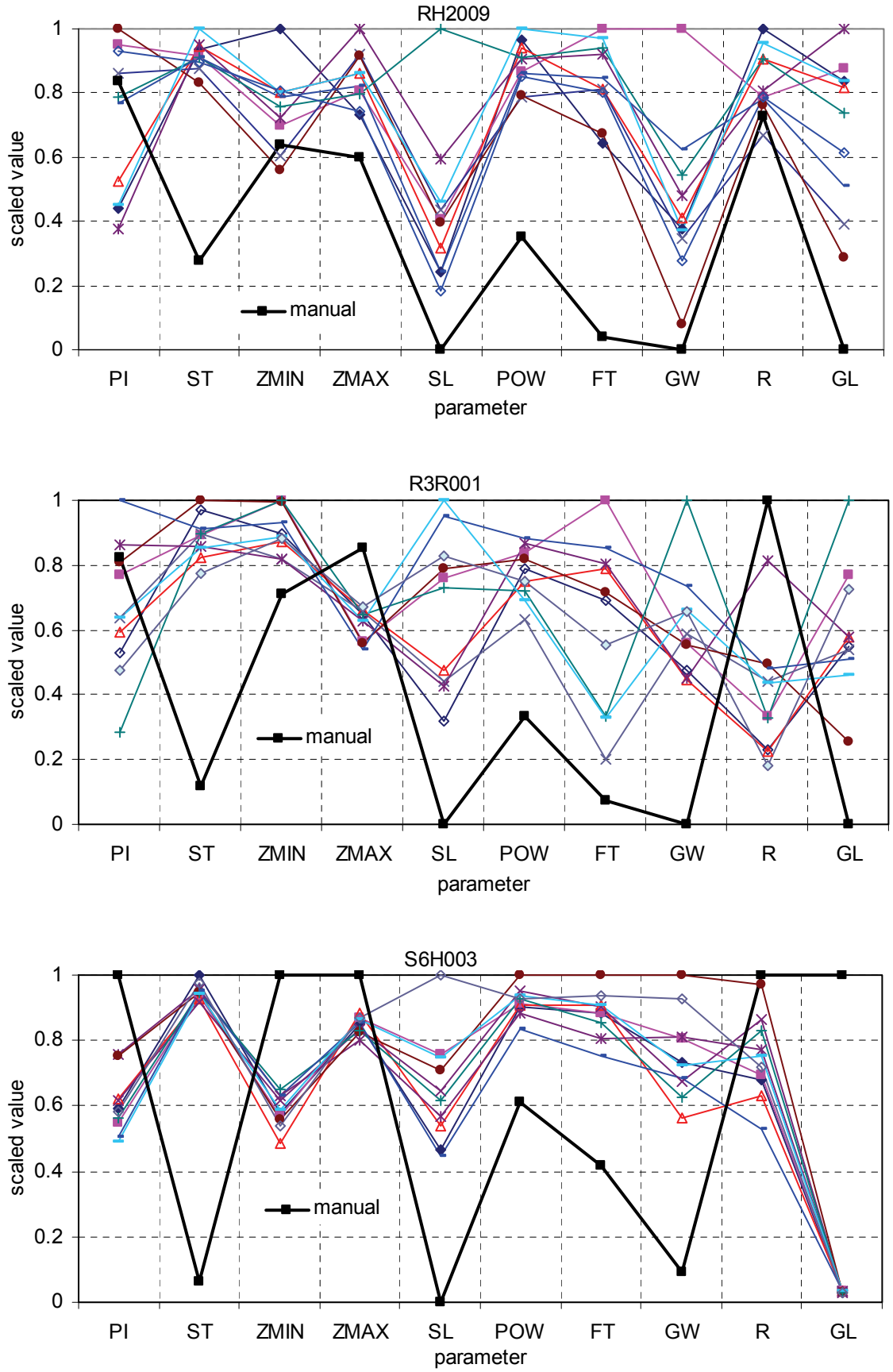

Figure 4.15 Comparison of scaled parameters from manual calibration and 10 automatic calibration runs for Amatole basin

Table 4.13 Calibration performance of Eastern Cape catchments using the hybrid objective function

Catchment R2H009								
Run	CE	CC	BIAS	CMAD	RMCC	MAR	STDEV	SI
1	-3.145	0.426	1.561	2.196	-1.208	0.003	-0.483	0.015
2	-3.696	0.409	1.69	2.285	-1.229	0.014	-0.499	0
3	-3.509	0.41	1.647	2.257	-1.18	0.007	-0.494	0.002
4	-3.367	0.405	1.63	2.217	-1.095	0.009	-0.512	0.008
5	-3.997	0.396	1.733	2.329	-1.206	0.004	-0.498	0.006
6	-3.264	0.403	1.589	2.197	-1.007	0.017	-0.502	0.002
7	-3.975	0.408	1.707	2.325	-1.275	0.003	-0.476	0.022
8	-3.485	0.41	1.648	2.249	-1.175	0.008	-0.503	0.004
9	-3.707	0.41	1.688	2.294	-1.268	0.001	-0.492	0.001
10	-3.191	0.418	1.585	2.193	-1.167	-0.001	-0.508	0.003
manual	-7.166	0.294	1.421	1.947	-1.396	0.061	-0.583	0.606

Catchment R3R001								
Run	CE	CC	BIAS	CMAD	RMCC	MAR	STDEV	SI
1	0.851	0.923	0.014	0.64	0.593	0.014	-0.06	0.002
2	0.843	0.92	0.02	0.655	0.586	0.02	-0.05	0
3	0.858	0.927	0.009	0.632	0.602	0.009	-0.068	0
4	0.854	0.925	0.008	0.638	0.59	0.008	-0.068	0.002
5	0.857	0.926	0.006	0.635	0.596	0.006	-0.071	0
6	0.843	0.92	0.013	0.654	0.581	0.013	-0.053	0.008
7	0.845	0.921	0.024	0.651	0.588	0.024	-0.05	0
8	0.842	0.919	0.014	0.656	0.581	0.014	-0.054	0.002
9	0.85	0.923	0.015	0.642	0.59	0.015	-0.06	-0.001
10	0.855	0.925	0.01	0.634	0.6	0.01	-0.064	0.001
manual	0.748	0.866	0.162	0.819	0.641	0.162	0.113	0.27

Catchment S6H003								
Run	CE	CC	BIAS	CMAD	RMCC	MAR	STDEV	SI
1	0.211	0.522	-0.36	0.608	0.302	-0.001	-0.002	0
2	0.225	0.533	-0.358	0.603	0.311	-0.002	0	0
3	0.234	0.539	-0.356	0.6	0.313	0	0	0.002
4	0.219	0.531	-0.359	0.606	0.31	0	0.003	0
5	0.198	0.515	-0.365	0.613	0.292	0	0	0.001
6	0.219	0.531	-0.357	0.607	0.312	0	0	-0.001
7	0.209	0.523	-0.36	0.609	0.303	0	0.001	0.002
8	0.209	0.521	-0.362	0.608	0.296	-0.001	0	0.001
9	0.225	0.533	-0.356	0.604	0.313	0	0	0.002
10	0.224	0.532	-0.356	0.604	0.312	0	0	-0.001
manual	0.319	0.659	-0.163	0.602	0.302	0.299	-0.021	-0.214

Table 4.14 Validation performance of Eastern Cape catchments using the hybrid objective function

Catchment R2H009								
Run	CE	CC	BIAS	CMAD	RMCC	MAR	STDEV	SI
1	-5.336	0.408	2.939	3.412	-0.237	4.98	7.587	-0.319
2	-5.842	0.399	3.203	3.622	-0.274	4.899	7.372	-0.314
3	-5.573	0.405	3.119	3.555	-0.214	4.91	7.299	-0.316
4	-5.407	0.401	3.144	3.534	-0.297	4.703	6.944	-0.31
5	-6.233	0.399	3.301	3.709	-0.261	4.917	7.321	-0.272
6	-5.209	0.402	3.07	3.477	-0.224	4.692	6.8	-0.286
7	-6.249	0.405	3.218	3.67	-0.23	5.034	7.677	-0.296
8	-5.556	0.4	3.134	3.555	-0.259	4.848	7.263	-0.306
9	-5.828	0.404	3.171	3.611	-0.217	4.983	7.468	-0.335
10	-5.209	0.401	3.014	3.448	-0.272	4.792	7.252	-0.332
Manual*	-5.16	0.396	2.399	2.757	-0.68	4.868	6.711	0.113

Catchment R3R001								
Run	CE	CC	BIAS	CMAD	RMCC	MAR	STDEV	SI
1	0.687	0.829	0.004	0.848	0.614	0.004	-0.184	0.005
2	0.677	0.824	0.016	0.863	0.625	0.016	-0.168	0.005
3	0.696	0.834	-0.003	0.837	0.609	-0.003	-0.186	-0.021
4	0.689	0.83	-0.007	0.846	0.607	-0.007	-0.199	0.015
5	0.694	0.833	-0.009	0.84	0.598	-0.009	-0.196	-0.017
6	0.676	0.823	0.007	0.864	0.622	0.007	-0.176	0.018
7	0.679	0.825	0.014	0.86	0.621	0.014	-0.176	0.018
8	0.674	0.822	0.009	0.867	0.621	0.009	-0.177	0.017
9	0.685	0.828	0.003	0.851	0.613	0.003	-0.187	0.01
10	0.692	0.832	-0.003	0.84	0.612	-0.003	-0.186	-0.003
Manual*	0.68	0.829	0.035	0.79	0.458	0.035	-0.119	-0.059

Catchment S6H003								
Run	CE	CC	BIAS	CMAD	RMCC	MAR	STDEV	SI
1	0.174	0.53	-0.378	0.656	-0.302	-0.158	-0.641	0.035
2	0.187	0.538	-0.379	0.653	-0.285	-0.159	-0.641	0.026
3	0.197	0.543	-0.38	0.648	-0.272	-0.162	-0.649	0.031
4	0.175	0.533	-0.377	0.661	-0.298	-0.154	-0.627	0.019
5	0.157	0.523	-0.379	0.665	-0.324	-0.156	-0.626	0.035
6	0.176	0.534	-0.376	0.661	-0.294	-0.152	-0.629	0.022
7	0.167	0.528	-0.376	0.663	-0.311	-0.152	-0.625	0.025
8	0.172	0.529	-0.38	0.656	-0.309	-0.16	-0.639	0.033
9	0.185	0.537	-0.376	0.655	-0.287	-0.155	-0.637	0.025
10	0.186	0.537	-0.377	0.652	-0.285	-0.157	-0.644	0.03
Manual*	0.208	0.601	-0.301	0.622	-0.737	-0.15	-0.437	0.201

* These are calibration and not validation results

Table 4.15 Calibration performance of Amatole catchments using the coefficient of mean absolute deviation as the objective function

Catchment R2H009								
Run	CE	CC	BIAS	CMAD	RMCC	MAR	STDEV	SI
1	0.111	0.427	-0.463	0.786	0.276	-0.672	-0.884	0.142
2	0.099	0.442	-0.501	0.785	0.256	-0.695	-0.91	0.214
3	0.095	0.43	-0.51	0.787	0.279	-0.708	-0.92	0.172
4	0.109	0.428	-0.497	0.786	0.234	-0.761	-0.912	0.154
5	0.102	0.434	-0.506	0.789	0.305	-0.684	-0.888	0.195
6	0.104	0.432	-0.503	0.786	0.252	-0.735	-0.915	0.225
7	0.113	0.44	-0.486	0.784	0.248	-0.716	-0.902	0.205
8	0.093	0.434	-0.517	0.785	0.257	-0.714	-0.901	0.187
9	0.104	0.423	-0.496	0.789	0.269	-0.735	-0.918	0.13
10	0.089	0.428	-0.519	0.786	0.255	-0.727	-0.929	0.128
manual	-7.166	0.294	1.421	1.947	-1.396	0.061	-0.583	0.606

Catchment R3R001								
Run	CE	CC	BIAS	CMAD	RMCC	MAR	STDEV	SI
1	0.885	0.951	-0.238	0.574	0.578	-0.238	-0.179	0.227
2	0.885	0.951	-0.223	0.574	0.58	-0.223	-0.176	0.203
3	0.885	0.951	-0.237	0.574	0.573	-0.237	-0.181	0.226
4	0.886	0.951	-0.215	0.572	0.585	-0.215	-0.176	0.185
5	0.886	0.95	-0.191	0.574	0.585	-0.191	-0.172	0.152
6	0.886	0.949	-0.199	0.573	0.588	-0.199	-0.162	0.179
7	0.885	0.951	-0.238	0.575	0.573	-0.238	-0.18	0.228
8	0.885	0.951	-0.233	0.574	0.574	-0.233	-0.181	0.218
9	0.885	0.952	-0.219	0.573	0.577	-0.219	-0.184	0.184
10	0.884	0.951	-0.243	0.576	0.569	-0.243	-0.183	0.235
Manual*	0.748	0.866	0.162	0.819	0.641	0.162	0.113	0.27

Catchment S6H003								
Run	CE	CC	BIAS	CMAD	RMCC	MAR	STDEV	SI
1	0.404	0.678	-0.319	0.539	0.48	-0.065	-0.003	-0.166
2	0.431	0.677	-0.254	0.535	0.454	0.079	0.132	-0.064
3	0.428	0.681	-0.284	0.532	0.446	0.032	0.062	-0.064
4	0.426	0.676	-0.266	0.536	0.463	0.049	0.101	-0.102
5	0.418	0.68	-0.306	0.534	0.462	-0.025	0.008	-0.109
6	0.407	0.669	-0.302	0.536	0.449	-0.008	0	-0.088
7	0.424	0.678	-0.273	0.536	0.473	0.021	0.074	-0.134
8	0.423	0.68	-0.296	0.533	0.442	0.014	0.041	-0.072
9	0.417	0.678	-0.297	0.533	0.451	-0.006	0.019	-0.11
10	0.434	0.687	-0.292	0.532	0.454	0.015	0.067	-0.072
Manual*	0.319	0.659	-0.163	0.602	0.302	0.299	-0.021	-0.214

Table 4.16 Validation performance of Amatole catchments using the coefficient of mean absolute deviation as the objective function

Catchment R2H009								
Run	CE	CC	BIAS	CMAD	RMCC	MAR	STDEV	SI
1	0.127	0.365	-0.131	1.006	-0.18	0.106	0.421	-0.36
2	0.148	0.395	-0.204	0.957	-0.104	0.09	0.318	-0.28
3	0.118	0.357	-0.216	0.979	-0.133	0.064	0.428	-0.311
4	0.117	0.362	-0.178	0.99	-0.177	-0.003	0.433	-0.344
5	0.113	0.353	-0.201	0.985	-0.219	0.068	0.468	-0.25
6	0.13	0.373	-0.196	0.977	-0.158	0.025	0.407	-0.287
7	0.142	0.384	-0.169	0.978	-0.149	0.079	0.415	-0.297
8	0.132	0.375	-0.22	0.963	-0.154	0.008	0.3	-0.311
9	0.103	0.345	-0.183	1.003	-0.172	0.039	0.503	-0.363
10	0.122	0.361	-0.23	0.971	-0.096	0.03	0.352	-0.383
Manual*	-5.16	0.396	2.399	2.757	-0.68	4.868	6.711	0.113

Catchment R3R001								
Run	CE	CC	BIAS	CMAD	RMCC	MAR	STDEV	SI
1	0.711	0.873	-0.282	0.717	0.542	-0.282	-0.346	0.062
2	0.713	0.872	-0.265	0.721	0.544	-0.265	-0.339	0.048
3	0.711	0.873	-0.279	0.718	0.54	-0.279	-0.348	0.059
4	0.714	0.873	-0.26	0.719	0.539	-0.26	-0.341	0.035
5	0.714	0.87	-0.234	0.726	0.54	-0.234	-0.333	0.02
6	0.716	0.868	-0.239	0.731	0.554	-0.239	-0.32	0.048
7	0.711	0.872	-0.279	0.72	0.541	-0.279	-0.348	0.07
8	0.711	0.873	-0.273	0.718	0.54	-0.273	-0.346	0.051
9	0.711	0.875	-0.263	0.716	0.532	-0.263	-0.35	0.024
10	0.71	0.872	-0.282	0.719	0.542	-0.282	-0.35	0.069
Manual*	0.68	0.829	0.035	0.79	0.458	0.035	-0.119	-0.059

Catchment S6H003								
Run	CE	CC	BIAS	CMAD	RMCC	MAR	STDEV	SI
1	0.322	0.665	-0.411	0.61	0.073	-0.258	-0.709	-0.163
2	0.381	0.667	-0.34	0.586	-0.026	-0.138	-0.647	-0.084
3	0.378	0.676	-0.368	0.591	-0.003	-0.173	-0.656	-0.097
4	0.368	0.663	-0.356	0.593	0	-0.166	-0.662	-0.111
5	0.352	0.674	-0.396	0.603	0.042	-0.222	-0.683	-0.133
6	0.349	0.659	-0.385	0.603	0.002	-0.197	-0.677	-0.105
7	0.359	0.665	-0.365	0.595	0.028	-0.187	-0.678	-0.138
8	0.37	0.676	-0.381	0.596	0.005	-0.19	-0.661	-0.113
9	0.356	0.67	-0.385	0.599	0.022	-0.204	-0.68	-0.13
10	0.379	0.685	-0.379	0.593	0.019	-0.192	-0.656	-0.114
Manual*	0.208	0.601	-0.301	0.622	-0.737	-0.15	-0.437	0.201

* These are calibration and not validation results

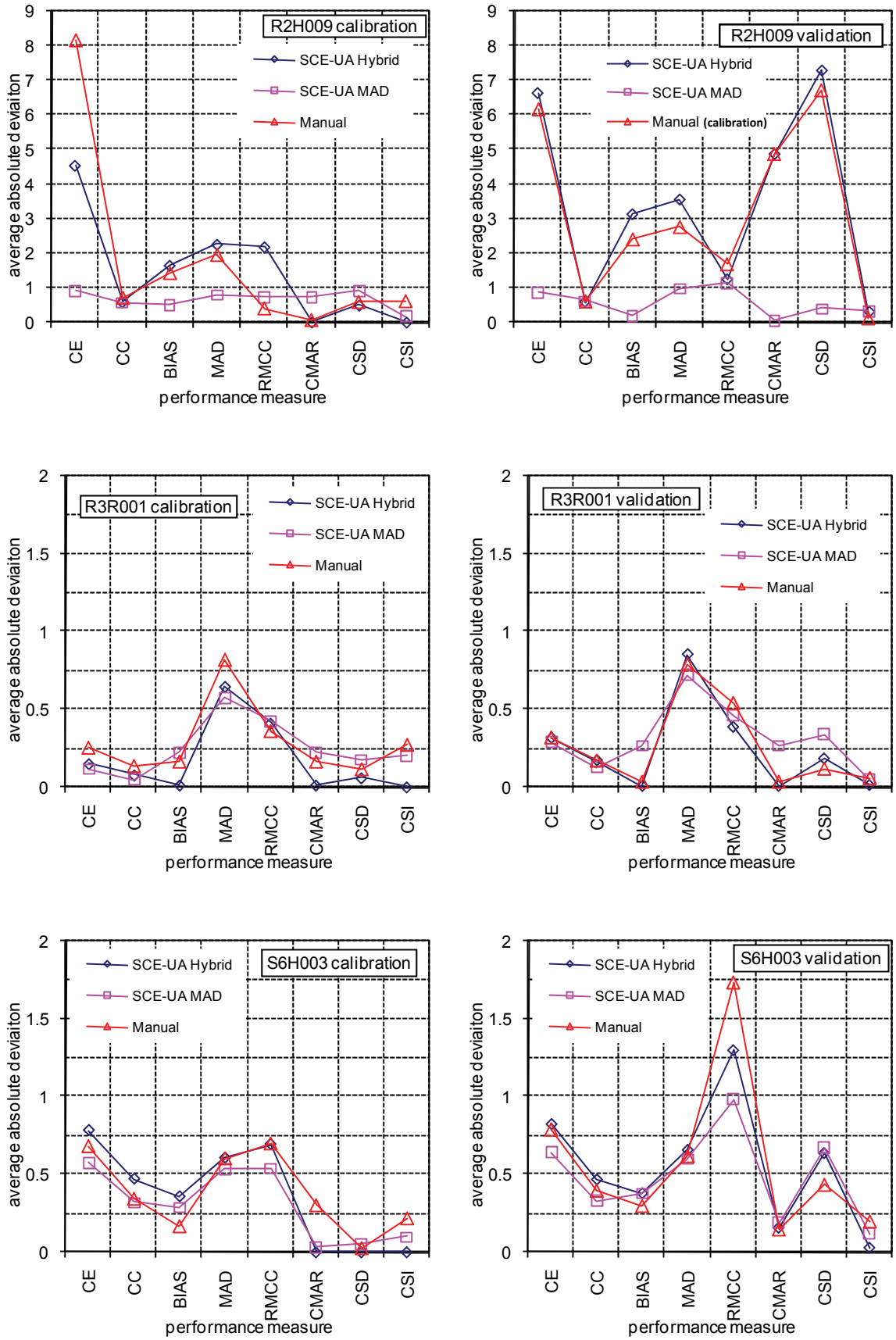

Figure 4.16 Comparison of manual and automatic calibration performance for Amatole catchments

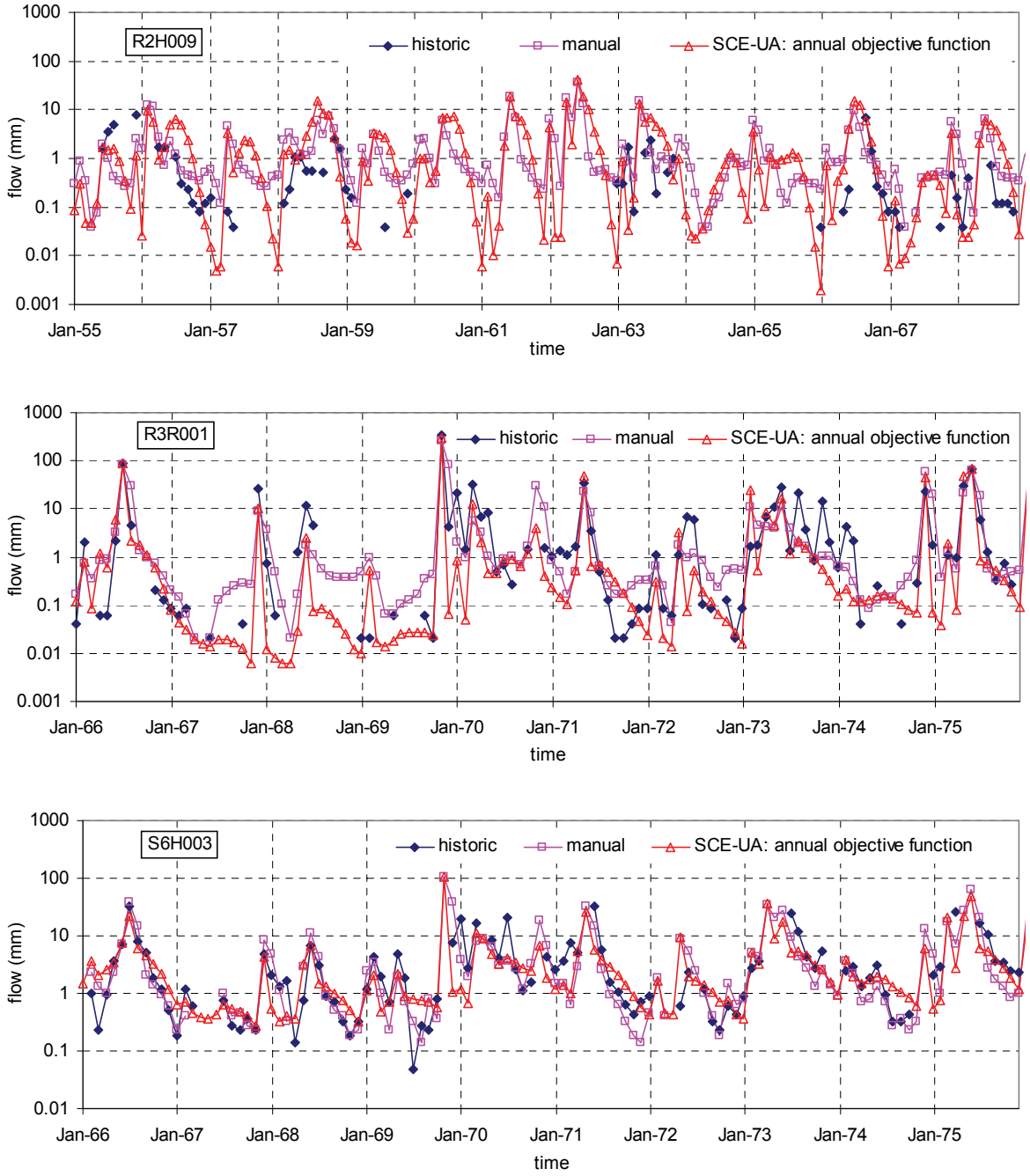

Figure 4.17 Comparison of observed and simulated time series for Amatole catchments

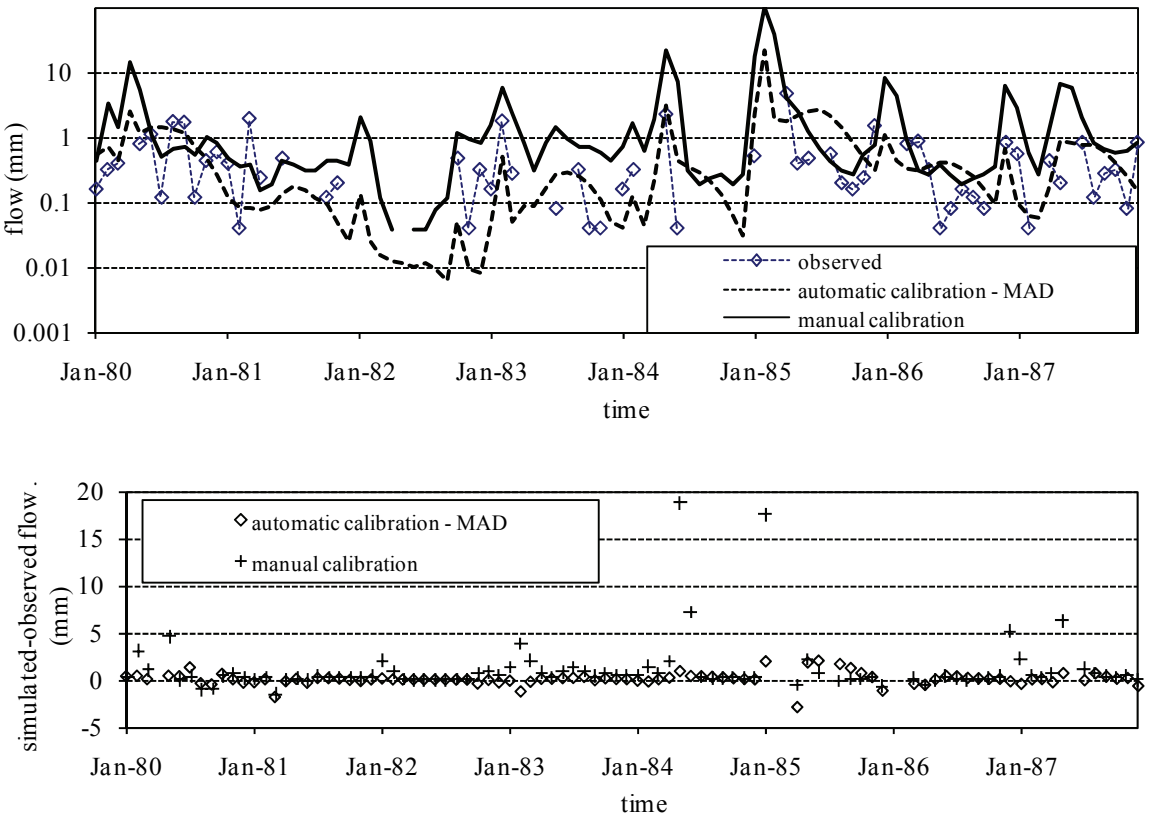

Figure 4.18 Comparison of manual calibration and automatic validation time series for Amatole catchment R2H009

4.4.3 Analysis of soil moisture – runoff relationships for Amatole basin catchments

In Section 4.4.2, one of the main differences between manual and automatic calibration was in the parameter values associated with the soil moisture-runoff relationship of the Pitman model. This relationship is therefore analyzed to some detail for the automatic calibrations. Details for manual calibration were not available so a comparison could not be carried out. The analysis however provided and an additional check for 'dangers' of automatic calibration. The soil moisture-runoff relationship in the Pitman model is modelled as illustrated in Figure 4.19. Runoff (Q) occurs once the soil moisture storage exceeds SL. If the storage is lower than SG, the storage corresponding to a runoff equal to GW, all the runoff is considered slow runoff and is lagged to a greater degree than the runoff in excess of GW. Parameter GL is the lag time in months modelled using Muskingum method for the runoff lower than or equal to GW. Runoff in excess of GW is lagged by TL months. ST represents the maximum storage and FT the maximum runoff from the soil.

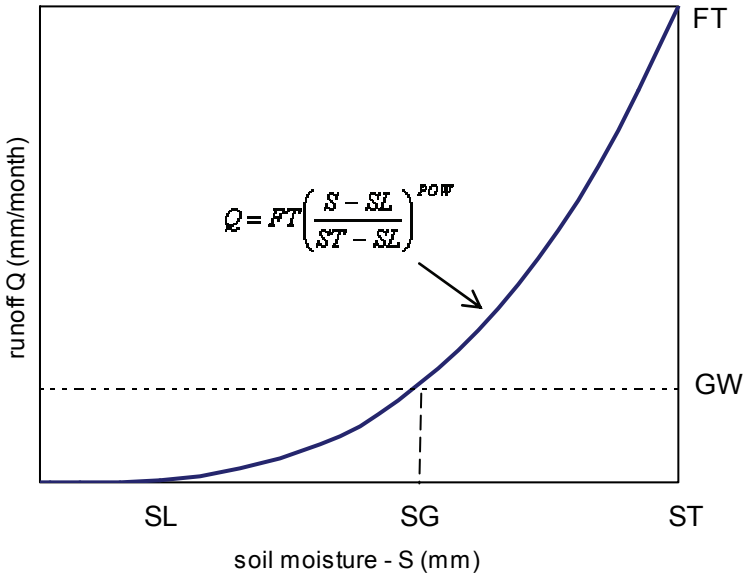

Figure 4.19 Soil moisture-runoff modelling in the Pitman model

Figure 4.20 shows representative soil moisture-runoff relationships for the three catchments. The single run out of ten giving the best objective function was selected as the representative for each catchment. The calibrations carried out using the annual (hybrid) objective function were used for this analysis. However as the calibration of R2H009 using the annual objective function was found inadequate in Section 4.4.2, the result obtained using the monthly (CMAD) objective function calibration is included as the fourth plot of Figure 4.20. The left hand side of the Figure show the soil moisture (S) versus runoff (Q) curves based on the calibrated parameters (Tables 4.11 and 4.12) plotted on a log-log scale. These plots also include the S-Q relationships from the manual calibration parameters. The plots on the right hand side are time series of the average monthly soil moisture obtained from 4 values of soil moisture that the Pitman model computes for each month.

It is observed from the plots that the soil moisture hardly exceeds SG (the soil moisture corresponding to GW) meaning that practically, all the soil moisture runoff is 'slow'. The lag periods represented by parameter GL are all less than 0.1 months (Tables 4.11 and 4.12) indicating negligible degree of lag. Parameter TL, the lag for the fast soil moisture runoff had been set to 0.5 months for all calibrations – a value higher than all the GL values and therefore conceptually wrong. Fast soil moisture runoff is however not generated according to Figure 4.20 and the calibrations are therefore valid. Figure 4.20 also shows that throughout the simulation period, with all three catchments, the monthly soil moisture does not go below 200 mm and exceeds 600 mm less than 0.5% of the simulation period (excluding the first plot based on an inadequate calibration of 2H009 using the annual objective function).

There are no field soil moisture measurements that could verify how reasonable the soil moisture time series' simulated by automatic calibration (Figure 4.20) are and there is no other observation to suggest that they are not realistic. The range of soil moisture depths obtained (200-600 mm) is considered realistic and all the three time series show the expected seasonal variation corresponding to the wet and the dry season. In addition, the expected inter-annual variability of soil moisture (reflecting dry and wet years) is also observed in the three time series.

The realistic soil moisture – runoff relationships obtained with automatic calibration with much higher POW values suggest that the recommended limit of POW to 3.0 is likely invalid. Previous manual calibration (Hughes, 2004; Mwelwa, 2004; Hughes et al., 2006), physically based calibration (Kapangaziwiri and Hughes, 2008) and automatic calibration (Ndiritu, 2001) of the Pitman model also strongly suggest that this guideline is not valid.

Figure 4.21 shows the runoff separation for the automatic calibrations using the annual objective functions and also the monthly objective function for catchment R2H009. There was no clear method of assessing how realistic this separation is for the three catchments as no field data or information was available for such assessment. The flow separation is however considered reasonable and realistic except for the annual calibration of R2H009 where the soil moisture flow component is considered excessive. This observation is again in agreement with the perceived inadequacy of this calibration (Figure 4.16, Tables 4.15 and 4.16).

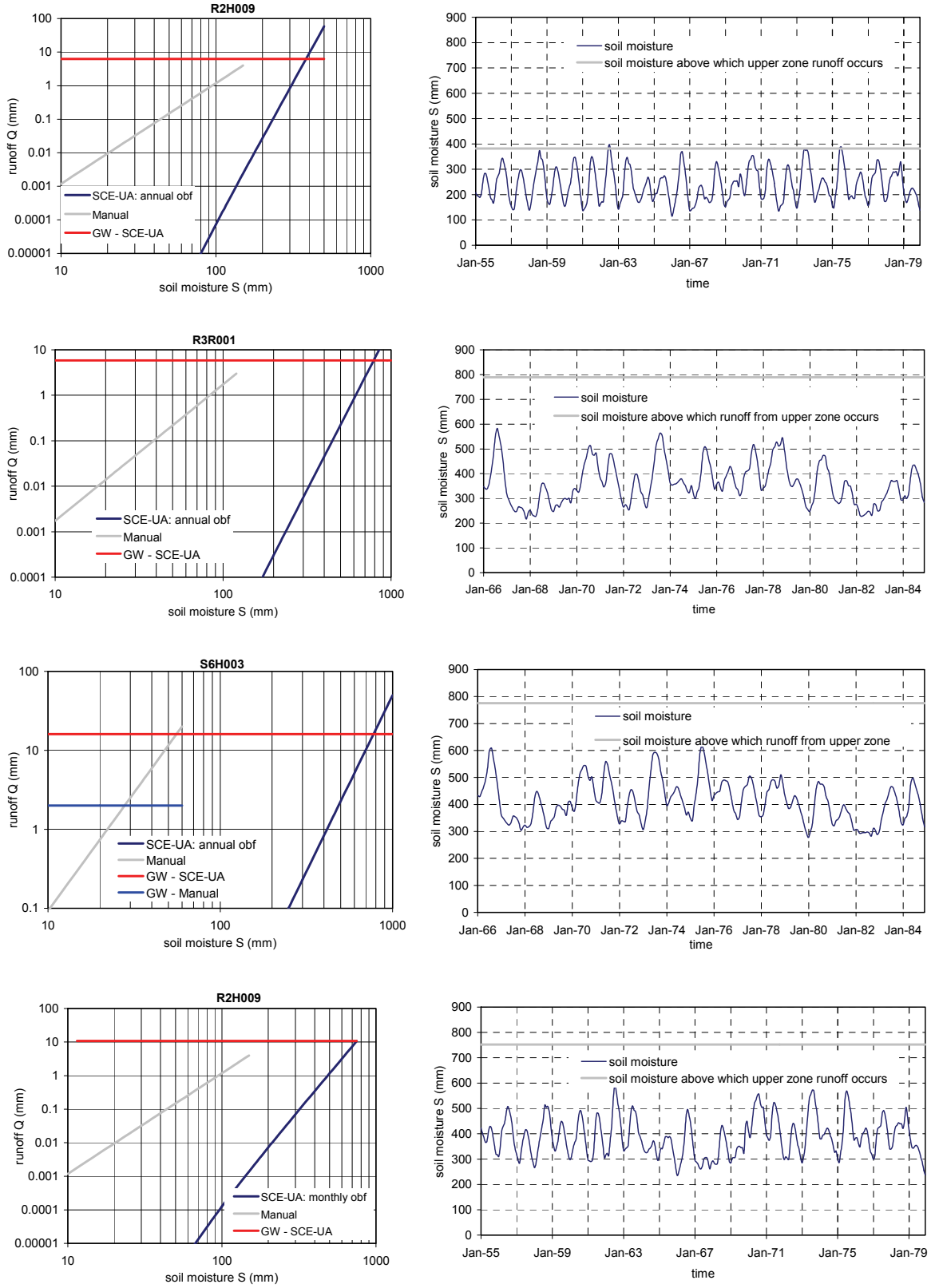

Figure 4.20 Soil moisture-runoff relationships for Amatole catchments

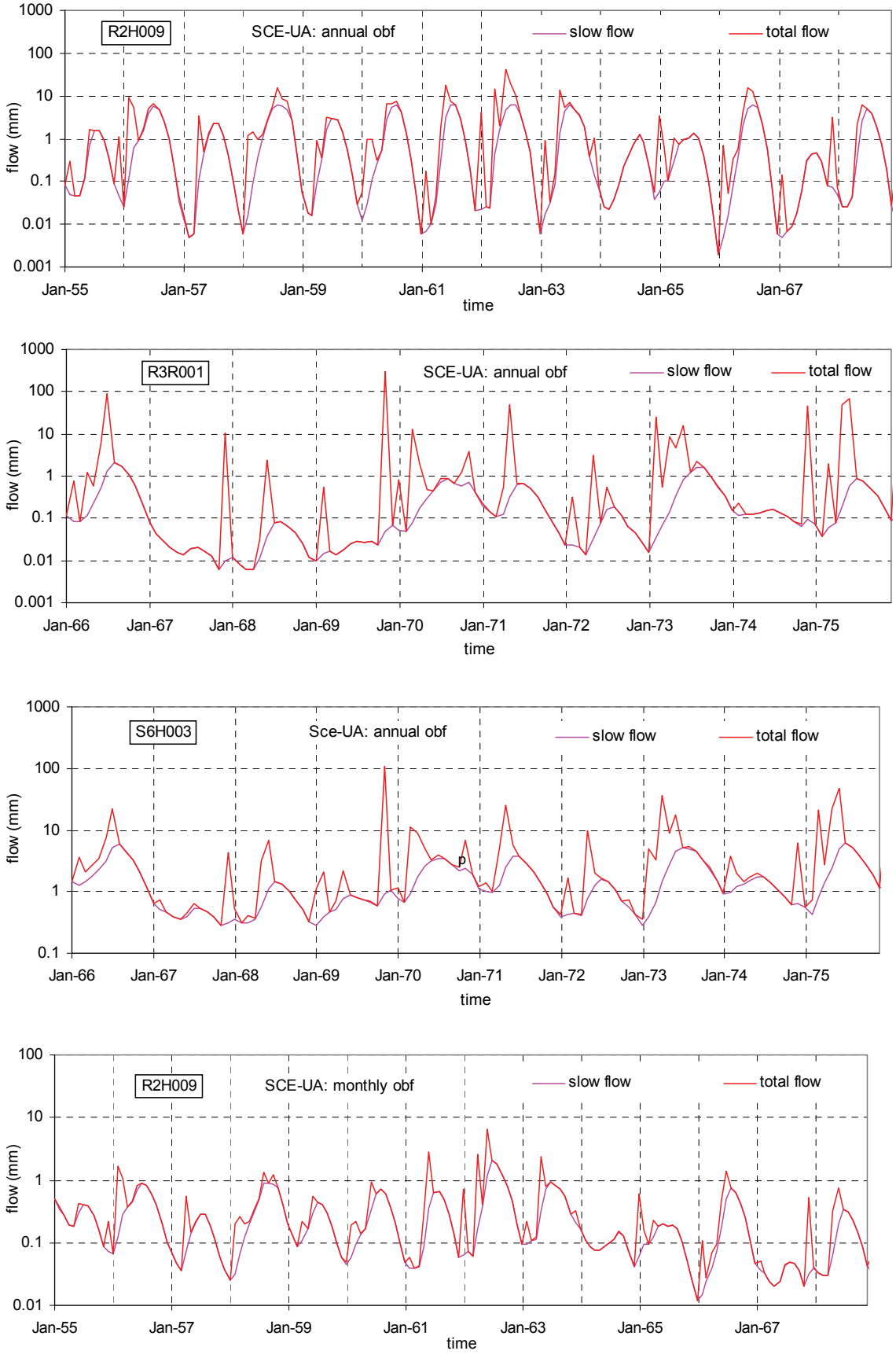

Figure 4.21 Flow separation for Amatole catchments

4.5 Potential dangers, challenges and advantages of automatic model calibration

The analysis in this Chapter and previous experience with automatic calibration has not revealed any glaring dangers of automatic calibration. The main danger that could arise would be to carry out calibration as a curve fitting exercise that may obtain model parameters that do not make hydrologic sense. This can be avoided by setting the parameter search range limits realistically – a task which is not difficult and that manual calibration also requires. The provision of an initial parameter search range and search range limits adopted in the automatic calibrations here allows the modeller to use his/her experience and judgement in selecting the starting point and the limits beyond which parameter values are not expected. If parameter values consistently locate at one limit in multiple randomly initialised calibrations, the search range limit is extended and the calibration runs limited. This gives a chance for the model and data to reveal processes that the modeller had not perceived or considered significant. A case in point was the calibration of Kafue basin (Section 4.3) where multiple automatic calibrations consistently lead to uncharacteristically high precipitation index (PI) and thereby revealed the significance of dambos in the basin and the likely inadequacy of the Pitman model in modelling them. These inferences from automatic calibration were not obtained by a comprehensive manual calibration of the basin (Mwelwa, 2004) although that study had recognized that dambos were expected to have a significant impact on several parameters of the model.

The conceptually inconsistent values of the lag for groundwater runoff GL and the lag for surface and soil moisture TL (GL < TL) for the Amatole catchments (Table 4.11 and 4.12) are an indication of the potential dangers of auto calibration. The soil moisture analysis for Amatole (Section 4.4.3) revealed that parameter TL is not activated and the auto-calibrations were therefore valid. This conceptual inconsistency of GL and TL was also observed in three instances of manual calibration: i) subcatchment G of Kafue basin by Mwelwa (2004) (GL=0, TL=0.25 months – see Appendix 2), ii) catchment R2H009 of Amatole basin by Kleynhans (2007) (GL=0, TL=0.5 months – see Tables 4.11 and 4.12) and iii) catchment R3R001 of Amatole basin by Kleynhans (2007) (GL=0, TL=0.5 months – see Table 4.11 and 4,12). It is most likely the case that both GL and TL were redundant in the manual calibrations although there is no evidence to show that this was verified. These inconsistencies show that unrealistic parameter sets can be obtained irrespective of whether automatic or manual calibration is applied. Furthermore, manual calibration may suffer from the application of invalid guidelines because its subjective nature makes it difficult to test such guidelines comprehensively. A case in point is the limitation of the power of the runoff-moisture storage relationship (POW) to 3.0 in the Pitman model (Bailey, 2008) as discussed in Section 4.4.3.

Realistic calibration, whether manual or automatic, requires the understanding of the model structure, the catchment processes including any unique features, a good dataset, a reasonable idea of the parameter search ranges, careful interpretation of ‘unexpected’ results and validation using an independent data set. The main challenges are usually the acquisition of a good data set and understanding the catchment processes. One needs data to gain insight and to understand the catchment processes but the data is often unavailable, too short, or unreliable.

The analysis here has revealed the ability of automatic calibration to enable parameter identification to be assessed clearly (see for example Fig 4.3 and 4.4) – a task that can only be carried out more subjectively with manual calibration. In addition, parameter interdependence within catchments (Figure 4.5) and across catchments (Figure 4.10) can also be revealed via automatic calibration. Again, manual calibration is only capable of carrying this out much more subjectively and tediously.

Automatic model calibration requires the specification of an objective function whose selection needs to be guided by the aim of the modelling and its ability to maximise utilization of data. The choice of the objective function is to a degree subjective but the literature does not suggest that this has been experienced as a drawback. Typically, manual calibration also requires the use of performance measures whose selection also involves subjective judgement. Different objective functions give different parameter sets as observed in the Amatole basin calibrations (Table 4.11 and 4.12). This however need not be viewed as a disadvantage of automatic calibration as it a reminder of the limitations of the model structure and applied data. It also compels the modeller to more closely relate the calibration exercise to the specific objective/s of the modelling.

It is important to note that the above advantages would not be achieved by making a single automatic calibration run but with **multiple randomly initialised** calibration runs. Statistical analysis may be applied to specify how many runs may be considered adequate but this may not add value to the task. In this study, 10 randomly initialised calibrations were applied and considered adequate for achieving the above mentioned advantages.

5 Conclusions and Recommendations

This study was aimed at evaluating automatic catchment model calibration in the light of a perception by many hydrological modellers in Southern Africa of automatic calibration as 'dangerous' and the consequent very limited application of automatic calibration in southern Africa. In order to achieve this, the widely used Pitman model was automatically calibrated on eleven catchments located in three southern African basins; the Buffelspruit and Amatole in South Africa and the North Western Kafue in Zambia. These catchments had been manually calibrated previously (by experienced modellers or under their guidance) thus allowing a comparison of automatic and manual calibration. The shuffled complex evolution (SCE-UA) method, arguably the most efficient and effective catchment model calibration technique to date was selected for automatic calibration.

The SCE-UA method was implemented in a generalized automatic calibration software that can be used to calibrate any catchment model with minor coding of the model to allow exchange of information with the calibration software. The method to implement this linkage is described in Chapter 3 and an example is included as part of the software (in the accompanying CR ROM). The SCE-UA was coded in Microsoft Power Station Fortran and a graphical user interface was developed in Delphi to enable user friendly calibration in a windows environment. The calibrator was designed to allow an initial search range and search range limits to be set thereby giving the modeller a chance to apply his/her experience and judgement in selecting suitable starting and limiting values of each parameter. The calibrator also allows for calibration to be repeated up to 20 randomly initialised times. Multiple randomly initialised calibrations help to; i) check the adequacy of optimization ii) identify parameters consistently locating at the set search limits and adjusting the limits if this is realistic, iii) assess the level of identification of parameters and finding out which are active and which are redundant, and iv) identify parameter inter-dependence within and across catchments. Ten randomly initialised calibration runs were applied in this project and were found adequate for the above mentioned tasks as illustrated in various Sections of Chapter 4.

For all 11 catchments, no evident danger of automatic calibration was observed and all the parameter values and simulated streamflow time series' were found to be realistic. Unexpectedly large values of the precipitation index (PI) with averages ranging from 9.0-13.4 mm for four catchments of Kafue basin were considered to represent interception on the extensive dambos found in the basin rather than canopy interception as in normal Pitman model applications. This inference was also found to be the likely explanation of the notably poorer validation for Kafue basin as the Pitman model structure does not include explicit modelling of dambos. Manual calibration of Kafue basin (Mwelwa, 2004) had failed to make these inferences although it had pointed out that dambos are expected to have significant impact on various parameters of the Pitman model. Although automatic calibration is often faulted on the basis of its inability to relate parameter values to physical features of the catchment, the results here indicate that automatic calibration may at times be better at this task than manual calibration.

Using several performance measured including the coefficient of efficiency, the coefficient of determination, the bias and a residual mass coefficient, automatic calibration was found to perform considerably better than manual calibration for the Buffelspruit and one of the three Amatole

catchments. Performance for other Amatole and the seven Kafue basin catchments was practically identical in manual and automatic calibration. These results suggest than automatic calibration using a powerful optimizer and appropriate objective functions may be less prone to obtaining sub-optimal calibrations than manual calibration.

No specific danger of automatic calibration was identified its use calls for careful identification of parameter search ranges and the use of all available information to try and obtain the best possible understanding of the hydrological processes and features in the catchment. In addition, thoughtful checking and interpretation of the calibration results is essential. These precautions obviate the obvious danger of using an optimizer to carry out a ‘blind’ curve fitting exercise in the name of automatic calibration. This study shows, on the other hand, that using an optimizer to search for suitable model parameters may hold many advantages over a purely manual search. The study reveals that for these advantages to be realised, multiple randomly initialised calibration runs would need to be carried out.

6 REFERENCES

AL-ABED N and WHITELY HR (2002) Calibration of the Hydrological Simulation Program FORTRAN (HSPF) model using automatic calibration and geographical information systems, *Hydrol. Processes* 16(6) 3169-3188.

ABDULLA FA, LATTENMAIER DP and LIANG X (1999) Estimation of the ARNO baseflow parameters using daily streamflow data. *J. Hydrol*. 222 37-54.

AJAMI KN, GUPTA HV, WAGENER T and SOROOSH SOROOSHIAN (2004) Calibration of a semi-distributed model for streamflow estimation along a river system. *J. Hydrol*. 298 112-135.

BAILEY A (2005) Personal communication on WRSM 2000 project.

BAILEY A (2008) Water resources simulation model for Windows, Theory Document PWMA 04/000/00/6107. (DWAF, WRC, SSI).

BANDARAGODA C, TARBOTON D and WOODS R (2004) Application of TOPNET in the distributed model intercomparison project. *J. Hydrol*. 298 178-201.

BOYLE DP, GUPTA HV and SOROOSHIAN S (2000) Toward Improved Streamflow Forecasts: Value of semidistributed modelling. *Water Resour. Res*. 37(11) 2749-2759.

BRATH A, MONTANARI A and TOTH E (2004) Analysis of the effects of different scenarios of historical data availability on the calibration of a spatially-distributed hydrological model. *J. Hydrol*. 291 232-253.

BELL LSJ, BINNING PJ, KUCZERA G and KAU PMH (2002) Rigorous uncertainty assessment in contaminant transport inverse modelling: A case study of floride diffusion through clay liners. *J. Contaminant Hydrol*. 57(1-2) 1-20.

BULLOCK, A. 1992a. The role of dambos in determining river flow regimes in Zimbabwe. *J. Hydrol.* 134: 349-372.

BULLOCK, A. 1992b. Dambo hydrology in southern Africa - review and reassessment. *J. Hydrol.* 134: 373-396.

CATCHMENT MODELLING TOOLKIT (www.toolkit.net.au/rrl) [accessed, July 6 2009],

CHENG CT, OU CP and CHAU KW (2002) Combining a fuzzy optimal model with a genetic algorithm to solve multi-objective rainfall-runoff model calibration. *J Hydrol*. 268 72-86.

CHENG S and WANG R (2002) An approach for evaluating the hydrological effects of urbanization and its application. *Hydrol. Processes* 16(7) 1403-1418.

CHIEW FHS and MCMAHON TA (1994) Application of the daily Rainfall-Runoff Model MODHYDROLOG to 28 Australian catchments. *J. Hydrol*. 147 1-36.

CONTRACTOR DN and JENSON JW (2000) Simulated effect of vadose infiltration on water levels in the Northern Guam lens aquifer. *J. Hydrol*. 229 232-254.

COOPER VA, NGUYEN VTV and NICELL JA (1997) Evaluation of global optimization methods for conceptual rainfall-runoff calibration. *Water Sci. and Tech*. 36(5) 53-60.

DAGNACHEW L, VALLET-COULOMB C and GASSE F (2003) Hydrological response to climate and land use changes in Tropical Africa: a case study South Central Ethiopia, *J Hydrol.* 275 67-85.

DI LUZIO M and ARNOLD JG (2004) Formulation of a hybrid calibration approach for a physically based distributed model with NEXRAD data input. *J. Hydrol*. 298 136-154.

DOHERTY J and JOHNSTON JM (2003) Methodologies for calibration and predictive analysis of a watershed model. *J. American Water Resour. Assoc*. 39(2) 251-265.

DUAN QY, SOROOSHIAN S and GUPTA V (1992) Effective and efficient global optimization for conceptual rainfall-runoff models. *Water Resour. Res*. 28(4) 1015-1031.

DUAN QY, GUPTA V and SOROOSHIAN S (1993) A shuffled complex evolution approach for effective and efficient optimization. *J. Optim. Theory Appl.* 76(3) 501-521.

DUAN QY, SOROOSHIAN S and GUPTA V (1994) Optimal use of the SCE-UA global optimization method for calibrating watershed models. *J. Hydrol*. 158 265-284.

ECKHARDT K and ARNOLD JG (2001) Automatic calibration of a distributed catchment model. *J Hydrol*. 251 103-109.

EUSUFF MM and LANSEY KE (2004) Optimal operation of artificial groundwater recharge systems considering water quality transformations. *Water Resour. Man*. 18(4) 379-405.

FRANCHINI M, GALEATI G and BERRA S (1998) Global optimization techniques for the calibration of conceptual rainfall-runoff models. *Hydrol. Sci.J.* 43(3) 443-458.

GAN TY, DLAMINI EM and BIFTU GF (1997) Effects of model complexity and structure, data quality, and objective functions on hydrologic modelling. *J. Hydrol*. 192(1-4) 81-103.

GOLDBERG DE (1989) *Genetic Algorithms in Search, Optimization and Machine Learning*, Addison-Wesley-Longman, Reading, Mass, 412pp.

GUPTA HV, SOROOSHIAN S and YAPO PO (1999) Status of automatic calibration for hydrologic models: Comparison with multilevel expert calibration. *J. Hydr. Eng. ASCE*. 4(2) 135-143.

GUPTA HV, SOROOSHIAN S and YAPO P (1998) Toward improvement of calibration of hydrologic models: Multiple and noncomensurable measures of information. *Water Resour. Res*. 34(4) 751-763.

HSIEH L and WANG R (1999) Semi-distributed parallel-type linear reservoir rainfall-runoff model and its application to Taiwan. *Hydrol. Processes* 13(8) 1247-1268.

HUGHES DA (1997) South African 'FRIEND' – The application of rainfall-runoff models in the SADC region. *WRC Report* No. 635/1/97.

HUGHES DA (2002) The development of an information modelling system for regional water resource assessments. *Proceedings of the 4th International FRIEND Conference*.

IAHS Publication 274.2002, 43-49.HUGHES DA (2004) Incorporating groundwater recharge and discharge functions into an existing monthly rainfall-runoff model. *Hydrol. Sci. J*. 49(2) 297-311.

HUGHES DA and METZLER W (1998) Assessment of three monthly rainfall-runoff models for estimating the water resource yield of semi-arid catchments in Namibia. *Hydrol. Sci. J.* 43(2) 283-297.

HUGHES DA, ANDERSON B, WILK J AND SAVENIJE HHG (2006) Regional calibration of the Pitman model for the Okavango River. *J. Hydrol.* 331: 30-42.

KAPANGAZIWIRI E AND HUGHES DA (2008) Towards revised physically based parameter estimation methods for the Pitman monthly rainfall-runoff model, Water SA, 34(2), 183-192.

JAKEMAN AJ and HORNBERGER GM (1993) How much complexity is warranted in a rainfall-runoff model? *Water Resour. Res*. 29(8) 2637-2649.

KLEYNHANS PJ (2007) Development of a Reconciliation Strategy for the Amatole Bulk Water Supply System, Report to the South African Department of Water Affairs and Forestry (DWAF).

KNIGHT PIESOLD, STEWART SCOTT and SRK CONSULTING (2003) Background to the Terms of Reference of the Water Resources of South Africa 2005 Study. *South African WRC Report No*. 1315/1/03.

KUCZERA G (1997) Efficient subspace probabilistic parameter optimization for catchment models. *Water Resour. Res*. 33(1) 177-185.

LEE R and WANG R (1998) Parameter estimation with colored noise effect for differential hydrological grey model. *J. Hydrol*. 208 1-15.

LIONG S, GAUTAM TR WEE L and VAN NGUYEN VT (2001) Alternative well calibrated rainfall-runoff model: Genetic programming scheme. *Proc. Urban Drainage and Modell. Conf*. Orlando. FL. USA. 777-787.

LYNCH, S. D., 2004, Development of a Raster Database of Annual, Monthly and Daily Rainfall for Southern Africa. *WRC Report No. 1156/1/04*. Water Research Commission, Pretoria, RSA

MADSEN H (2000) Automatic calibration of a conceptual rainfall-runoff model using multiple objectives. *J hydrol*. 235 276-288.

MADSEN H (2003) Parameter estimation in distributed hydrological catchment modelling using automatic calibration with multiple objectives. *Advances in Water Resour.* 26(2) 205-216.

MADSEN H, WILSON G and AMMENTORP HC (2002) Comparison of different automated procedures for calibration of rainfall-runoff models. *J Hydrol*. 261 48-59.

McCARTNEY M. P., 2000. The Water Budget of a Headwater Catchment Containing a Dambo. *Physics and Chemistry of the Earth.* 25 (7-8): 611-616.

MERTENS J, MADSEN H, FEYEN L, JACQUES D and FEYEN J (2004) Including prior information in the estimation of effective soil parameters in unsaturated zone modelling. *J. Hydrol*. 294 251-269.

MIDGLEY DC, PITMAN VW and MIDDLETON BJ (1994) Surface Water Resources of South Africa. *WRC Report* No. 298/1/94.

MWELWA EM (2004) The application of the monthly step Pitman Rainfall-Runoff Model to the Kafue River Basin of Zambia, MSc thesis, Rhodes University, South Africa.

NDIRITU JG (2001) Using validation to evaluate model calibration adequacy. *Proc. 10th South African Nat. Hydrol. (SANCIAHS) Symp.* Pietermaritzburg South Africa.

NITTIN M and LIONG S (2004) superior exploration-exploitation balance in shuffled complex evolution. *J. Hydr. Eng. ASCE* 130(12) 1202-1205.

PITMAN V (1973) A mathematical model for generating monthly river flows from meteorological data in South Africa. *Report No. 2/73, Hydrological Research Unit, Univ. of the Witwatersrand.*

PITMAN WV, BAILEY AK and KAKEBEEKE JP (2000) The monthly WRSM2000 model.

SCOTT RL, SHUTTLEWORTH W, JAMES K, TIMOTHY O and WARRICK AW (2000) Modelling multilyear observations of soil moisture recharge in the semiarid American Southwest. *Water Resour. Res.* 36(8) 2233-2247.

SENARATH SUS, OGDEN FL, DOWNER CW and SHARIF HO (2000) On the calibration and verification of a two-dimensional, distributed, Hortonian, continuous watershed model. *Water Resour. Res.* 36(6) 1495-1510.

SOIL WATER ASSESSMENT TOOL (www.brc.tamus.edu/swat/) [accessed, July 6 2009],

SOROOSHIAN S, DUAN Q and GUPTA VK (1993) Calibration of Rainfall-Runoff Models: Application of Global Optimization to the Sacramento Soil Moisture Accounting Model. *Water Resour. Res*. 29(4) 1185-1194.

TANAKAMARU H and BURGES SJ (1996) Application of global optimization to parameter estimation of the TANK model, *Proc., Int. Conference, Water Resour. and Environ. Res*. Kyoto Japan 2, 39-46.

THIEMANN M, GUPTA HV, FUNKE R and SOROOSH SOROOSHIAN (1998). Calibration of a distributed rainfall-runoff model using global optimization strategies. *Proc. Int. Water Resour. Eng. Conf.* 2 1362-1367.

THYER M, KUCZERA G and BATES BC (1999) Probabilistic optimization for conceptual rainfall-runoff models: comparison of the shuffled complex evolution and simulated annealing algorithms. *Water Resour. Res*. 35(3) 767-773.

VAN GRIENSVEN A and BAUWENS W (2003) Multiobjective auto calibration for semidistributed water quality models. *Water Resour. Res*. 39(12) SWC91-99.

VRUGT JA, GUPTA HV, BOUTEN W and SOROOSH SOROOSHIAN (2003a) A Shuffled Complex Evolution Metropolis algorithm for optimization and uncertainty assessment of hydrologic model parameters. *Water Resour. Res*. 39(8) SWC1-1-SWC1-16.

VRUGT JA, GUPTA HV, BASTIDAS LA, BOUTEN W and SOROOSH SOROOSHIAN (2003b) Effective and efficient algorithm for multiobjective optimization of hydrologic models. *Water Resour. Res.* 39(8) SWC5-1-SWC5-19.

VRUGT JA, SCHOUPS G, HOPMANS JW, YOUNG C, WALLENDER WW, HARTER T and BOUTEN W (2004) Inverse modelling of large-scale spatially distributed vadose zone properties using global optimization. *Water Resour. Res*. 40(6) W06503-1-W06503-20.

XIA Y, PITMAN J, GUPTA HV, LEPLASTRIER M, HENDERSON-SELLERS A and BASTIDAS LA (2002) Calibrating a land surface model of varying complexity using multi-criteria methods and the Cabauw dataset. *J. Hydrometeorol*. 32(2) 181-194.

YAPO PO, GUPTA HV and SOROOSH SOROOSHIAN (1996) Automatic calibration of conceptual rainfall-runoff models: sensitivity to calibration data. *J. Hydrol*. 181 23-48.

YAPO PO, GUPTA HV and SOROOSHIAN S (1998) Multiobjective global optimization of hydrologic models. *J. Hydrol.* 204 83-97.

YU P-S AND YAG T-C (2000) Fuzzy multi-objective function for rainfall-runoff model calibration, *J Hydrol*, 238 1-14.

WINSEMIUS HC, SAVENIJE HHG, GERRITS AMJ, ZAPREEVA EA, and KLEES R (2006) Comparison of two model approaches in the Zambezi river basin with regard to model reliability and identifiability, *Hydrol. Earth Syst. Sci.,* 10, 339-352.

ZITLER E and THIELE L (1999) Multi-objective Evolutionary Algorithms: A comparative case study and the strength Pareto approach. *IEEE Trans. Evol. Comput.* 3(4) 257-271.

APPENDICES

Appendix 1 Manually calibrated parameters for Buffelspruit catchment

Parameter	Notation	Value
Rain distribution factor		1.2
Proportion of impervious area	*AI*	0
Intercept cap. (*Veg1*)	*PI*	1.5
Intercept cap. (*Veg2*)	*PI*	4.0
% Area of *Veg2*	*AFOR*	0
Veg2/*Veg1* Pot. evap. ratio	*FF*	1.4
Min. abs. rate (mm month-1)	*ZMIN*	25
Mean abs. rate (mm month-1)	*ZAVE*	320
Maximum abs. rate (mm month-1)	*ZMAX*	520
Maximum storage capacity	*ST* (mm)	400
No runoff below storage	*SL* (mm)	0
Power of the storage–runoff curve	*POW*	2.3
Runoff rate at *ST* (mm month-1)	*FT*	22.0
Max. groundwater flow/recharge (mm month-1)	*GW*	8.0
Evaporation–storage coefficient	*R*	0.5
Surface runoff time lag (months)	*TL*	0.25
Groundwater time lag (months)	*GL*	2.5

Source: Hughes (2004)

Appendix 2 Calibrated parameters for 7 Kafue River Basin sub catchments

Pitman Model Parameters	Kafue river basin subcatchment						
	A	C	D	E	F	G	H
Rain Distribution Factor (RDF)	0.80	0.80	0.800	0.800	0.800	0.800	0.800
Proportion of impervious area (AI)	0.00	0.00	0.00	0.00	0.00	0.00	0.00
Summer interception capacity (Veg1) (PI1s)	1.50	1.50	1.50	1.50	1.50	1.50	1.50
Winter interception capacity (Veg1) (PI1w)	1.50	1.50	1.50	1.50	1.50	1.50	1.50
Summer interception capacity (Veg2) (PI2s)	4.00	4.00	4.00	4.00	4.00	4.00	4.00
Winter interception capacity (Veg2) (PI2w)	4.00	4.00	4.00	4.00	4.00	4.00	4.00
Percentage Area of Veg2 (AFOR)	20.00	20.00	35.00	5.00	10.00	30.00	10.00
Veg2/Veg1 Potential Evapotranspiration Ratio (FF)	1.40	1.400	1.400	1.400	1.400	1.400	1.400
Power of Veg. recession curve	1.00	1.00	1.00	1.00	1.00	1.00	1.00
Annual Pan Evaporation (mm) (PEVAP)	1640.00	1504.00	1604.00	1504.00	1464.00	1464.00	1464.00
Summer minimum absorption rate (mm/month) (ZMINs)	200.00	200.00	200.00	200.00	200.00	200.00	200.00
Winter minimum absorption rate (mm/month) (ZMINw)	200.00	200.00	200.00	200.00	200.00	200.00	200.00
Mean absorption rate (mm/month) (ZAVE)	500.00	500.00	500.00	500.00	600.00	600.00	600.00
Maximum absorption rate (mm/month) (ZMAX)	1200.00	1200.00	1200.00	1200.00	1200.00	1200.00	1200.00
Maximum storage capacity (ST)	1200.00	1200.00	1200.00	1300.00	1300.00	1300.00	1300.00
No runoff below storage (SL)	0.00	0.00	0.00	0.00	0.00	0.00	0.00
Power: storage-runoff curve (POW)	4.00	4.00	4.00	4.00	4.00	4.00	4.00
Runoff rate at ST (mm/month) (FT)	105.00	105.00	105.00	55.00	55.00	55.00	55.00
Maximum groundwater flow (mm/month) (GW)	10.00	10.00	10.00	5.00	5.00	5.00	5.00
Evaporation-storage coefficient (R)	0.20	0.20	0.20	0.20	0.20	0.20	0.20
Surface runoff time lag (months) (TL)	0.25	0.25	0.25	0.25	0.25	0.25	0.25
Groundwater time lag (months) (GL)	3.00	3.00	3.00	3.00	3.00	0.00	3.00
Irrigated area (km^2) (AIRR)	0.00	0.00	0.00	0.00	0.00	0.00	91.300
Irrigation return flow fraction (IWR)	0.00	0.00	0.00	0.00	0.00	0.00	0.00
Non-Irrigation Direct Demand (Ml/year)	0.00	58000.00	0.00	78000.00	13000.00	0.00	21000.00

Source: Mwelwa (2004)

Note: The calibration here is not entirely manual as a genetic algorithm was initially applied to obtain initial parameter estimates.